ESR STUDIES ON SOME NAPHTHALENE DERIVATIVES

—

A thesis

submitted in partial fulfilment

of the requirements for the Degree

of

Doctor of Philosophy in Chemistry

in the

University of Canterbury

by

M.G. Bakker

—

University of Canterbury

1985

PREFACE

This thesis contains the results of an original study by the author, and is not substantially the same as any which has already been submitted. Unless stated otherwise the experimental results are those of the author.

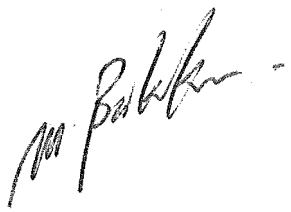

To

my Parents

ACKNOWLEDGEMENTS

I wish to sincerely thank my supervisor, Dr R.F.C. Claridge, for his help, encouragement and enthusiasm during the course of this project. My thanks must also go to my family for their support and encouragement, to the academic and technical staff of the Chemistry Department of the University of Canterbury for their asistance, and to Mr A.J. M^{c}Kinley for many helpful discussions.

CONTENTS

ABSTRACT

ESR Spectroscopy has been used to study conformational interconversion and addivity relationships in a number of series of naphthalene derivatives. Oscillation of the alkyl rings in 1,2,3,6,7,8-hexahydropyrene ions, and the ions of the related 5, 6 and 7 membered ring compounds has been studied. The temperature dependance of the ESR spectra have been used to assign the coupling constants. The aromatic ring coupling constants in the asymmetric compounds have been assigned on the basis of an additivity relationship.

The ESR spectra of a number of methylnaphthalene anions have been recorded and analysed to give the coupling constants. Improved additivity relationships for both the proton and methyl coupling constants have been determined. The temperature dependence of the spectrum of 1,2,3,4-tetramethylnaphthalene has been analysed in terms of an interconversion between a tight and loose ion pair.

The ESR spectra of a number of methylnaphthalene cations have been generated using $AlCl_3/SO_2$ and their spectra recorded and analysed . For those methylnaphthalenes which did not have methyl substituents in the 1 and 4 or 1 and 5 positions, a series of compounds with g=2.008 were recorded. Evidence is presented to show that these compounds are methyl derivatives of naphtho[1,8-cd]-1,2-dithiole. An additivity relationship for the

proton coupling constants of these compounds has also been found. ESR spectra from the methylperylenes formed in the Scholl Condensation of the methylnaphthalene cations were also observed and analysed

Changes in the ESR spectra of 1,8-dimethylnaphthalene$^+$ and octamethylnaphthalene$^+$ were ascribed to the effect of hindered rotation of the methyl groups.

Coupling constants for the ESR spectra of tetracyclopentanaphthalene have been determined.

CHAPTER ONE

INTRODUCTION

Since the first observation of Electron Spin Resonance (ESR) by Zavoisky (44Zav) in 1944, this technique has been used to provide structural and other information on a wide variety of systems. One particular chemical problem on which ESR has shed considerable light, is the study of molecular motions particularly conformational interconversions. Investigations in this area are continued in this study. A second major objective was to study the quantitative relationships between the coupling constants of a structurally related series of compounds known as additivity relationships. These two aims required the analysis of a number of very complex ESR spectra. Because of the complexity of these spectra, the usual methods of analysis were unsatisfactory. It therefore became necessary to improve the available methods for analysing ESR spectra. These three areas, conformational interconversion, additivity relationships and analytical methods, form the basis of this study.

Improved methods of analysing ESR spectra are contained in chapter 2, which also contains details of the experimental method.

The conformational interconversion of different alkyl carbon rings of different lengths is discussed in chapters 3 and 6. The between a loose and tight ion pair is discussed in chapter 4. The hindered rotation of methyl groups is a third example of conformation interconversion and is discussed in Section 5.4.2

Additivity relationships are reviewed in Section 1.2 and examples occur in Chapters 3, 4, and 5.

Neither basic theory nor practice of ESR are discussed in this work, as both are discussed in a number of standard texts (72Wer, 67Car, 83Poo). Changes in the form of the ESR spectra of systems undergoing molecular motion of some form are discussed in Section 1.1 of this chapter. Section 1.2 contains an introduction and review of previous work in the area of additivity relationships, which relate the coupling constants of a structurally related series of compounds. Included are applications of this approach to a number of series of compounds, for which sufficient data is available for additivity relationships to be calculated, but for which no such calculation has been reported.

In the interests of clarity the reviews for the various, specific topics covered has been included at the beginning of the relevant chapters, i.e. chapter 3 begins with an introduction to and a review of previous work for peri alkyl substituted naphthalenes, chapter 4 contains introduction to and review of methylnaphthalene anions, and chapter 5 contains introduction to and review of methylnaphthalene cations.

Section 1.1

Linewidth Effects Resulting from Molecular Motions

The bulk magnetisation of a large assembly of spins, when a constant magnetic field is applied, is described by the Bloch Equations (46Blo, Eqn 1.1)

$$\frac{dM_x}{dt} = \omega_0 M_y - \frac{M_x}{T_2}$$

$$\frac{dM_y}{dt} = -\omega_0 M_x - \frac{M_y}{T_2} \qquad \text{Eqn 1.1}$$

$$\frac{dM_z}{dt} = -\frac{(M_z - M_0)}{T_1}$$

where M_x, M_y, M_z are the components of the bulk magnetic moment of the sample in the x, y, z, directions respectively. The static magnetic field is assumed to be applied parallel to the z axis, ω_0 is the frequency at which the spin vector precesses around the magnetic field (the Larmor Frequency), M_0 is the magnetic moment at equilibrium, T_1 is the spin-lattice relaxation time, and T_2 is the spin-spin relaxation time.

Integration of the Bloch Equations gives the lineshape of the transistions (lines) in an E.S.R Spectrum in the absence of any exchange processes. This is a Lorentzian curve as given in Eqn 1.2

$$g(\omega) = \frac{T_2}{\omega} \frac{1}{1 + T_2^2(\omega-\omega_0)^2} \qquad \text{Eqn 1.2}$$

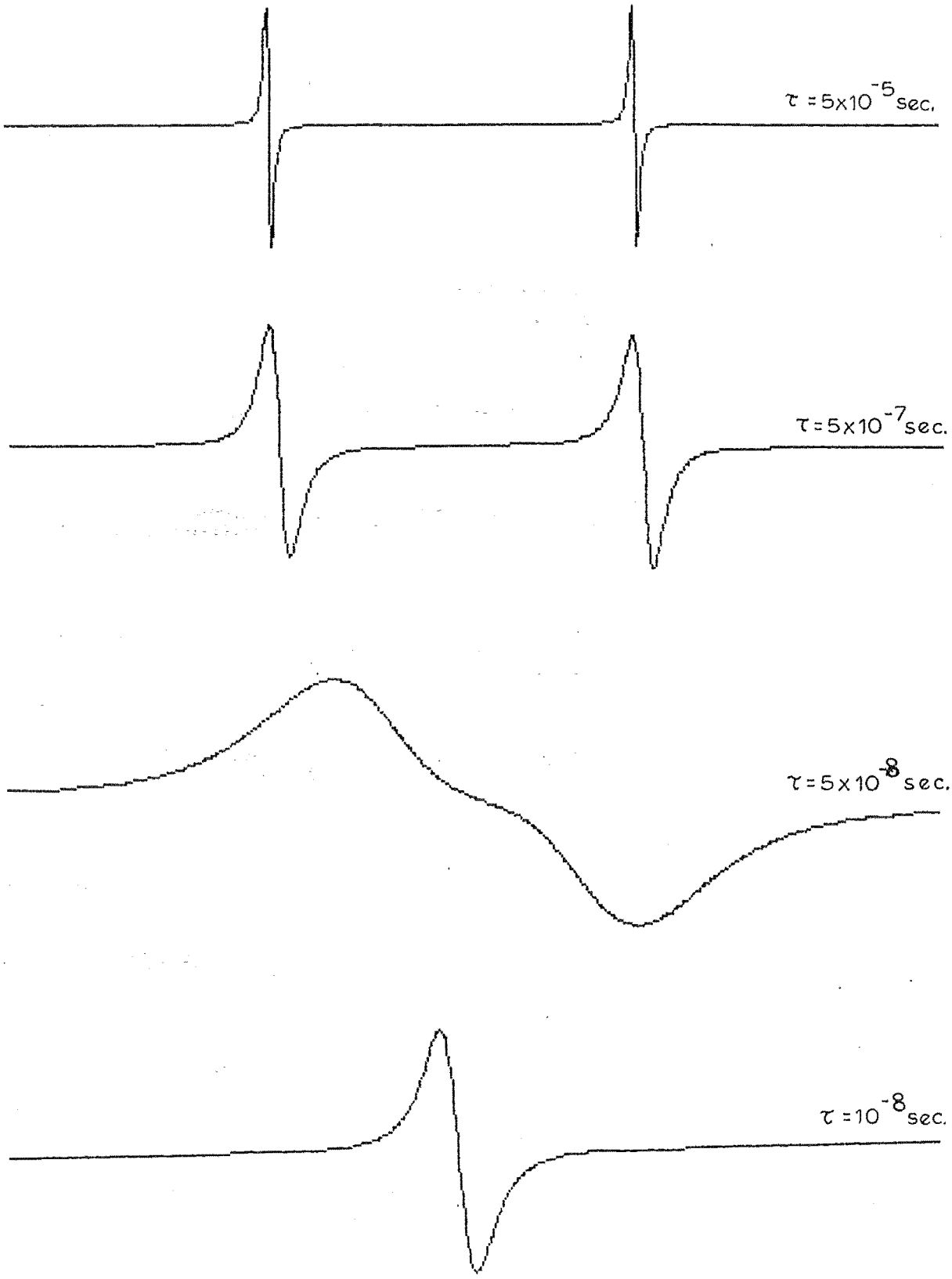

Figure 1.1 Simulated ESR Spectra for two Inconverting Species

where $g(\omega)$ is the microwave power absorbed at frequency ω and ω_0 is the resonant frequency.

Molecular processes which result in the exchange of magnetic nuclei between chemically non-equivalent sites will alter the lineshape, and position of lines in an E.S.R spectrum. By suitable modification of the Bloch Equations (53Gut), the form of the E.S.R spectrum can be calculated. Consider a process in which the average lifetime of the molecule in state A is τ_A and in state B is τ_B. For E.S.R it is required that the spin of the electron changes but that no nuclear spin changes state. For a spin state in state A with frequency $\omega_1+\delta\omega/2$ and corresponding spin state in state B of $\omega_1-\delta\omega/2$ the intensity of microwave absorption is given by Eqn 1.3

$$g(\omega)= \frac{\omega_0 M_0((1+\tau/T_2)P+QR)}{P^2+R^2} \qquad \text{Eqn 1.3}$$

where $P= \tau((1/T_2^{\,2})-(\Delta\omega)^2+(\delta\omega/2)^2)+1/T_2$

$Q= \tau(\Delta\omega-(\delta\omega/2)(p_A-p_B))$

$R= \Delta\omega(1+2\tau/T_2))+(\delta\omega/2)(p_A-p_B)$

$\Delta\omega= \omega-\omega_1$

$\tau=\tau_A\tau_B/(\tau_A+\tau_B)$ and p_A, p_B are the proportion of the total in each state.

For states of equal probability i.e. $p_A = p_B$ this yields the set of spectra in Fig. 1.1

When considering E.S.R spectra as a whole rather than individual transitions, there are two types of modulation (70Sul). In-phase modulation is defined as a modulation or motion which causes hyperfine splittings to increase or decrease in

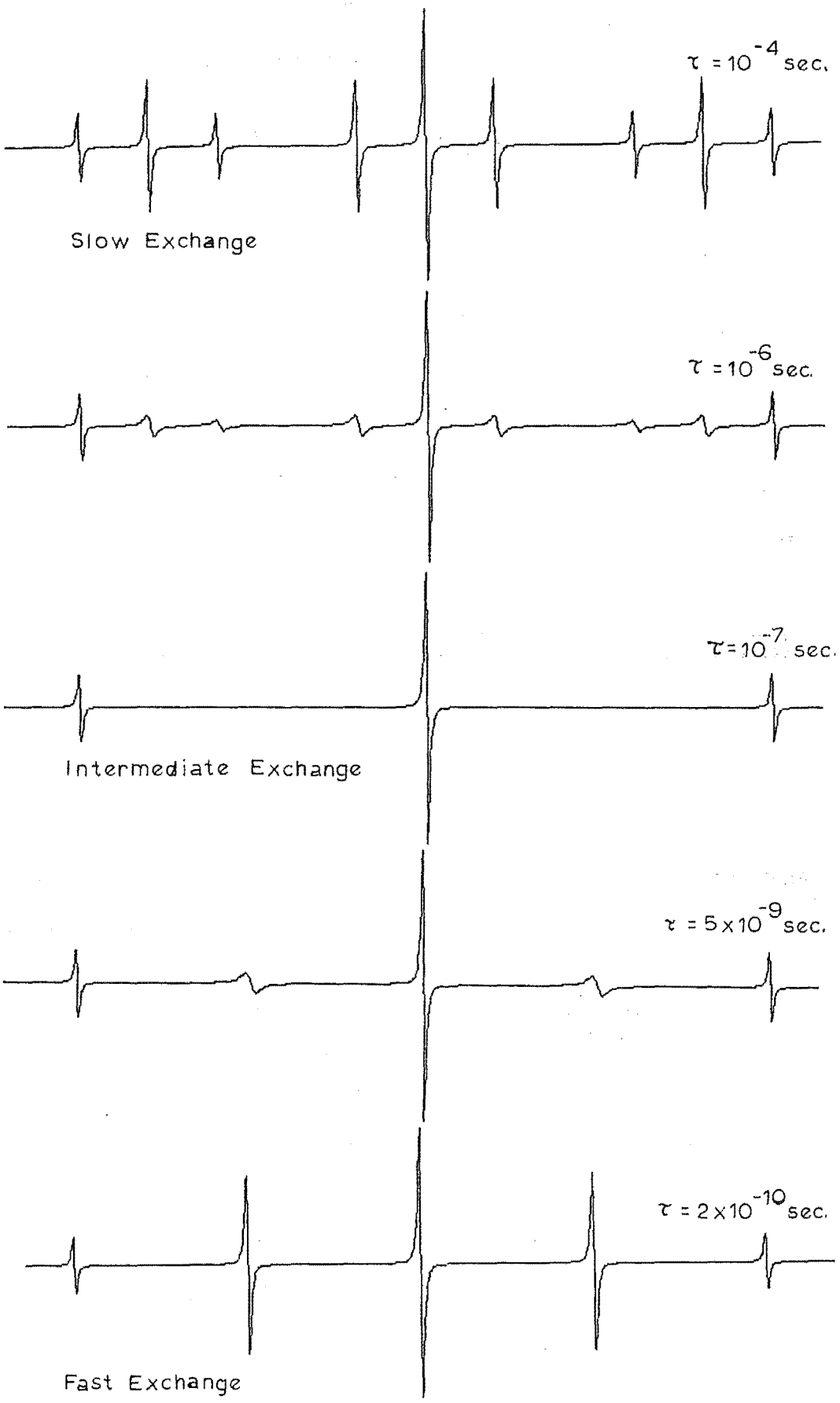

Figure 1.2 Alternating Linewidth Effect in ESR Spectra

unison. For out-of-phase modulation a pair of hyperfine splittings is exactly out of phase i.e. one decreases when the other increases. A special case of out-of-phase modulation occurs when the change in a pair of hyperfine splittings is equal and opposite. This leads to what is known as the alternating linewidth effect where alternate groups of lines are unchanged, and broadened. The broadened groups of lines can disappear altogether. Consider a system with two, non-equivalent hydrogen doublets, undergoing an out-of-phase modulation in which the two doublets are interchanged. The spectra over a range of rates of exchange is shown in Fig. 1.2. At intermediate rates of exchange alternate lines remain sharp. These are lines produced by transitions for which the value of M_I, the total spin, is the same for both doublets. The ratio of the heights of the these lines is 1:4:1.

The number of states in a system is normally described by the number of 'jumps' e.g. a system with two different states would be fitted by a 'two jump model', similarly a system with four non-equivalent states would be fitted by a 'four jump model' even though the number of exchange processes that would need to be considered is actually 6. A quick method of determining if a two jump or four jump model is required, for systems in which either model might be valid, is by an analysis of the amplitudes of the sharp lines at intermediate exchange. For example, in hexahydropyrene anion (see Fig. 3.1 V and Fig. 3.3) the eight β hydrogens can interconvert either by a two jump model, in which all eight hydrogens change coupling constants at once, or by a four jump model in which only four hydrogens change coupling

constants at once. The two jump model predicts that the amplitudes at intermediate exchange are 1:16:32:16:1 whereas the four jump model predicts that the amplitudes are 1:8:18:8:1.

Another approach used to analyse the ESR spectra of compounds undergoing conformational interconversion is the relaxation method of Freed and Fraenkel (63Fre). Since this method applies only to the fast-exchange region it can not be used to describe a number of the compounds covered in this study and will not be discussed further.

Section 1.2

Introduction and Review of Additivity Relationships

It has long been recognised (59Ven) that the effect of introducing two or more identical, substituents into an aromatic system on the coupling constants of that aromatic system can be accurately estimated from the sum of the effects of substituents individually. That is, if the coupling constant of a nucleus at position A is A, and substitution at positions B and C gives coupling constants $A+A_B$ and $A+A_C$ respectively, then the coupling constant at position A for substitution at <u>both</u> B and C will be $A+A_B+A_C$. This relationship is known as an additivity relationship, and can be theoretically justified on the basis of Perturbation Theory. It should be noted that in symmetric substrates the following convention will be used; if the coupling constant at some arbitrary position X is being evaluated, then

the molecule is reoriented so that X is transformed into the lowest possible position. e.g. for the hydrogen coupling constant for position 7 in 2,3-DMN (see Fig. 4.1) the molecule is reoriented so that the 7 position is transformed to the 2 position and the two methyl groups are at positions 6 and 7. The coupling constant for this hydrogen will then be $B+B_F+B_G$. Throughout this work the nomenclature that will be used is as above. Where other authors have used a different nomenclature this will also be given.

Such an additivity relationship was first applied by Venkataraman et al for methyl and chloro substitution in semiquinones radicals (59Ven) and extended to cover t-butyl, thiobenzyl and thiophenyl substitution in semiquinones (74Ped). Barton and Fraenkel (64Bar) developed such a relationship to describe methyl substitution in pyrazine cations. As did Cavalieri et al. (71Cav) to assign coupling constants in a range of diazine and naphthyridine anions, indicating that such additivity relationships hold for quite large perturbations. There have also been reports of additivity relationships for deutero substituted naphthalenes (67Law), methyl substituted naphthalenes (69Mos, 75Kir) and t-butyl substituted naphthalenes (77Gol). Huffadine, Peake and Deady (75Huf) used such a relationship to assign the coupling constants of t-butylacenaphthene anions.

In order to evaluate the accuracy of the additivity relationship a number of other series of compounds were investigated. These were series for which sufficient data had been published, but for which no determination of the additivity

relationships had been reported. A standard linear least squares regression program was used (program REGRES in 69Bev).

Using least squares refinement, a fit of the additivity relationship to Lawler and Fraenkel's data for deutero substituted benzene anions (68Law) gave a set of parameters which predicted coupling constants that differed by less than 20mG from the experimental results. The full least squares analysis is given in Appendix 1.1, Table A.

Similar analysis of methyl substituted biphenyl anions did not give such good results, with a difference of 220mG between experimental and calculated coupling constants being found. This is despite the neglect of 2,4,6-trimethylbiphenyl for which the fit was so poor that doubt must be expressed as to the correctness of the fitting of the ESR spectrum (65Ish). It is noteable that for the later ENDOR results (73Chr) the difference between the coupling constants calculated on the basis of the additivity relationship and those found experimentally is much smaller than for the earlier ESR results. It therefore appears that the poor agreement between the additivity relationship and the experimental data is the result of poor data rather than any fault in the additivity relationship. There is also doubt about one of the assignments. Ishizu (77Ish) assigns the value of 2.71G to the 2' position in 3-methylbiphenyl and 2.43G to the 6 position whereas the additivity relationship would predict the reverse assignment. The full least squares analysis of the data for the methyl substituted biphenyls is given in Appendix 1.1 Tables B, C, D and E.

Other systems investigated were the methyl substituted benzene anions (72Bal, 73Jon, 75Rou, 75Nel, 77Jon), and the cyano substituted benzene anions (63Rei) (Appendix 1.1 Tables F and G respectively). In the former differences between experiment and calculated coupling constants of 280mG were observed and in the later 1.63G. The deviations in the methyl substituted benzenes appear to be due to poor data, but those in the cyano substituted benzenes could well be due to a break-down in the assumption that substitution is a small perturbation.

Examination of the t-butyl substituted acenaphthenes anions reported by Huffadine, Peake and Deady indicated that incorrect assignments had been made. A least squares refinement of the additivity relationship for these compounds using these authors assignments gave a standard deviation of 400mG, reassigning the coupling constants gave a standard deviation of 0.071mG. This analysis supports Nelsen and Gillespies assignments of the α coupling constants in pleiadane, and the assignments of the α coupling constants in acenaphthene and phenalene which had been based on MO calculations. (see Section 3.3.1 for further details) The complete least squares analysis of the t-butyl substituted acenaphthenes is given in Appendix 1.1 Tables H and I.

It is clear from the above that, for alkyl-substitued aromatics at least, the deviations from the additivity relationships are more likely to be due to experimental error than to a break-down in the relationships themselves.

CHAPTER TWO

EXPERIMENTAL

This chapter covers the details of the experimental method used. Section 2.1 deals with the ESR Spectrometer and accessories. Section 2.2 covers the sources and purity of the chemicals used and the details of sample preparation. Section 2.3 covers the hardware portion of the computing interfacing done in the course of this work, i.e. equipment purchased, built and interfaced. Section 2.4 covers the software, i.e. programs written. Neither section is comprehensive in coverage, since thoroughness in covering the technical details is not required to appreciate the accuracy of the results. Sufficient detail has been given to illustrate the interplay between hardware and software, the accuracy and quality of the results obtained, and the ease, (or otherwise) with which those results were obtained. Further technical details are given in the Appendices to this chapter, and in the documentation kept with the equipment. Computer applications to ESR have been reviewed recently (81Van) and, because of limited relevance, will not be discussed further.

Section 2.1

E-12 ESR Spectrometer and Accessories.

The ESR spectra were recorded on a Varian E12 spectrometer using an E-112, Century series high frequency amplifier module. The frequency was measured using a Systron Donner Model 6016 Frequency Counter. Magnetic field measurements were made using a Micro-now Instrument Co., Model 515 NMR Gaussmeter. The cavity used was a Varian E231, TE_{102} rectangular cavity fitted with a Varian V4557 temperature controller. The sample temperature was measured using a chromel-alumel thermocouple connected to a calibrated digital volt meter. The thermocouple was calibrated using the freezing points of water, carbontetrachloride, chlorobenzene, chloroform, ethylacetate, and toulene. The temperature was found to be constant to within $3^{0}C$ over a scan. The coolant used for the temperature controller was compressed air at 40psi. The air was dryed using zeolite and silica gel columns. The columns themselves were vacuum dried at $180^{0}C$. Surges in the air flow were found to cause changes in the microwave frequency equivalent to 0.1 Gauss. The incidence of surging could be substantially reduced by putting liquid-air in the dewar some hours prior to using the spectrometer, and ensuring that there was always some liquid air in the dewar.

Section 2.2
Chemicals and Sample Preparation

Section 2.2.1 Chemicals

1,2-dimethoxyethane (DME) : BDH

tetrahydrofuran (THF) : Fluka Purum

2-methyltetrahydrofuran (MTHF) : Eastman Organic Chemicals White Label

diethylether (DEE) : Riedel-de Haen

dichloromethane : Hoechst

perylene : Koch Light Laboratories Ltd.

naphthalene : BDH

1,6-; 2,3-; 2,6-dimethylnaphthalene (DMN) : L. Light and Co. Ltd.

1,4-; 1,3-; 1,5-DMN : Fluka Co.

2,7-; 1,2DMN : K and K Laboratories.

1,7-DMN : prepared by R.F.C. Claridge and D.A.R. Happer from a succinic acid condensation and subsequent methylation.(33DeB)

1,8-DMN : prepared by S. Blackstock from the reduction of naphthalic anhydride. (62Mit)

1,2,3,4- and 1,3,5,7-tetramethylnaphthalene (TMN) : supplied by B.M. Peake, prepared according to Canonne and Renault (67Can)

1,2,3,4,5-pentamethylnaphthalene : supplied by B.M. Peake

1,2,3,4,5,8-hexamethylnaphthalene : supplied by B.M. Peake, prepared according to Oku et al (67Oku)

octamethylnaphthalene : supplied by B.M. Peake, prepared according to Oku et al (67Oku)

tetracyclopentanaphthalene : prepared by R.P. Thummel and T. Fuchigami (81Thu)

1,2,5,6,7,8-hexahydro-cyclohepta[fg]acenaphthylene : prepared by D.R.A. Leonard and A. Fischer (71Fis)

1,2,3,6,7,8-hexahydropyrene : K and K Laboratories.

2,3,6,7,8,9-hexahydro-1H-cyclohepta[cd]phenalene : prepared by D.R.A. Leonard (71Fis)

1,2,3,4,7,8,9,10-octahydro-dicyclohepta[de,ij]naphthalene : prepared by D.R.A. Leonard (70Fis)

2,8- and 3,9-dimethylperylene : supplied by B.M. Peake, prepared according to Anderson et al (60And)

aluminium trichloride : Riedel-de Haen

potassium : BDH

sodium : BDH

sulphur dioxide : BDH

The solvents were purified by standard methods,(64Bol, 71Pea). Sulphur dioxide was distilled directly onto the vacuum line without purification. A check on the purity of the sulphur dioxide with a mass-spectrometer, showed no mass peak larger than 1% of the parent ion. All other materials were used without further purification.

Section 2.2.2 Sample Preparation

The preparation of the anion samples was similar to the standard methods (64Bol, 71Pea), purified sodium and potassium mirrors were formed by distilling the metal three times.

The cation samples were prepared using aluminium trichloride with sulphur dioxide in dichloromethane. The sample tube used for preparing cation samples was substantially the same as that used for anion samples.(see 71Pea for details) Three pairs of constrictions were made in the side arm, a small wad of glass-wool was placed between the two constrictions of each pair. Aluminium trichloride was placed at the open end of the side arm, which was then sealed. The aluminium trichloride was sublimed along the side arm by heating the side arm with a flame. As the aluminium trichloride sublimed through each wad of glass-wool, the redundant section of the side arm was cut off. The glass-wool was found to be necessary to prevent the aluminium trichloride bumping from one end of the side arm to the other. This triple sublimation of the aluminium trichloride was found to substantially improve the quality of the samples prepared.

Section 2.3
The Computer to ESR Spectrometer Interface

Section 2.3.1 The SBC-100 Microcomputer and Existing Interfacing

The computer used for data collection and analysis was an SD Systems SBC-100 microcomputer purchased from Microprocessor Developments Ltd of Auckland. The microcomputer consisted of a nine slot Wameco "Little Mother" S-100 mother board. Into the mother board were slotted an SBC-100 CPU Board, an EXPANDORAM memory expansion board, a VERSAFLOPPY disk controller, a Vector Graphics Analog to Digital Conversion Board, a Jade Computer Products I/O Board and four other boards built subsequent to the purchase of the microcomputer.

The SBC-100 CPU Board consisted of a Z80A microprocessor (CPU) chip, 1024 bytes RAM, 2048 bytes of EPROM, a serial port, a parallel port, a four channel counter/timer, a non-maskable interrupt and four maskable, vectored interrupt inputs. The serial port can accept either RS-232 or 20mA and was used to drive the operator's terminal. The EPROM contained a simple monitor and the programs required to load and start the operating system supplied with the machine. The counter/timer circuit allowed the CPU to be performing one operation and then, at preprogramed times, to interrupt this operation to perform some other, second operation. On completion of this second operation the CPU would return to the first operation. Alternately the counter/timer circuit could be used to provide accurately known time intervals or to measure the time between events. The

maskable, vectored interrupts allowed the operation of the CPU to be interrupted by some external event. The parallel port was connected to an interface which controls the ESR Spectrometer. This interface (the design is given in Appendix 2.1) was built by Mr J. Sheriff of this department in conjunction with Mr A. Alloway, to a design produced by the author and Mr Sheriff prior to commencement of this project. The interface allowed the computer to step the plotter one step at a time in either direction, return the plotter to either the left or right margin, and allow the Y-axis input of the plotter to come from either the ESR Spectrometer or the Computer. Since the magnetic field was set by the position of the plotter this effectively allowed the computer to scan the magnetic field within the limits set on the ESR Spectrometer console. There were also a set of manual switches which allowed control of either plotter axis to be given to the computer.

The VERSAFLOPPY disk controller board controlled two 8 inch Shugart, single sided, single density, floppy disk drives. The data was tranferred between the floppy disk and the computer's memory by Direct Memory Access (DMA), which gave extremely rapid data access. (ca. 4 microseconds per byte)

The EXPANDORAM was fully populated, therefore 64K bytes were available to the operating system. When the operating system was in place only 48K bytes were available to the user.

The Jade I/O board had one parallel and two serial ports.These ports were used to interface to a variety of printers and other accessories.

The Vector Graphics Analog to Digital Conversion Board, which converted the ESR signal into a form that the computer can manipulate, will be dealt with in Section 2.3.2.

The operating system provided was CP/M. The original version purchased was 1.4, (version 2.2 became available and was used from 1981 onwards). CP/M came with a debugger (DDT and later ZSID), an editor (ED), an assembler (ASM and ZASM) and a loader (LOAD), Microsoft FORTRAN-80 was also provided. Later the M-80 macro-assembler was acquired. Apart from these programs, there were also the usual utilities, plus three different versions of BASIC. No further mention will be made in this section of any hardware or software, any further details will be given as required in the various sections, and in Appendices 2.1, 2.2, 2.3, 2.4, and 2.5.

Section 2.3.2 Analog to Digital Conversion Board to Spectrometer Interface

The Analog to Digital Conversion board purchased from Vector Graphics, consisted of two 12 bit Digital to Analog Converters (DACs) and a set of 8 precision comparators. The DACs converted a 12-bit digital number, in the range 0 to 4096 (or in the more usual, hexadecimal form, 0 to 0FFFH), into an analog output that varied over 4096 discrete voltage levels. The comparators compared two voltages and gave a signal indicating which of the two voltages was higher.

The method used by this board to convert an analog signal to a digital signal was successive approximation, otherwise known as

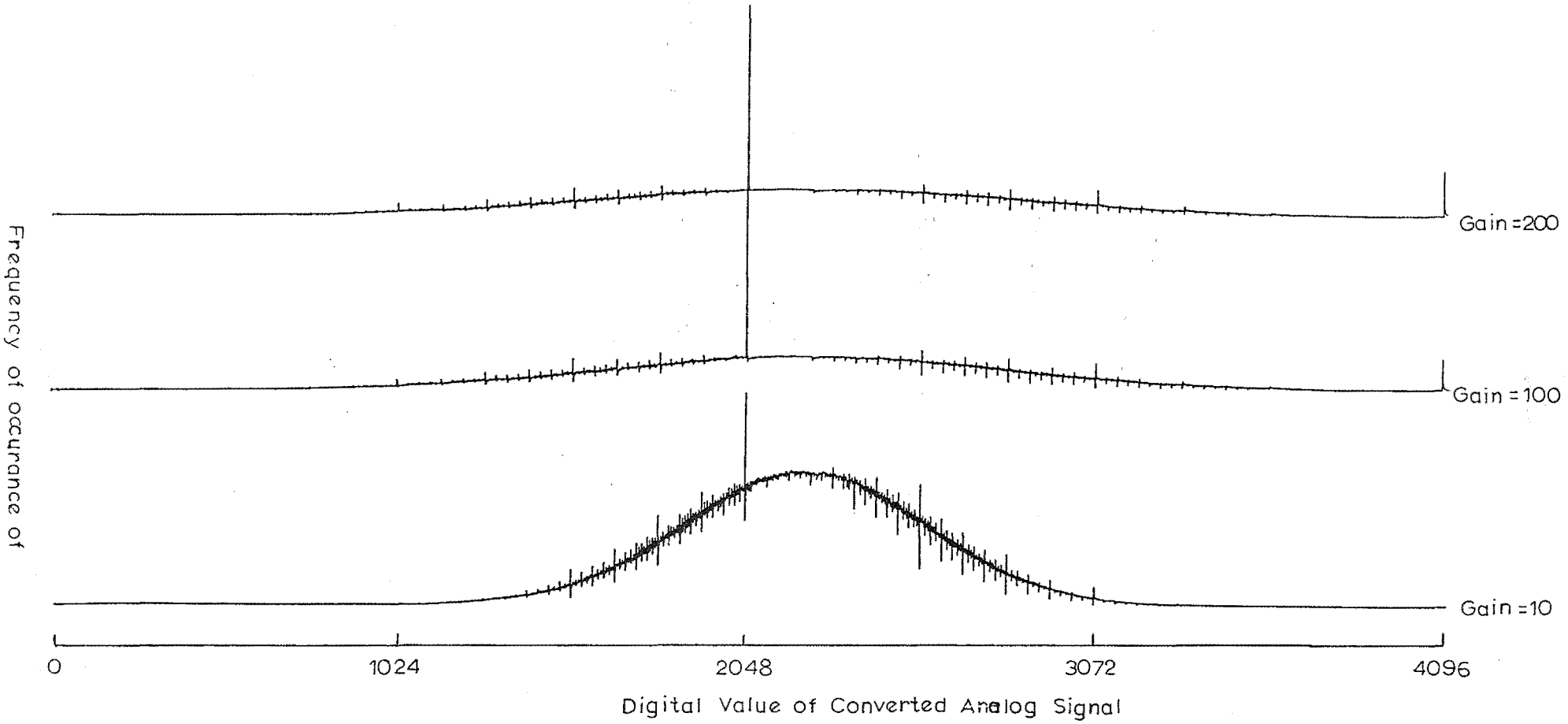

Figure 2.1 Digital Signal Histogram

a logrithmic search, as the number of approximations required is equal to $\log_2$ of the range of the input value. The analog to digital (A to D) conversion is done by the CPU and is therefore very slow, requiring 0.36 millseconds per conversion. Giving a conversion rate of 3Hz. Conversion rates of 100KHz are more usual in this type of application.

When the board was tested, it was found that the response of the A to D converter was not linear. The result of this test is shown in Fig. 2.1, which is a set of three histograms of the frequency with which a given digital value is produced, versus the digital value. For an ideal, noiseless signal only one digital value would result. The effect of noise is to broaden the histogram so that digital values above and below the ideal (average) digital value are also recorded. The histogram should then show a gaussian (normal) distribution. In Fig. 2.1 the three histograms are recorded at three different noise levels and do show the expected gaussian characteristics. However there are a number of sharp spikes present. These spikes result from a failure of the sample and hold circuit.

The role of the sample and hold circuit is to hold the analog signal received by the A to D at a constant value while an A to D conversion is taking place. If the value of the signal received by the A to D changes in the middle of an A to D conversion then the result is as shown in Fig. 2.1, i.e. digital values in which the least significant bits are all 0 or all 1 are more probable than those with mixtures of the two. Tests showed that the sample and hold circuit could not be significantly improved, and that the fault lay in the slowness of the A to D

conversion as compared to the very fast fluctuations that occur in the analog signal. Further tests showed that so long as a large number of A to D conversions were made for each value of the magnetic field, the average digital value determined was very close to the correct value.

Section 2.3.3 Microwave Corrections

In the course of the project, it became necessary to accurately fit calculated spectra to experimental spectra. For simple spectra of three or four coupling constants, this proved relatively simple. However, for more complicated spectra of seven and eight coupling constants, or worse still two species, it proved very difficult to accurately fit the calculated to the experimental spectra over the complete range of the spectra. The best that could be managed was to get the 'shape' of the calculated spectra right, and to apply a 'sliding factor' to make the calculated and experimental spectra agree. For the more complicated compounds, especially the peri-alkyl substituted naphthalenes (see Chapter 3) this approach proved unsatisfactory. The outer most lines could be fitted accurately, but as further coupling constants were added, the discrepencies would accumulate. By the time the last coupling constants had been added, the differences between the experimental and calculated spectra were so large as to cast doubt on the correctness of the solution.

The first approach taken to correct this problem was to use least squares fitting of the line positions, as will be described

in Section 2.4.4. This approach did produce better fits of calculated to experimental spectra. However the improvement was not sufficient to yield satisfactory fits of the calculated to the experimental spectra. In the course of this least squares analysis, suspicions arose as to the stablitiy of the microwave frequency. Subsequent experiments showed that changes in the microwave frequency across a scan could produce apparent movements of 200 mGauss in the positions of lines.

The optimum solution to this problem of microwave drift would have been the purchase of a field frequency lock (65Hyd), however the price of such an accessory was prohibitively high. The approach decided on was to use the computer to read the microwave frequency from the Systron Donner Model 6016 Frequency Counter attached to the Spectrometer. This counter had a TTL compatible input/output port, which made available, in digital form, the output of the counter. There was also a number of control lines available which allowed the attenuation, and ranges to be set by the computer. A design for the board was produced (see Appendix 2.2), and a wirewrap prototype was constructed by the author.

During testing it was found that proper earthing was essential. Absence of a good earth resulted in the value of the counter being misread, leading to erroneous microwave values. The error could be as much as 1 GHz, i.e. 350 Gauss. Even with satisfactory earthing, an incorrect reading might occur once or twice within a 12 hour period. This problem was circumvented by programing the computer to check any suspicious microwave readings. This will be discussed further in Section 2.4.1

The details of the algorithm used to correct for microwave frequency drift will be given in Section 2.4.1. The correctness of this algorithm and of the application of this algorithm was tested by visually comparing a series of repeated scans. All scans were collected under the same conditions. (In this study a collected spectrum will be one converted by the A to D converter and stored on disk, a recorded spectrum will be one plotted directly onto paper.) The comparison indicated that those collected spectra for which the microwave correction had been made showed less variation in line position than those for which no microwave correction had been made. However, there were still some variations in the precise positions of the lines, even in the set for which corrections had been made for the changes in microwave frequency. When the full least squares regression analysis became available (see Section 2.4.4), it became clear that there were still considerable errors present in the positions of the lines in the ESR spectra, even when changes in the microwave frequency had been accounted for. From the difference between the positions of the lines in the experimental spectra and calculated spectra the residual error was estimated to be as much as 100 mGauss for a 20G scan.

Section 2.3.4 Magnetic Field and Plotter Linearisation

The linearity of the magnetic field as a function of the position of the plotter was checked by collecting a series of spectra from the perylene anion, and moving the centre of the spectra between each successive scan. This test showed clearly

that the function relating the magnetic field to the position of the plotter was not linear, varying by as much as 1% from linearity. Program MAGLIN was written to accurately determine the relationship between position and magnetic field using the NMR Gaussmeter. Tests showed that, because of play in the drive mechanism it was necessary to scan the plotter in one direction only. MAGLIN was used to find the exact value of the magnetic field as a function of plotter position for all the scan ranges used in this study i.e 10G, 20G, 40G and 100G scan ranges. The difference between the magnetic field measured at each 100 step interval and the least squares fitted best line was used as a rough correction co-efficient, to correct for the non-linearities in the magnetic field.

The nonlinearity of the plotter itself was measured by plotting a series of lines at 100 step intervals across a page and then using a travelling microscope to accurately measure the distance between the lines. The largest difference found between the measured position and the least squares regression line was 0.5mm

The corrections for the nonlinearities, in the magnetic field as a function of plotter position and in the physical position of the plotter, were incorporated in programs COLLECT and GRAPH. After the drive belt was replaced, MAGLIN was again used to measure the linearity of the magnetic field, and it quickly became clear that the linearity of the relationship between magnetic field and position changed considerably as the belt aged. The determination of the non-linearities is a time consuming task, which needs to be done regularly. In view of the

small error introduced, there are few applications which would justify this correction being made.

Section 2.3.5 Determination of g-values

The method used in this study to determine the g-value of a compound was to use a sample of the perylene anion, standardise the NMR Gaussmeter against this, and then measure the g of the unknown relative to the NMR Gaussmeter. In practice this involved collecting a spectrum of perylene with a series of markers on it. The markers were generated using the pushbutton connected to the computers interrupt line. When the NMR Gaussmeter was reading correctly, the pushbutton was pressed, causing the computer to interrupt the data collection, switch the frequency counter onto the MHz frequency range and read the frequency of the NMR Gaussmeter. The position of the plotter (in steps from the left hand margin) and the NMR frequency were then output to the console. The computer also put a mark in the output file. When the file was plotted back, this mark showed as a discontinuity, i.e., as a sharp downward spike in the plot. Program ESRCON (section 2.4.4) was then used to fit the calculated spectrum to the experimental perylene spectrum. This program also determined the position of the centre of the spectrum (in steps from the left hand margin). The offset for the Gaussmeter was then determined from Eqn. 2.1

$$\text{Offset} = \frac{h\nu}{g\beta} - (P_C - P_M)*SR - \frac{h\nu_P}{g_P\beta_P} \qquad \text{Eqn. 2.1}$$

Where P_C is the position of the centre of the perylene spectrum, P_M is the position of the marker (both in plotter steps), SR is the scan range (in Gauss per plotter step), ν_P is the frequency of the Gaussmeter. Using a similar equation the g-value of the unknown was determined. The errors in the g-value came primarily from the uncertainty in the determination of the centre of the spectra and from uncertainties in the measurement of the NMR frequency. The uncertainties in determining the centres of the spectra should have totalled less than 3 plotter steps, i.e. 12mGauss, and the uncertainties in the measurement of the NMR frequencies approximately 20mGauss. This gave a total error of 30mG and a g-value with an error of $\pm$0.00002

A set of measurements made on the perylene anion, at the same conditions, indicated that this estimate of the accuracy of the g-value determination was somewhat in error. The set consisted of five measurements on perylene$^-$/Na$^+$/DME and five on perylene$^-$/K$^+$/DME. The scatter in the offsets determined was 300mG, giving the error for the g-value determination as $\pm$0.0002. It is this latter estimate of error that will be quoted in this study. There are two likely reasons for the inaccuracy of the g-value determination. First; the sample tubes were not sitting in the same position in the cavity, and are therefore not experiencing the same magnetic field. Second; the determination of the centre of a spectrum was not accurate to 1 plotter step.

During the course of the project, a surplus Varian Associates A-60 NMR Spectrometer, became available. At about this time also, the work load of the ESR Spectrometer was such as to limit the amount of time available to plot out the simulated spectra. An interface between the computer and the A-60 was therefore built to allow the computer to control the plotter component of the A-60 Spectrometer.

Section 2.4
Data Collection and Analysis Programs

Section 2.4.1 Data Collection Program : COLLECT

Program COLLECT was written to collect an ESR spectrum from the E-12 Spectrometer and store the spectrum in a retrievable form on a disk file. COLLECT is written in a mixture of Z-80 assembler code and FORTRAN-80. The object code produced by the Z-80 assembler is not compatible with LINK, the linker used. This means that the machine instructions required to call the assembly language subroutines need to be inserted by the programmer using ZSID. Ideally the assembly language section would have been written/rewritten in a format compatible with the M80 macroassembler. In this form the L80 linker could link the assembly language section directly to the FORTRAN section, thereby saving any human intervention. However, the time involved in the conversion of format far out-weighs the benefits.

COLLECT has a number of modes of operation and a variety of options. (see Appendix 2.5, Section 1 for an example of the input and output of this program)

The file format used is a mixture of ASCII and core image. The file header, which is in ASCII, contains all the relevant information about the file . The file header can be examined directly by the operator using the CP/M TYPE command. Details of the format of the file header can be found in Appendix 2.3

The flow chart, which describes the algorithim used to correct for changes in the microwave frequency, is given in

Figure 2.2 Flow Diagram for Algorithm to Correct for Microwave Drift

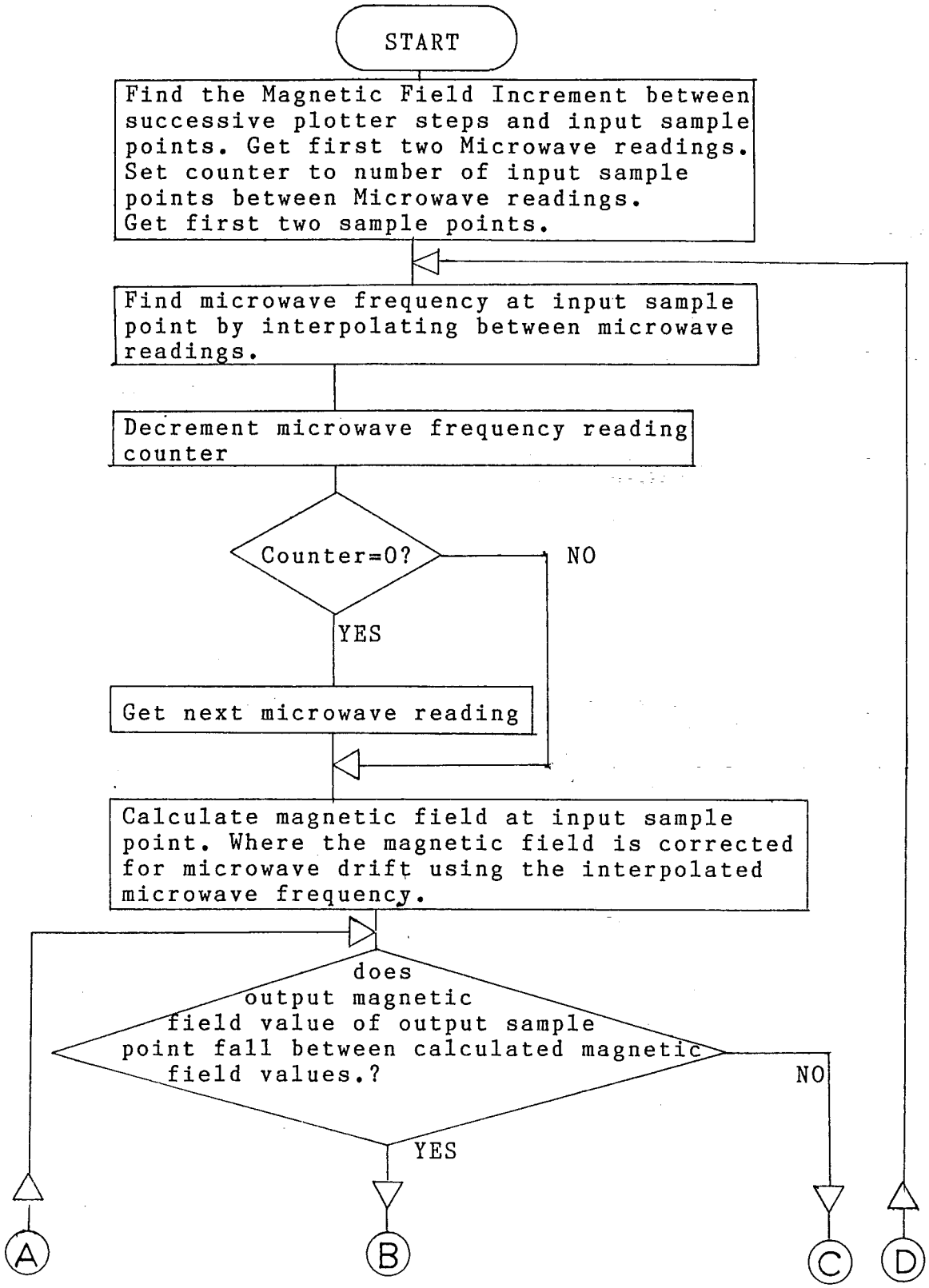

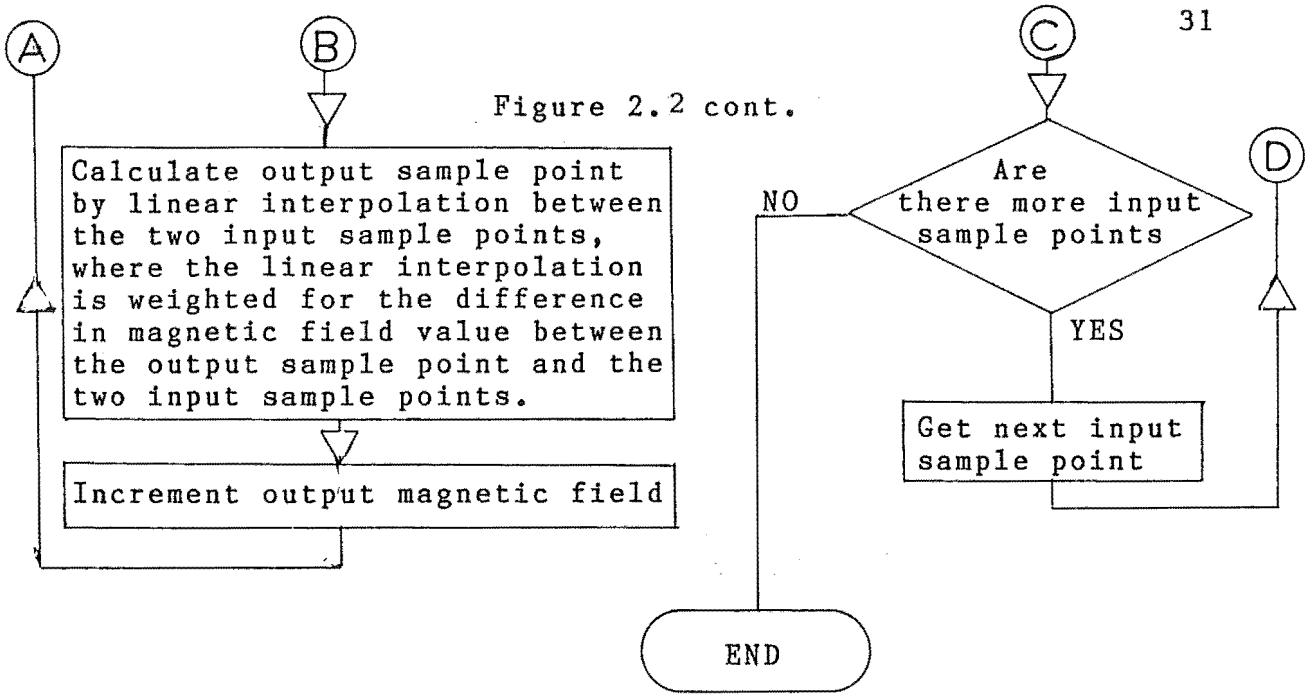

Fig. 2.2. The method used is that of linear interpolation between data points. The microwave frequency at each data point is calculated by linearly interpolating between successive microwave frequency readings. The value of the ESR signal at each successive output data point is then calculated by linearly interpolating between the input data points.

Generally when COLLECT is being used, the time constant would be one or two settings lower than when a normal scan of similar scan time is being recorded. This is by way of insurance against loss of resolution resulting from having the time constant set too high. Since only one amplitude is output at each channel by COLLECT, any noise present will automatically be averaged. It is important also that the oscilloscope modulation be turned off. If not, the spectrum collected will have an effective 5 or 10 Gauss modulation instead of the more usual 0.005 Gauss modulation.

Section 2.4.2 Spectrum Simulation

Simulation of first and second order, solution spectra is carried out using a set of five programs. These are programs STICK, SORT, LINESHA, GRAPH and LNLOAD. All five programs are written in FORTRAN-80 and accept input from the terminal. Details of operation etc., are given in Appendices 2.4 and 2.5. Data is transferred between the various programs via disk files. Details of the file formats are given in Appendix 2.3. The simulation programs use a number of temporary files, which are closed and renamed when control is passed from one program to another. This transfer of control is done automatically, once the operator has told the program running what the next program to load is.

(1) STICK, this program accepts input from the console to generate a Stick file. STICK will also accept Stick output files as an input file and generate further Stick files. STICK can calculate the second order perturbation for nuclei of spin 1/2. Any number of coupling constants can be entered.

(2) SORT, sorts the Stick files produced by STICK into ascending order. Files with less than 1900 lines can be handled internally using the sorting routine of Peake (71Pea). Files larger than this are sorted by splitting them into groups of 1900 lines, transferring the groups into two files and then doing a merge sort between the two files.

(3) LINESHA, produces a Lineshape file from a sorted Stick file. The spectrum generated can be a gaussian or lorentzian, absorption, first or second derivative curve of either phase. The usual algorithm is used, i.e. the required lineshape is generated

and stored in an array, from which it is read for each line of the spectrum. This algorithm therefore includes an implicit rounding of the coupling constant to the difference in Gauss between successive steps on the plotter.

(4) GRAPH, plots the output files produced by COLLECT and LINESHA on either the spectrometer plotter or the A-60 plotter. A number of plotting options are available, which give considerable control over the scale of both axes and the position of the plot produced.

(5) LNLOAD, is a file manipulation program. LNLOAD will add or subtract any two Stick or two Lineshape/Collect files, with offsets along both axes and variable weighting being provided.

Section 2.4.3 Data Transfer Programs.

A large number of systems studied did not yield satisfactory fits of calculated to experimental spectra, when simulation methods using visual comparison of the experimental and simulated spectra were used. For this reason the least squares regression programs of section 2.4.4 were produced. These programs run on the mainframe computers operated by the Computer Centre of the University of Canterbury, and require the collected data to be available to the Burroughs 6920 or Prime 750 mainframe computers.

A modified version of GRAPH was used to output a file to 8-inch floppy disk. This disk file contained all the points of the spectrum in ASCII form, with the points being separated by a carriage return and linefeed. From there a number of different

methods were used to get the data onto the target mainframe computer. The method finally used was to take the ASCII files to the SBC-100 machine in the Computer Science Department of the University of Canterbury. The disk would then be read by the SBC-100 and transferred to the Data General Eclipse machine via a direct line. A modified version of program PIP (provided with the CP/M operating system) was written to do this data transfer. The program to allow input of the files onto the Eclipse was the standard RDOS program XFER, using the /A option. From the Eclipse the data was written onto 9-track magnetic tape, and this tape could be read directly onto the Prime 750 using the Prime utility program MAGNET. Once on the Prime 750, the files were transformed into a useful form using progam TRANSLATE. TRANSLATE was a slightly modified version of a program written by Mr G. Davies of the Computer Science Department, whose assistance is gratefully acknowledged.

Section 2.4.4 Least Squares Regression Analysis

When it became apparent that simple simulation methods would not give adequate agreement between calculated and experimental ESR spectra, it was decided to produce a program that would find the best fit of the coupling constants to the position of the lines in the ESR spectra (64Bol). Best fit is here used in the sense that the sum of the squares of the differences between the calculated and experimental positions of the lines in a spectrum is a minimum. The program ORGLS (Oak Ridge General Least Squares) was acquired, and modified to

calculate the positions of the lines generated by a given set of coupling constants. This modification would also deal with coupling constants large enough to require a second order approximation to be used. The program runs on the Prime 750 under the name PORGLS. The physical distance between the centre of each line and a fixed point was measured. Fits obtained for hexahydropyrene (see Section 3.2.1) gave coupling constants with standard deviations of 0.0007Gauss.

The use of least squares fitting of line position suffers from the limitation that the position of many lines in complex spectra can not be accurately determined because of overlap. In some spectra this overlap is so great that the position of only a handful of lines might be able to be determined, whereas there may be as many as 6000 lines in the entire spectrum. One way to overcome this is to use least squares regression analysis on all the points in a spectrum. A program to do this was produced by modifying a program by J. Heinzer and acquired from the Quantum Chemistry Programs Exchange (program Number 197, 'ESRCON'). The details of the modifications made are given in Appendix 2.6

Section 2.4.5 Fitting Technique.

In this study the series of steps taken to find the best fit to the ESR of a given cation or anion was as follows;

(1) the spectrum was collected using program COLLECT. Usually a number of spectra were collected, with long slow scans often being used to find the outer most line of the spectrum.

(2) the spectrum was fitted from the outer most lines inwards using the simulation programs running on the SBC-100. This fitting was usually done by fitting each successive coupling constant, before the next one was added. It was not unusual for 80 to 120 simulations to be carried out before the best fit possible by simulation was achieved. On a number of occasions the coupling constants could not be accurately fitted in this manner and it was necessary to use ESRCON before all the coupling constants had been found. Examples of this are 1- and 2-methylnaphthalene anions where the first six coupling constants were readily found. The other two coupling constants proved intractable due to errors in the values of the other six coupling constants. By using ESRCON to refine the first six coupling constants, the remaining two were then quickly found.

(3) the collected spectra were transferred onto the Prime 750 for use with ESRCON.

(4) Once acceptable trial values for the coupling constants had been found, ESRCON was used to refine the trial coupling constants. Generally the spectra were fitted by fitting the smallest coupling constant to the outermost lines, and then adding each successive coupling constant, while fitting a successively larger part of the spectrum. This process was found to be necessary, otherwise ESRCON would not converge to a satisfactory solution, or would not converge at all.

(5) The final calculated and experimental spectra were plotted out on the Calcomp flat-bed plotter by ESRCON. The two spectra were plotted directly one upon the other, with the

calculated spectra dashed. This enabled the goodness of fit to be evaluated by eye.

The units of the coupling constants output by ESRCON were points or steps. As discussed in Section 2.3.3 the conversion factor in Steps per Gauss for each scan range had been determined using MAGLIN, and these conversion factors were used to convert the values output by ESRCON. On a number of occasions the best fit required accidental equality of coupling constants, or some other special relationship. When this occurred the ESR spectrum was usually repeated, with an attempt being made to resolve the "degenerate" coupling constants.

Section 2.5
Miscellaneous Programs

Section 2.5.1 Exchange Broadening Simulation Program YKEXCH

YKEXCH was obtained from the University of York, and was used with only minor modifications. In YKEXCH, Modified Bloch Equations are used to describe the exchanging system. The number of interconverting species the program can handle is limited only by the size of the arrays, which were increased considerably beyond those of the version of the program received. Simulations involving more than two interconverting species used a different, and considerably slower, algorithm.

Section 2.5.2 High Resolution Plotting Program GRAPHS

The resolution of both the E-12 Spectrometer and the A-60 plotters is considerably higher than the resolution normally used. Both COLLECT and GRAPH use only 5000 points rather than the possible 10,000 point resolution of the E-12 plotter, and 5000 points rather than the 35,000 point resolution of the A-60 plotter. For some applications, particularly high quality plot preparation, the higher resolution is useful. For such applications, a wider choice of scaling options is also required. GRAPHS is a modified version of GRAPH which uses the full resolution of both plotters. Scaling options allow any choice of scale from 1/99 th to 99 times the scale of the input file to be selected, e.g. a scale of 13/87 ths of the input file could be selected. The plotting speed of GRAPHS is considerably lower than that of GRAPH. Details of GRAPHS are given in Appendix 2.5

CHAPTER 3

PERI-ALKYLNAPHTHALENES

Section 3.1
Introduction and Review

Saturated peri- substituted alkylnaphthalenes have been the subject of intensive investigation using ESR during the past two decades. Acenaphthene(ACN), pyracene(PYC), hexahydropyrene(HP), phenalene, pleiadane(P) and dipleiadane(DP) (see Fig. 3.1) have all been studied using ESR. The ESR spectrum of $ACN^{-\cdot}$ has been studied by a number of groups (58deB, 64Col, 67Her, 72Cla1, 74Red, 67Iwa) and the ion pairing effects observed are well understood. Similarly $PYC^{-\cdot}$ (65deB, 71Red, 72Fas).

In peri-alkylnaphthalenes which contain 6- or 7-membered rings, the 6- or 7-membered ring does not lie in the plane of the molecule (see Fig. 3.2) It would be expected therefore that β_{ax} and β_{eq} would be different as might γ_{ax} and γ_{eq}. This non-equivalence of the β and γ hydrogens has been observed for phenalene anion (72Cla1, 72Cla2, 72Pas, 71Pea). In pleiadane anion (72Cla1, 72Cla2, 71Pea) only the β hydrogens were found to

Figure 3.1 Some Peri-alkylnaphthalenes

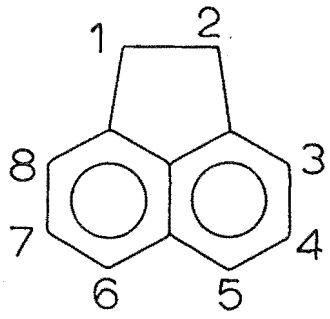

I acenaphthene (ACN)

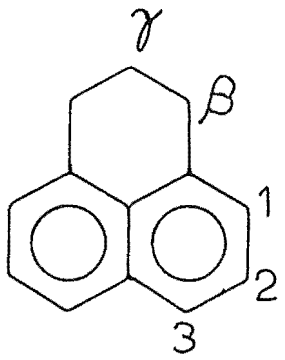

II phenalene

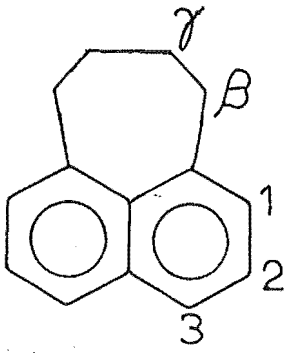

III pleiadane (P)

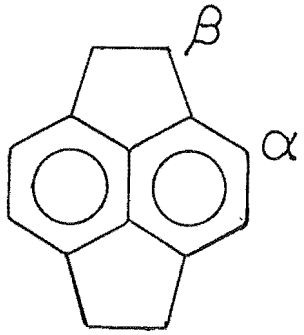

IV pyracene (PYC)

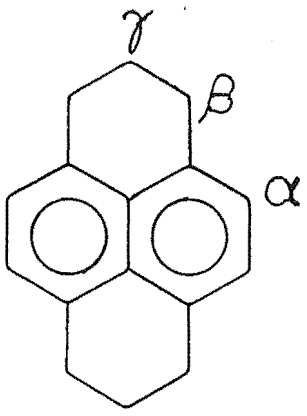

V hexahydropyrene (HP)

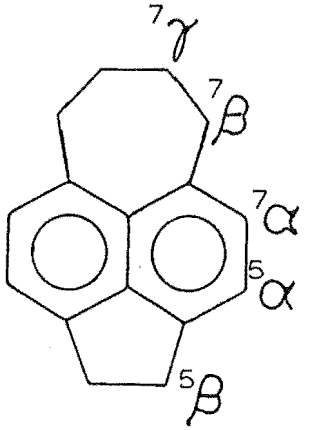

VI hexahydro-cyclohepta[fg]-acenaphthylpleiadane (5,7PN)

Figure 3.1 cont.

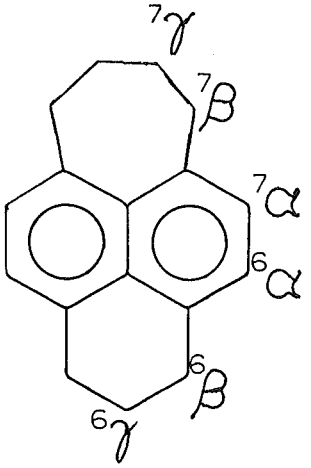

VII hexahydro-1H-cyclohepta[cd]-phenalene (6,7PN)

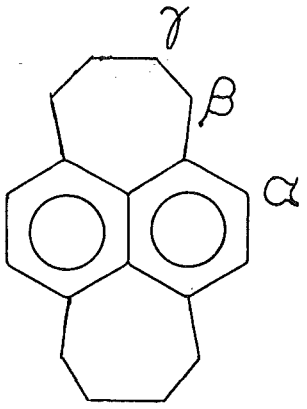

VIII dipleiadane (DP)

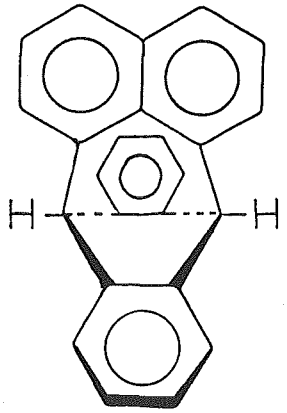

IX

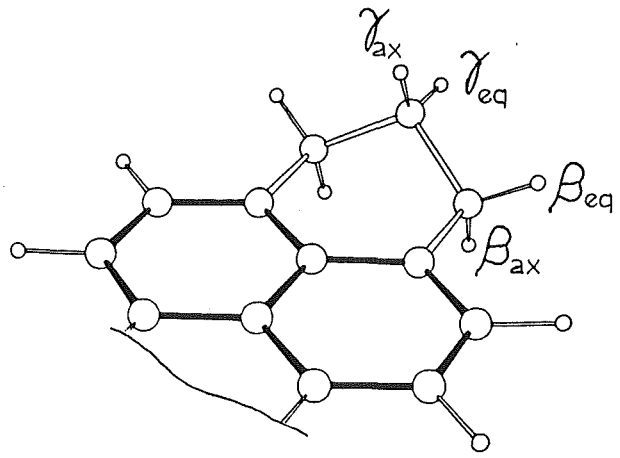

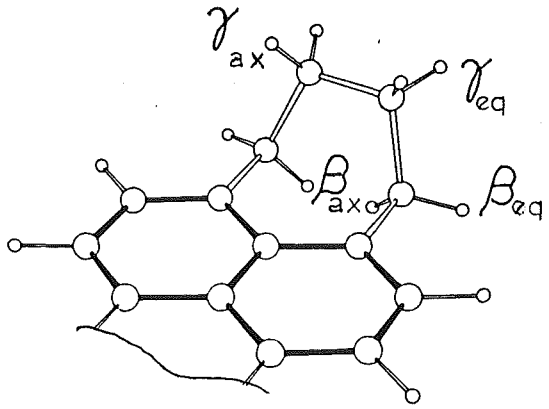

Figure 3.2 Conformation of 6- and 7-membered Peri-alkyl Rings*

* Reproduced from 71 Pea

be non-equivalent. In both phenalene and pleiadane anions the observed spectra changed with temperature. It was shown by simulation that this effect was attributable to the ring oscillating between a position above the plane of the molecule and the equivalent position below the plane.

If a molecule has two 6- or 7-membered rings, the possibility arises that the molecule might exist in more than one conformation. For example in HP, which has two 6-membered rings, both γ carbons can lie above (or below) the plane of the molecule, or one can lie above and the other below. The first conformation is termed a boat conformation and the second a chair conformation. (see Fig. 3.3). In $HP^{\cdot-}$ the coupling constants of the chair and boat conformers were found to be the same within experimental limits (70C1a, 72C1a1, 71Pij, 71Pea). At higher temperatures linebroadening was observed. Simulation required a four-jump model indicating that the interconversion was between chair and boat conformations. By simulating the spectra over a range of temperatures the rate of interconverion as a function of temperature was found and this allowed the entropy and enthalpy of the interconversion to be found (72C1a1, 71Pij).

$DP^{\cdot-}$ can also exist in chair and boat conformations, and accurate simulation of the low temperature spectra required that the coupling constants of the two conformations be different (71C1a, 72C1a1, 72C1a2, 71Pea). Claridge and Peake simulated the spectra of $DP^{\cdot-}$ over a range of temperatures and were able to calculate the entropy and enthalpy for the interconversion.

de Boer and Praat (64deB) reported that HP^{+} also existed as two conformers, and that the coupling constants of the two

Figure 3.3 Chair and Boat Conformations in HP and DP*

HP

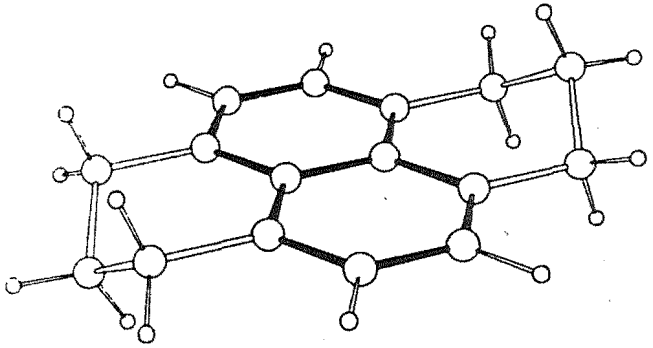

Chair

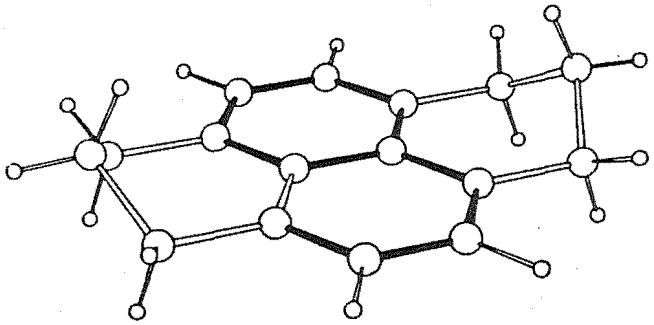

Boat

DP

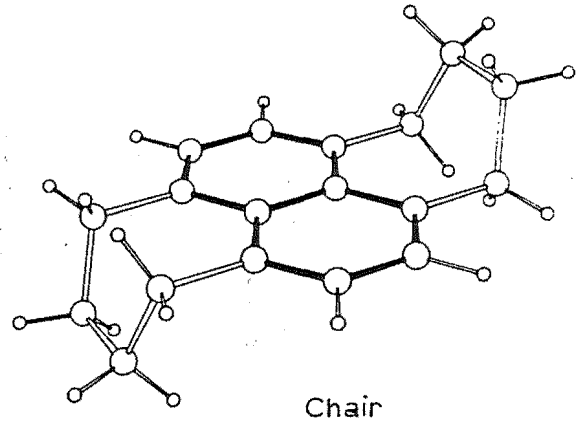

Chair

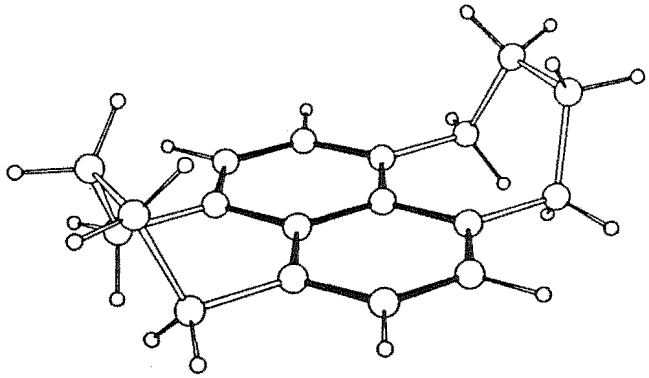

Boat

*Reproduced from 71Pea

conformers were different. Pijpers et al (71Pij) determined the enthalpy and entropy of the chair/boat interconversion. The only other study on peri-alkyl bridged naphthalene systems is that of Nelsen and Gillespie (73Nel) on pleiadane derivatives, and on peri-alkylnaphthalenes with 8, 9 and 10 membered rings.

A number of ENDOR studies have been carried out on these compounds. Shain in 1971 (71Sha) confirmed the coupling constants found by Claridge and Peake for $HP^{\bar{\cdot}}$. Iwazumi (80Iwa) in 1980 reported an ENDOR study of the temperature dependence of the coupling constants of $HP^{\bar{\cdot}}$, and calculated the entropy and enthalpy of the chair/boat interconversion. Claridge in 1977 (77Cla) recorded the ENDOR spectra of phenalene anion, pleiadane anion, $DP^{\bar{\cdot}}$, $HP^{\bar{\cdot}}$, DP^{+}, HP^{+} and of the cations and anions of 1,2,5,6,7,8-hexahydro-cyclohepta[fg]acenaphthylene (5,7PN), and 2,3,6,7,8,9-hexahydro-1H-cyclohepta[cd]phenalene (6,7PN). However the coupling constants determined by Claridge from ENDOR reproduced the ESR spectra of $HP^{\bar{\cdot}}$ only. The simulations using the ENDOR coupling constants did not satisfactorily reproduce the ESR spectra of the other systems.

One objective of this section was therefore to reconcile the coupling constants, as found by ENDOR, with the ESR spectra.

A common method of gaining conformational information from coupling constants is by use of the relationship proposed by M^{c}Connell and Heller in 1960 (60Hel). The relationship (Eqn 3.1) relates the observed hyperfine coupling of a hydrogen atom bonded to the β carbon, to the angle between the carbon-hydrogen bond and the symmetry axis of the π orbital containing the unpaired electron.

$$a = \rho_{\alpha}^{\pi} (B_0 + B_2 \cos^2\theta) \quad \text{Eqn 3.1}$$

Where a is the β hydrogen hyperfine coupling constant, ρ_{α}^{π} is the spin density on the aromatic carbon to which the β carbon is attached, B_0 is the contribution made by spin delocalisation through the C_{α}-C_{β} bond, B_2 is the contribution made by hyperconjugation, θ is as shown in Fig. 3.4. The common assumption made is that B_0 is 0, and that the angle between the two β hydrogens is 120^0. Studies by Bauld et al (72Hud, 71Bau) suggest that B^0 can be as much as $0.16B_2$ and therefore is not negligible.

The major objective of this section was to investigate the conformation of the alkyl rings.

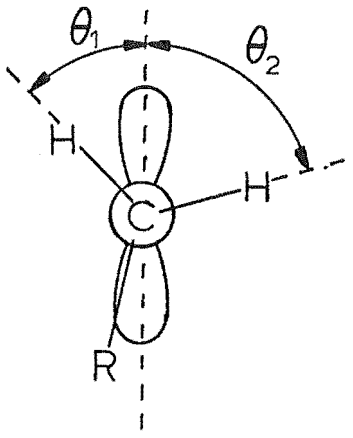

Figure 3.4 The dihedral angles between β protons and the adjacent carbon π orbital

Table 3.1

Coupling Constants of Peri-alkylnaphthalene Ions

Compound	Assignment[1]		Value (in Gauss)			
		This work (±0.005)	Peake[2]	Claridge[3]	other	
Acenaphthane$^{-\cdot}$	5_β				8.29[4]	
	5,6				4.17	
	4,7				2.42	
	3,8				1.04	
Phenalene$^{-\cdot}$	γ_{eq}		0.36		0.36[5]	
	γ_{ax}		0.53		0.53	
	1		1.54		1.52	
	2		1.92		1.89	
	β_{eq}		2.30		2.24	
	β_{ax}		8.68		8.62	
HP$^{-\cdot}$	γ_{eq}		0.36	0.36	0.50[6]	0.36[7]
	γ_{ax}		0.53	0.50	0.50	0.50
	α		1.69	1.67	1.69	1.71
	β_{eq}		2.02	2.03	2.02	2.10
	β_{ax}		7.92	7.97	8.03	8.08
HP$^{+\cdot}$	Species I	γ 0.404		0.40	0.40[7]	
		α 1.874		1.89	1.90	
		β_{eq} 3.593		3.62	3.63	
		β_{ax} 14.553		14.63	14.70	

Table 3.1 cont.

HP†	Species II	γ	0.398	0.40	0.40
		α	1.888	1.89	1.90
		β_{eq}	3.848	3.87	3.70
		β_{ax}	14.497	14.63	14.63
DP†	Species I	γ_{eq}	0.087	0.07	
		β_{eq}	1.272	1.27	
		γ_{ax}	1.738	1.77	
		α	1.777	1.77	
		β_{ax}	11.909	12.12	
	Species II	γ_{eq}	0.086	0.07	
		β_{eq}	1.272	1.27	
		γ_{ax}	1.742	1.77	
		α	1.775	1.77	
		β_{ax}	12.057	12.23	
5,7PN†		γ_{eq}	0.00	0.00	
		$^{7}\beta_{eq}$	0.721	0.69	
		$^{5/7}\alpha$	1.555	1.58	
		γ_{ax}	1.977	1.96	
		$^{7/5}\alpha$	2.330	2.30	
		$^{5}\beta$	12.688	12.80	
		$^{5}\beta$	12.753	12.80	
		$^{7}\beta_{ax}$	13.584	13.60	

Table 3.1 cont.

6,7PN^{+}	Species I	$^{7}\gamma_{eq}$		0.07
		$^{6}\gamma$		0.38
		$^{7}\beta_{eq}$		1.03
		α		1.86
		$^{7}\gamma_{ax}$		1.86
		$^{6}\beta_{eq}$		3.66
		$^{7}\beta_{ax}$		12.60
		$^{6}\beta_{ax}$		14.33
	Species II	$^{7}\gamma_{eq}$		0.07
		$^{6}\gamma$		0.38
		$^{7}\beta_{eq}$		1.03
		α		1.86
		$^{7}\gamma_{ax}$		1.86
		$^{6}\beta_{eq}$		3.55
		$^{7}\beta_{ax}$		12.60
		$^{6}\beta_{ax}$		14.33
5,7PN$^{-\cdot}$		γ_{eq}	0.180	0.17
		$^{7}\beta_{eq}$	0.522	0.51
		γ_{ax}	0.734	0.72
		$^{5}\alpha$	1.225	1.22
		$^{7}\alpha$	2.032	2.06
		$^{7}\beta_{ax}$	6.049	6.02
		$^{5}\beta$	6.918	6.93

Table 3.1 cont

6,7PN$^{\cdot-}$		$^{7}\gamma_{eq}$			0.20
		$^{6}\gamma_{eq}$			0.35
		$^{6}\gamma_{ax}, ^{7}\gamma_{ax}$			0.51
		$^{7}\alpha$			1.15
		$^{7}\beta_{eq}$			1.62
		$^{6}\alpha, ^{6}\beta_{eq}$			2.06
		$^{7}\beta_{ax}$			6.17
		$^{6}\beta_{ax}$			8.06
Pleiadane$^{\cdot-}$		γ_{eq}	0.22	0.22	0.21
		γ_{ax}	0.53		0.53
		β_{eq}	1.22	1.22	1.22
		1	1.58	1.58	1.55
		2	1.80	1.80	1.80
		3	4.61	4.64	4.61
		β_{ax}	6.78	6.79	6.78
DP$^{\cdot-}$	Species I	γ_{eq}	0.22	0.22	0.21
		γ_{ax}	0.45	0.22	0.45
		β_{eq}	1.50	1.35	1.46
		α	1.69	1.57	1.66
		β_{ax}	6.23	6.28	6.22
	Species II	γ_{eq}	0.22	0.22	0.21
		γ_{ax}	0.45	0.22	0.45
		β_{eq}	1.69	1.57	1.66
		α	1.69	1.57	1.66
		β_{ax}	6.12	6.16	6.08

[1] see Figs. 3.1, 3.2 and 3.3 for positions

[2] 71Pea

[3] 77Cla, ENDOR

[4] 64Col

[5] 72Pas

[6] 64deB

[7] 71Sha, ENDOR

SECTION 3.2

Experimental

Section 3.2.1 Hexahydropyrene Cation ($HP^{\cdot+}$)

Hexahydropyrene (HP) reacted readily with $AlCl_3/SO_2$ in CH_2Cl_2 to give an olive green coloured solution. A strong ESR signal was present in the solution. After a number of dilutions the minimum linewidth was attained. Initially 100kHz modulation was used to collect the spectrum, but because of the narrow linewidth (25mG), this lead to line broadening due to modulation side bands and the observation of spurious lines. Subsequently 25kHz modulation was used. From spectra at low temperature ($-85^{0}C$), the outer most lines were collected. The simulated spectrum reproduces the outermost lines and all other features of the spectra (see Fig. 3.5). The simulated spectra was refined using ESRCON (Section 2.4.4) and fits the collected spectra extremely well. The difference in g-value found for the two species was 0.012 ± 0.004 G. The ratio of the concentrations of the two species was $50\%:50\%\pm4\%$

At higher temperatures line broadening occurs. This line broadening was found to be reversible with temperature. Simulation using program YKEXCH (Section 2.5.1) showed that this is effect is caused by interconversion between the chair and boat conformers. The assignments given in Table 3.1 for $HP^{\dagger}$ were determined by simulation using YKEXCH. At temperatures above $-40^{0}C$ all lines except those for which $M_I(\beta_{ax}) = M_I(\beta_{eq})$ had disappeared. It was therefore concluded that $\beta_{ax}+\beta_{eq}$ = 18 Gauss so that the 3.8, 3.6, 14.5, and 14.6 Gauss coupling constants must be assigned to the β positions.

In two samples it was observed that at temperatures above $0^{0}C$ a second signal would appear (see Fig 3.6). The strength of this second signal increased with time and did not decrease as the temperature was lowered. Simulations using coupling constants of 5.30G (4 hydrogens), 2.12G (4 hydrogens) and 1.20G (2 hydrogens), satisfactorily fitted the spectra of this second species. Lewis and Singer (65Lew) reported the coupling constants of pyrene cation to be 5.38G, 2.12G and 1.18G. These values are in reasonable agreement with those found indicating that pyrene is being formed. This is not unreasonable, given the reaction conditions. $HP^{\dagger}$ is found to have a g-value 0.00009 ± 0.00001 lower than $pyrene^{\dagger}$. This agrees with the difference in g-value reported by Makela et al (84Mak)

The fits obtained with YKEXCH were not considered to be sufficiently accurate to allow any meaningful estimate of the enthalpy or entropy of the interconversion between the two conformers to be made. At lower temperatures YKEXCH did not accurately simulate the change of the second order splitting. At

Figure 3.6 HP^+ Spectra at 0°C

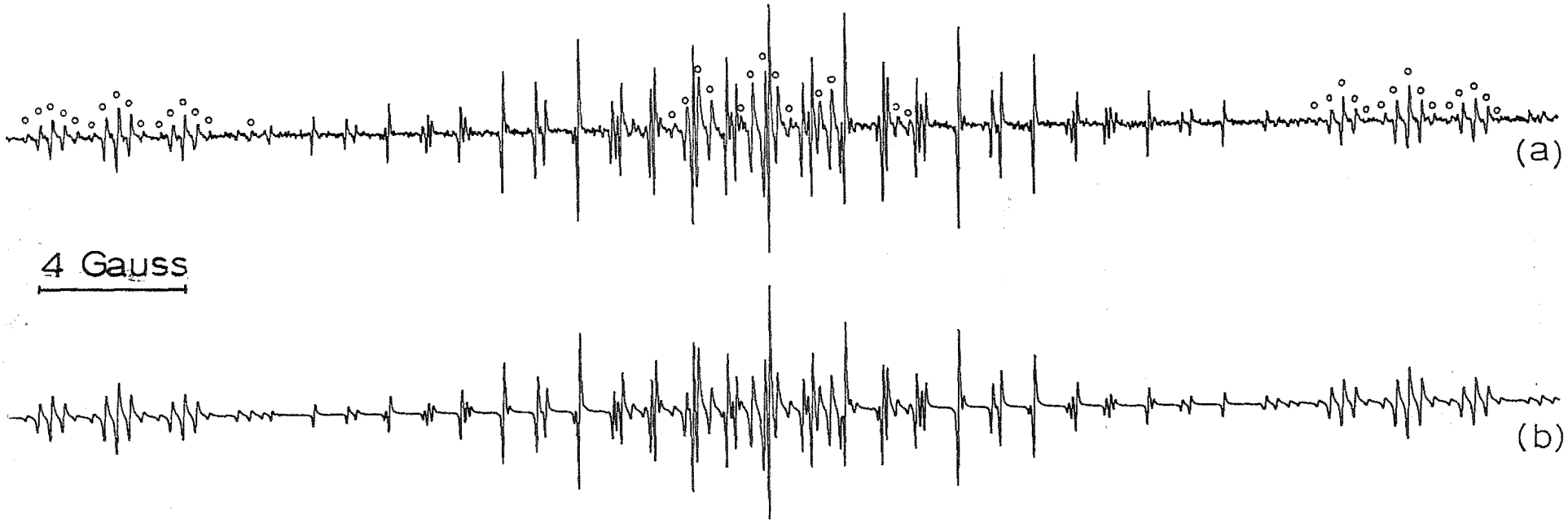

(a) experimental
(b) calculated
HP^+ lines marked.

Figure 3.7
Dipleiadane$^{+\cdot}$ Spectra at 27°C

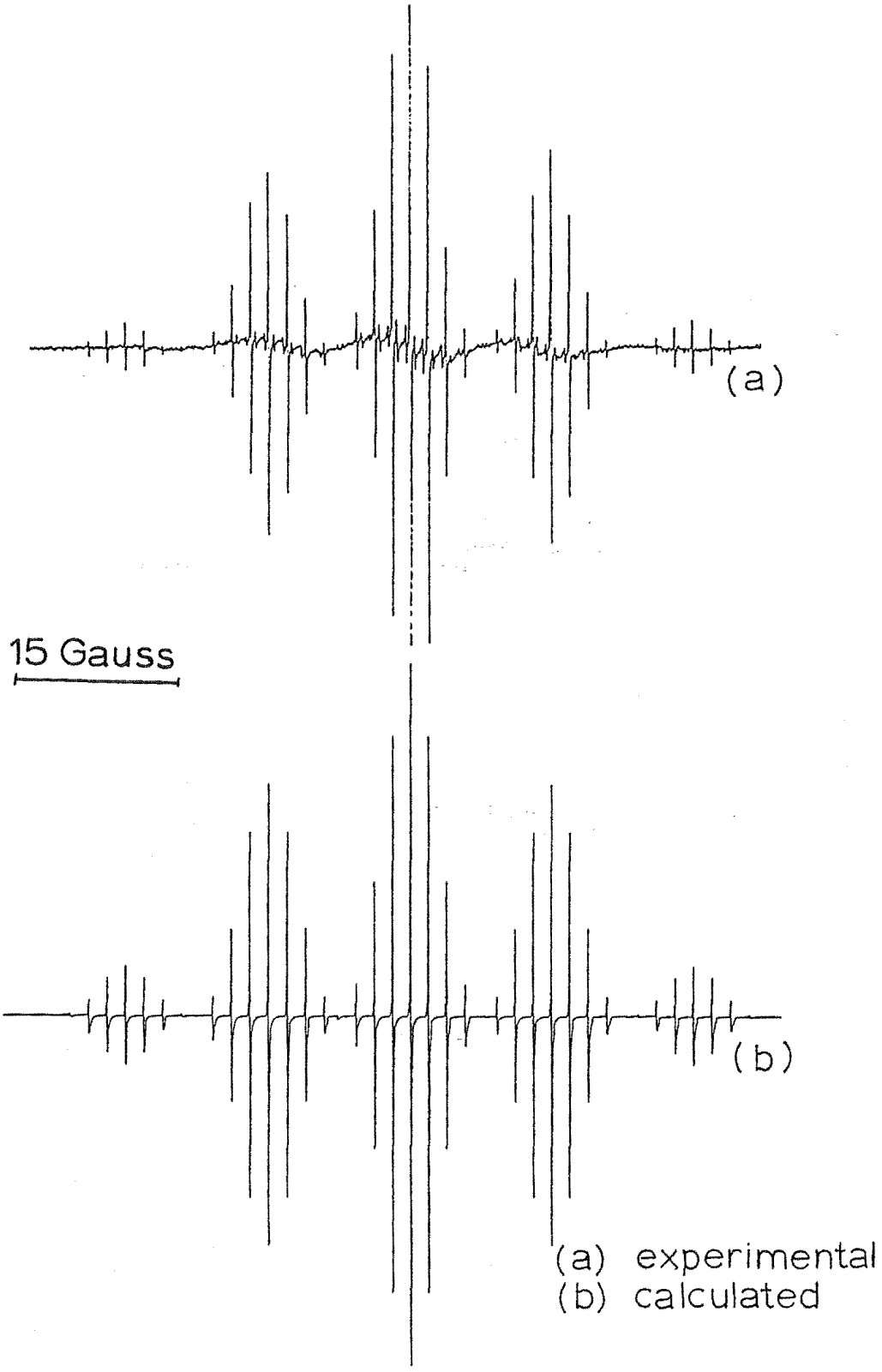

the higher temperatures it proved possible to satisfactorily fit the linewidths, positions and amplitudes of the various lines but not simultaneously, i.e. the linewidth, or the positions or the amplitudes would be correct but not all three at once.

The coupling constants found for HP^{+} at low temperature are in agreement with those found by de Boer and Praat (64deB) and Claridge using ENDOR (77Cla).

Section 3.2.2 Dipleiadane Cation (DP^{+})

Dipleiadane (DP) gave a very pale green coloured solution when reacted with $AlCl_3/SO_2$ in CH_2Cl_2. The observed ESR spectrum had an extremely narrow linewidth (18mG). Spectra were collected in the range -89^0 to $+52^0$. At temperatures above -70^0 line broadening occurred. From approximately -40^0 to the highest temperature at which spectra were collected DP^{+} exhibited an alternating linewidth effect. It was found that the spectra at intermediate exchange (see Fig. 3.7) could be simulated with 13.3G (4 hydrogens) and 1.8G (8 hydrogens). The only reasonable combination that would give this result was $\beta_{ax}+\beta_{eq}$ = 13.3G and $\alpha=\gamma_{ax}+\gamma_{eq}$=1.8G. Once this was understood, the spectra were successfully simulated. (see Fig.3.8). The simulation required two species with slightly different g-values. The difference in g-value found by ESRCON was 0.021 ± 0.005G. Simulations of just the centre part of the spectrum indicate that the actual difference is closer to 0.017G. The ratio of the concentrations of the two species found was $43\%:57\%\pm4\%$.

Simulation of the temperature dependance of DP^{+} proved to be impossible. The size of the arrays required for YKEXCH to simulate the spectra exceeded the limitations of the operating system of the Burroughs computer on which the program runs. Some smaller simulations did indicate the basic correctness of the analysis given. The simulated coupling constants and assignments are given in Table 3.1

Section 3.2.3 1,2,5,6,7,8-Hexahydro-cyclohepta[fg]acenaphthylene Cation ($5,7PN^{+}$)

1,2,5,6,7,8-hexahydro-cyclohepta[fg]acenaphthylene (5,7PN) reacted with $AlCl_3/SO_2$ in CH_2Cl_2 to give a pale green/black coloured solution. Spectra were recorded in the range $-90^{0}C$ to $+40^{0}C$. The best least squares fit obtained using ESRCON is given in Table 3.1. The experimental and simulated spectra are shown in Fig. 3.9. The correctness of this analysis is confirmed by simulation, using YKEXCH, of the spectra of $5,7PN^{+}$ at higher temperatures (above $-70^{0}C$) where the alternating linewidth effect is evident (see Fig. 3.10). The assignments given in Table 3.1 were determined from this simulation. A number of simulations using YKEXCH were run to test the various possible assignments, and that given is the only assignment that successfully simulates the higher temperature spectra. The coupling constants determined agree with the ENDOR values found by Claridge (77Cla), including a requirement that one coupling constant is 0.0 Gauss.

The values of 12.688G and 12.753G found for the $^{5}\beta$ coupling constants are smaller than expected on the basis of the coupling

Figure 3.9 5,7PN‡ Spectra at -87°C

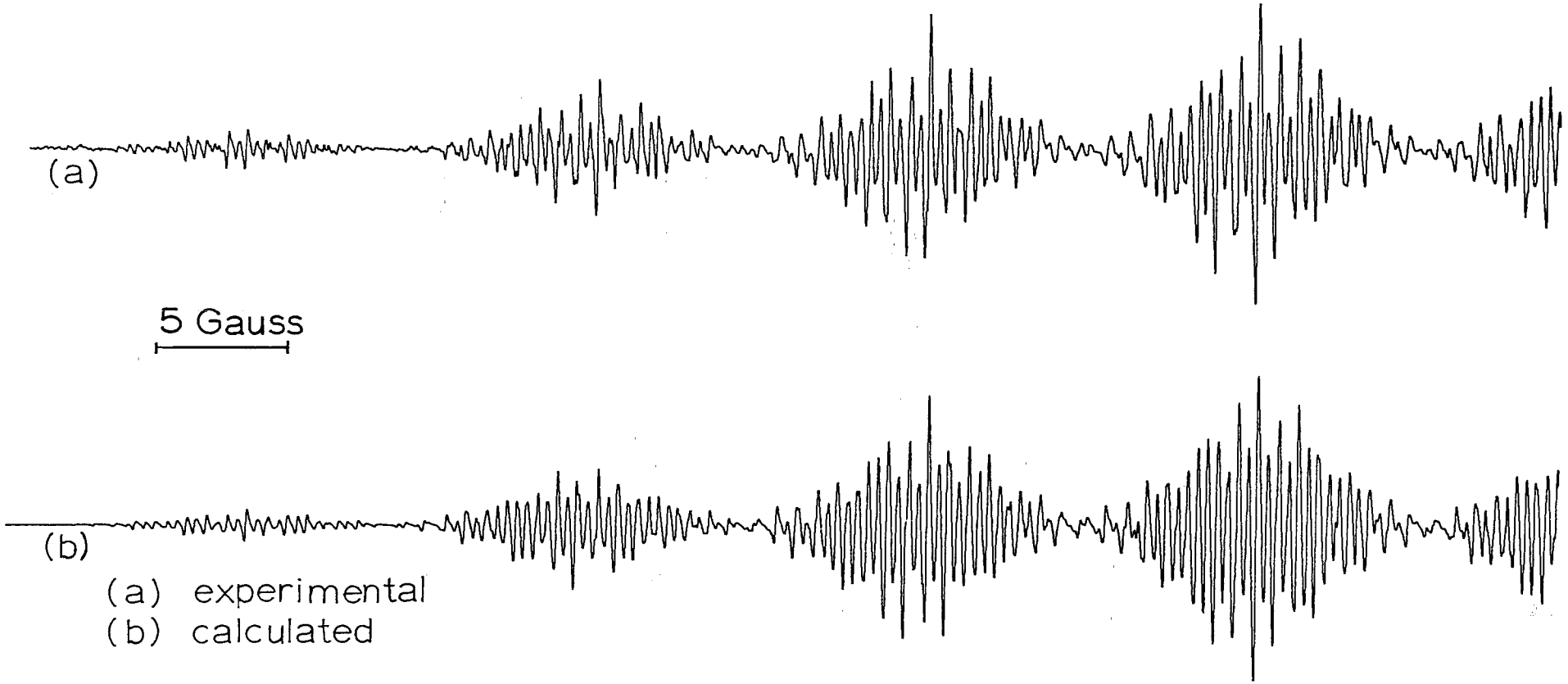

Figure 3.10 5,7PN‡ Spectra at -51°C

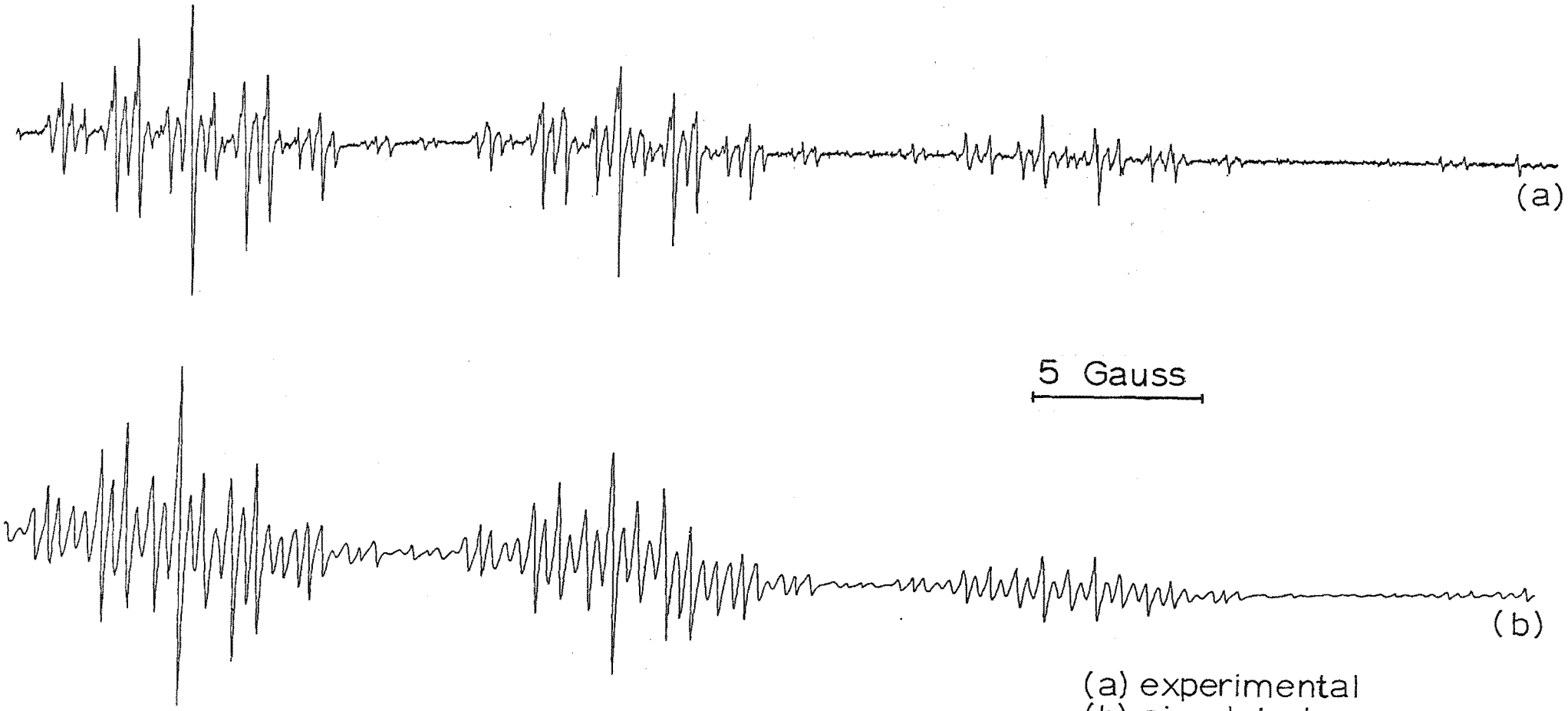

(a) experimental
(b) simulated

Figure 3.11 67PN‡ Spectra at 18°C

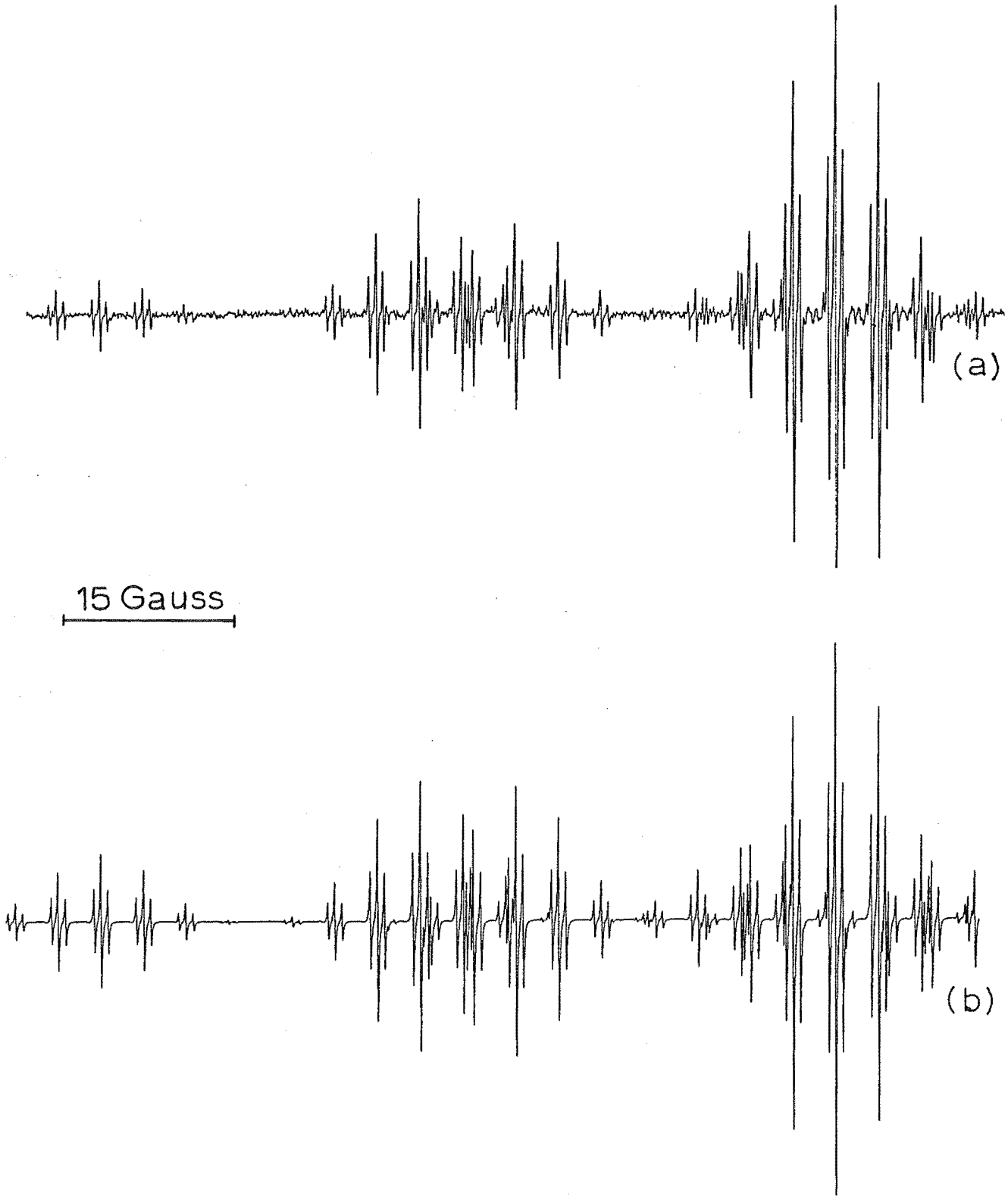

(a) experimental
(b) simulated

coupling constants in acenaphthene^{+}, where the $^{5}\beta$ coupling constant found by Buchanan et al. was 13.18 Gauss (80Buc).

Section 3.2.4 2,3,6,7,8,9-Hexahydro-1H-cyclohepta[cd]phenalene Cation (6,7PN^{+})

2,3,6,7,8,9-hexahydro-1H-cyclohepta[cd]phenalene (6,7PN) reacted with $AlCl_3/SO_2$ in CH_2Cl_2 to give a pale olive green coloured solution. Spectra were collected between -90^{0}C and $+29^{0}$C. Because of the complexity of the spectrum it proved impossible to satisfactorily simulate the spectrum at the lowest temperature studied. The general form of the spectrum is very similar to that found for DP^{+}. At higher temperatures, where the spectrum had simplified because of the alternating linewidth effect, it proved possible to simulate the spectra (see Fig 3.11). The simulated spectra given is a standard first-order ESR spectra calculated using the simulation programs on the SBC-100 rather than the correct simulation using YKEXCH. This is because the correct simulation requires considerably larger array allocations than are currently available on the Burroughs computer. The analysis of the spectra exhibiting the alternating linewidth effect resulted in the assignments for α, $^{7}\beta$, $^{7}\gamma$, and $^{6}\beta$ coupling constants found by Claridge (77Cla) given in Table 3.1. The complexity of the spectra at low temperatures indicates that the $^{6}\beta_{ax}$ and $^{7}\beta_{ax}$ coupling constants probably differ in the two species. The resolution of the ENDOR is estimated to be 30mG, whereas that of the ESR at the lowest temperatures used in this study is 20mG. Errors in the simulated coupling constants of 10mG

Figure 3.12 5,7 PN : Spectra at -69°C

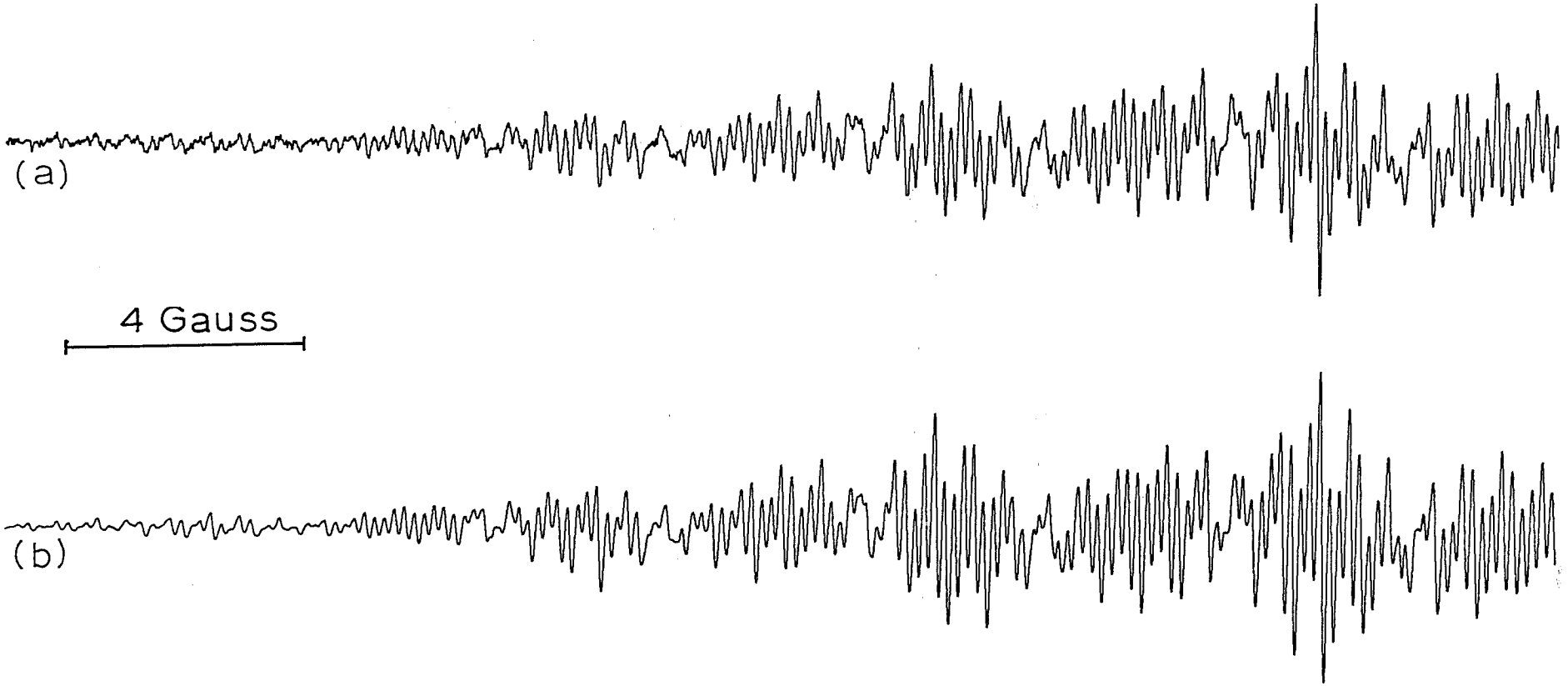

(a) experimental
(b) simulated

are readily apparent. The $^{6}\beta_{ax}$ and $^{6}\beta_{eq}$ coupling constants were assigned on the basis of the coupling constants in $HP^{+\cdot}$.

Section 3.2.5

1,2,5,6,7,8-Hexahydro-cyclohepta[fg]acenaphthylene Anion ($5,7PN^{-\cdot}$)

5,7PN reacted with potassium in DME, the resulting ESR spectra were collected in the range $-90^{0}C$ to $-20^{0}C$. The best least squares fit found using ESRCON is that given in Table 3.1 (see Fig 3.12). The assignments however, are tentative only. Attempts to simulate the spectra at higher temperatures, where the alternating linewidth effect is evident, were completely unsuccessful. The α coupling constants were confirmed from the simulations using YKEXCH, however no combination of linewidth, assignments, and interconversion rate could be found that would successfully simulate the other features of the spectrum. As the variations of the spectra were reversible with temperature it can be assumed that the variations observed are not due to reaction products, but to $5,7PN^{-\cdot}$. The assignments of the α coupling constants were determined on the basis of the least squares fit for the addivity relationships for the α coupling constants in a variety of systems. This will be discussed further in Section 3.3.1

Figure 3.14 Pleiadane⁻ Spectra at -95°C

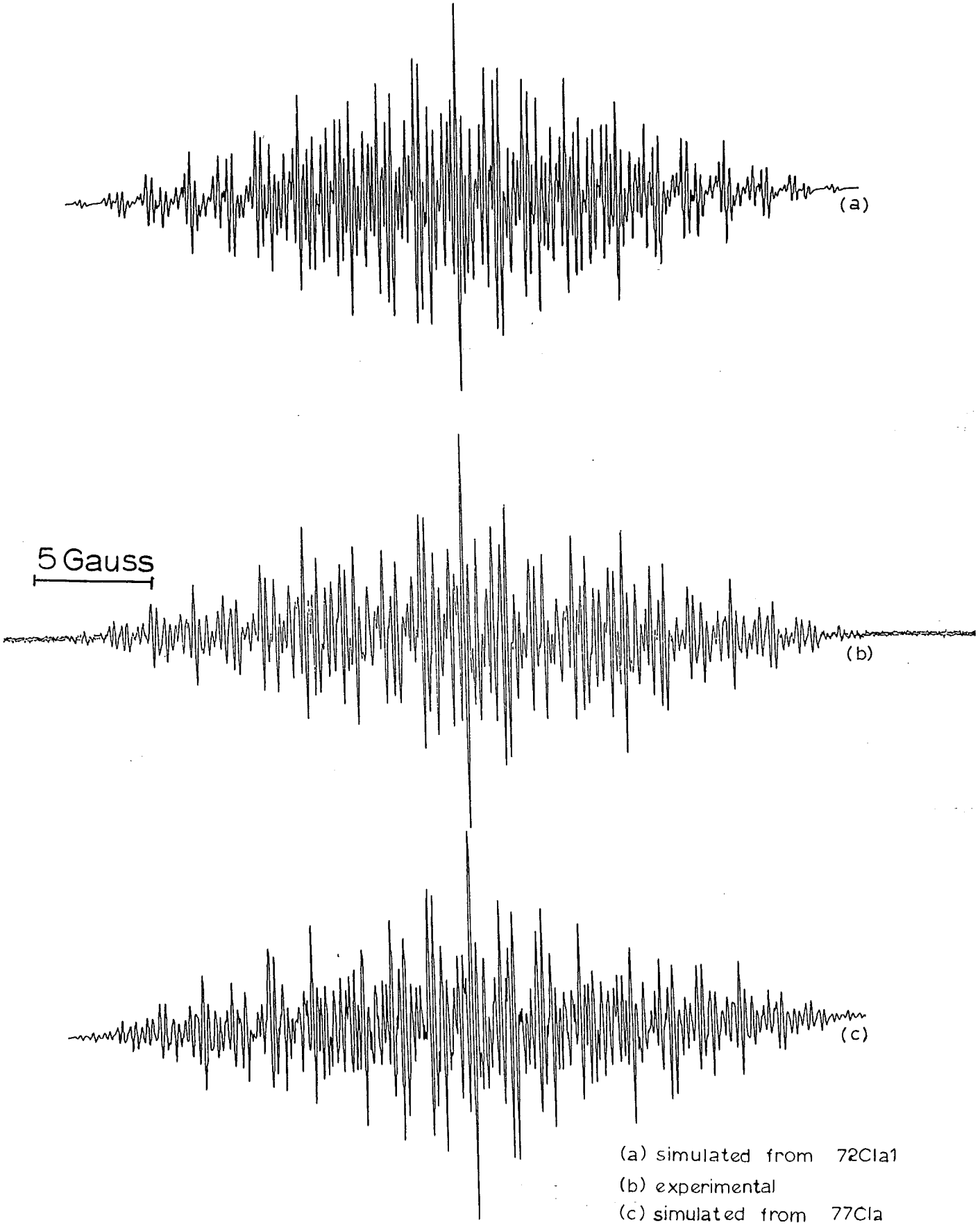

(a) simulated from 72Cla1
(b) experimental
(c) simulated from 77Cla

Section 3.2.6 2,3,6,7,8,9-Hexahydro-1H-cyclohepta[cd]phenalene Anion ($6,7PN^{\cdot-}$)

6,7PN reacted readily with potassium in DME to give a deep olive green coloured solution. A strong, poorly resolved ESR signal was present. Attempts to improve the resolution by diluting the sample were unsuccessful. The temperature variation of the spectrum between $-90^{0}C$ and $0^{0}C$ did not result in any simplification of the spectrum. No attempt was made to simulate this spectrum. The ENDOR coupling constant assignments given in Table 3.1 were all assigned by comparison with $HP^{\cdot-}$, $DP^{\cdot-}$ and $5,7PN^{\cdot-}$. Because of the doubts in the assignments in $DP^{\cdot-}$ and $5,7PN^{\cdot-}$ the assignments in $6,7PN^{\cdot-}$ must therefore be treated with caution.

Section 3.2.7 Pleiadane and Dipleiadane Anions ($P^{\cdot-}$ and $DP^{\cdot-}$)

When the coupling constants found from ENDOR were compared with those found from ESR it was seen that the two techniques agreed for all the ions studied with the exception of the pleiadane and dipleiadane anions. It was therefore decided to check the simulations for these two species. The original spectra recorded by B.M. Peake (71Pea) were available and were used. Fig. 3.13 shows the recorded and simulated spectra of pleiadane anion in DME at $-95^{0}C$. Spectrum (b) is the experimental spectrum, (a) is the simulated spectrum using the parameters given by Claridge and Peake (71Pea, 72Cla1, 72Cla2), (c) is the simulated spectrum using the parameters given in the first column of Table 3.1. The

simulated spectrum (c) clearly fits better than spectrum (a). Analysis of the pleiadane spectra at -10^{0}C, where the alternating linewidth effect has simplified the spectrum, indicates that the 1.58G, 1.80G and 4.64G coupling constants are due to naphthalene ring protons. The value of 8.1G was found for the sum of the β coupling constants, resulting in the assignment of the 6.79G coupling constant to β_{ax} and 1.22G to β_{eq}. The remaining two coupling constants must be due to the γ coupling constants.

After the success in improving the fit to $P^{\cdot-}$, attempts were made to fit $DP^{\cdot-}$ on the basis of the ENDOR results. The simulated spectrum produced (see Fig 3.14 (c)) was in better agreement with the experimental spectra than that given by Claridge and Peake (71Cla, 71Pea, Fig 3.14 (a)) but the agreement between the experimental spectrum (Fig. 3.14(b)) and the simulated spectra is still very poor. This would indicate that there may be some other effect which is not being taken into account. It is possible that there is some line broadening, at this temperature, caused by ion pairing or by conformational interconversion.

Figure 3.14 Dipleiadane$^{-\cdot}$ Spectra at -95°C

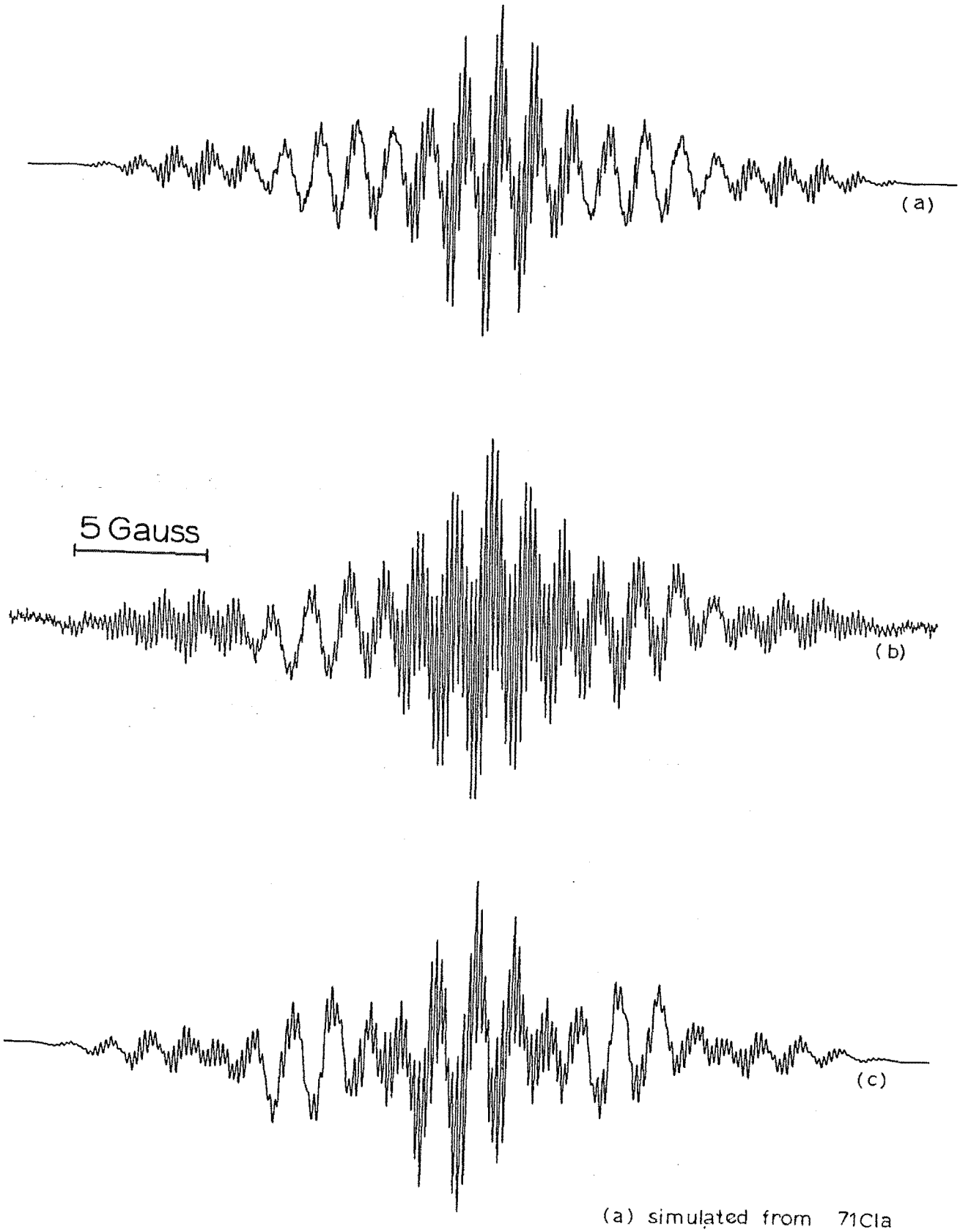

(a) simulated from 71Cla
(b) experimental
(c) simulated (this work)

SECTION 3.3

Discussion and Conclusions for Peri-alkylnaphthalene Ions

Section 3.3.1 α Coupling Constants

Enough data on the α coupling constants of peri-alkylnaphthalene anions exists to allow a set of additivity relationships to be calculated. The assignments are based on the assignment in acenaphthene$^{-\cdot}$(Fig. 3.1). The assumption is made that the coupling constant at position 4 is larger than that at position 3. There are 14 equations in 7 variables so the system is considerably overdetermined. The largest difference between an experimental coupling constant and the value calculated on the basis of the additivity relationship is 85mG. The full least squares analysis is given in Appendix 3.1 The α coupling constants in 5,7PN$^{-\cdot}$ were initially assigned on the basis of this set of additivity relationships, before being confirmed by the analysis of the temperature dependence of the 5,7PN$^{-\cdot}$ spectra. The assignment of 1.22G to $^{5}\alpha$, and 2.06G to $^{7}\alpha$ in 5,7PN$^{-\cdot}$, and 2.06G to $^{7}\alpha$ and 1.15G to $^{6}\alpha$ in 6,7PN$^{-\cdot}$ was determined solely on the basis of the additivity relationships.

The 5- and 6-membered rings have similar influences on the coupling constants, whereas the effect of a 7-membered ring is much smaller, only perturbing the coupling constant of the hydrogen at the 3 position by 60mG and that at the 4 position by 300mG. By comparison the 5- and 6-membered rings produce perturbations of 500mG at the 3 position and 750mG at the 4 position. This implies that 5- and 6-membered rings are more efficient at

delocalising spin density than is a 7-membered ring. Alternately 5- and 6-membered rings may cause a greater distortion in the naphthalene rings than a 7-membered ring.

There are insufficient data to allow the additivity relationship for the α coupling constants in the cations to be determined. In 5,7PN^{+} the 2.33G and 1.555G coupling constants must be assigned to the $^{5}\alpha$ and $^{7}\alpha$ positions. However without an additivity relationship these two coupling constants cannot be unambiguously assigned, e.g. the 2.33G coupling constant could be assigned to either the $^{5}\alpha$ or $^{7}\alpha$ positions. The $^{6}\alpha$ and $^{7}\alpha$ coupling constants in 6,7PN^{+} are not resolved so the ambiguity does not occur in 6,7PN^{+}.

Section 3.3.2 Ring Conformation

In order to apply the M^{c}Connell-Heller relationship (Eqn. 3.1) to the peri-alkylnaphthalenes, a number of constraints of one form or another need to be introduced to reduce the number of variables. In the general form of the equation there are four variables; B_0 and B_2, θ, and ρ_{α}^{π} the spin density on the α carbon (see Fig. 3.4). The presence of two hydrogens increases the number of data available, but also increase the number of variables. The evaluation of the conformation from this relationship requires that a number of assumptions be made. Table 3.2 gives the results for a number of different assumptions. Assumption 1 is that $\theta_2=\theta_1+120^{0}$, and that $\rho_{\alpha}^{\pi}=0.18$, this allows

Table 3.2

Angle about β Carbons in some peri-alkylnaphthalenes

Compound	Assumption 1			Assumption 2	Assumption 3	
	B_0	B_2	θ_1	θ_2	θ_1	θ_2
$P^{\cdot-}$	6.45	38.30	25.4^0	6.4^0	30.3^0	-69.9^0
$HP^{\cdot-}$	6.26	38.68	9.0^0	0.7^0	15.7^0	-61.9^0
$HP^{\cdot+}$	6.58	74.83	5.0^0	10^0	14.7^0	-62.3^0
	7.12	73.76	3.9^0	0^0	15.1^0	-61.2^0
$DP^{\cdot-}$	8.00	32.32	24.2^0	0.9^0	31.6^0	-65.8^0
	9.07	30.18	24.1^0	-0.8^0	32.5^0	-64.7^0
$DP^{\cdot+}$	6.82	74.36	26.7^0	13.2^0	29.2^0	-75.4^0
	6.67	74.66	26.0^0	13.4^0	28.5^0	-75.4^0
$5,7PN^{\cdot+}$(7)	1.87	84.26	20.8^0	20.4^0	21.0^0	-80.5^0
(5)	81.24	-42.28	60.3^0	29.9^0,120^0	25.3^0	25.6^0
$6,7PN^{\cdot+}$(7)	4.91	78.17	24.2^0	16.2^0	26.0^0	-77.4^0
(6)	7.75	72.50	5.4^0	0.6^0	16.3^0	-62.0^0
(6)	7.61	72.77	5.9^0	1.2^0	16.3^0	-62.5^0

B_0, B_2 and θ_1 to be found. Assumption 2 is that most often used, this is that $\theta_2=\theta_1+120^0$ and that B_0/B_2 is some given value. Nelsen and Gillespie (73Nel) made the assumption that $B_0/B_2=0.02$, based on work by Allendoerfer, Gallagher and Lansbury (72All) on a compound for which θ was constrained to be 90^0 (Compound IX in Fig. 3.1). Assumption 3 is that $B_0/B_2=0.02$ and that $\rho^{\pi}_{\alpha}=0.18$. This then allows the two angles to be calculated directly and thereby gives a check on the assumption that $\theta_2=\theta_1+120^0$. It was found necessary to solve the equations

resulting from the first two sets of assumptions numerically. There were two solutions to these equations. One of which generally involved θ_1 ca. 60^0, and was not used.

The ratio B_0/B_2 found under assumption 1 varies from 0.16 to 0.33 in the anions and from 0.10 to 0.06 in the cations. This would tend to suggest either that the spin density on the carbon could vary from one compound to another or that the alkyl ring(s) produce a substantial distortion of the naphthalene rings. The third alternative is that the assumption that $\theta_2=\theta_1+120^0$ could be invalid. The angles found under assumption 3 indicate that the angle between the two hydrogens may well vary. In no case does the sum of the two angles found equal 120^0. The nearest any come is for the 7-membered ring systems where the sum is ca. 100^0. It appears likely then that the ratio B_0/B_2, ρ_α^π and $\theta_1+\theta_2$ all vary, and that no conclusion can be reached about the absolute magnitude of any of the parameters of interest. It is however possible to draw some conclusions from the trends in the various parameters.

Within a given set of assumptions there is considerable selfconsistency in the angles found, e.g. under assumption 1 θ_1 for 6-membered rings varies from 4^0 to 9^0, and for 7-membered rings it varies from 20.8^0 to 26.7^0. The low value for θ_1 in 5,7PN$^+$ is consistent with the observation that the $-(CH_2-CH_2)-$ bridge distorts the naphthalene ring (57Ehr). The bridge across the peri positions decreases the separation of the two bridged carbons and increases the separation of the corresponding carbons on the opposite side of the ring. This conclusion is reinforced by the observation that $^7\beta_{ax}$ is 1.5G larger in 5,7PN$^+$ than in

$DP^{\dagger}$. No such change in θ_1 is observed in $6,7PN^{\dagger}$ indicating that the presence of the 6-membered ring produces only a minor distortion of the naphthalene ring.

In the four cases where two conformers were distinguished, only small changes in θ_1 were observed. On the basis of the observed changes in θ_1 the species in both $DP^{\dagger}$ and DP^{-} with the smaller θ_1 would be presumed to be the boat form. No such conclusion can be made for any 6-membered ring because of the uncertainty in the sign of θ_1.

CHAPTER FOUR

METHYLNAPHTHALENE ANIONS

This chapter covers work done on methylnaphthalene anions. Section 4.2 covers the experimental observations made, the details of the experimental method being covered in Chapter 2. Section 4.3, which contains the discussion and any conclusions reached, is subdivided into three parts. The first part is that comparing the present study of the 1- and 2-methylnaphthalenes with the study carried out by Brumby (80Bru). The second part contains details of the additivity relationship derived. The third part consists of discussion of the linewidth effects seen in 1,2,3,4-tetramethylnaphthalene. The coupling constants determined are given in Appendix 4.1, the details of the least squares fit of the additivity relationship for various assignments is given in Appendices 4.2 and 4.3

Section 4.1
Introduction and Review

Methylnaphthalene anion radicals have been studied by a large number of groups since de Waard and Henning's study in 1963 (63deW). Gerson, Weidmann and Heilbronner (64Ger) reported the

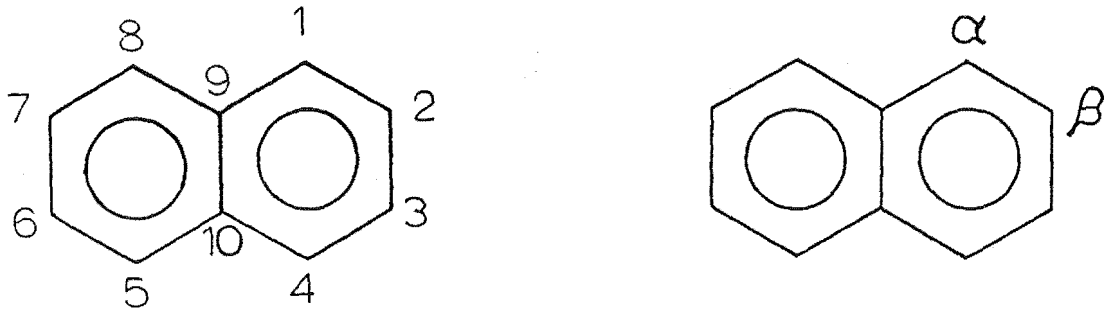

Figure 4.1 naphthalene

coupling constants for the symmetric dimethylnaphthalenes in Na/DME. Rieke and associates reported linewidth effects and temperature dependence of the coupling constants of 2,3-DMN in K/DME (68Rie) and K/DME/HMPA (74Rie) due to ion pair formation. In 1969 Moss et al. (69Mos) reported the coupling constants for 1- and 2-methylnaphthalene and 1,4,5,8-tetramethylnaphthalene in Na/DME. Moss et al. also cited Bolton's coupling constants (63Bol) for 2,3,6,7-tetramethylnaphthalene^{-}, and developed an additivity relationship between the coupling constants in the various methylnaphthalenes. Peake (71Pea) reported coupling constants of some symmetric DMNs in a variety of solvents. In 1972 Gerson, Peake and Whitesides (72Ger) reported the coupling constants for 1,2,3,4-tetramethylnaphthalene in K/DME and Na/DME. More recently Kirk (75Kir) reported a detailed study of ion pairing effects on the symmetric DMNs in a variety of solvents and over a range of temperatures. Kirk also reported the coupling constants for the asymmetric DMNs in K/DME. Brumby (80Bru) re-examined the coupling constants for 1- and 2-methyl-naphthalenes in Na/DME and Na/THF over a range of temperatures, and made calculations of the changes of the coupling constants with temperature, which allowed assignment of the coupling constants to be made. The assignments given by Brumby disagreed with the previously accepted assignments of Moss et al. (69Mos).

The existence of ion pairs was first postulated by Bjerrum in 1926 (26Bje) to explain the low conductivity of sodium chloride in liquid ammonia. In 1954 Fuoss (54Sad) and Winstein (54Win) independently proposed the existence of two forms of ion pair. One type of ion pair consists of a tightly bond cation and

anion, in which there are no solvent molecules between the cation and the anion. This will be referred to as a tight ion pair. In the second type of ion pair the cation and anion were separated by a sheath of solvent molecules. This will be referred to as a loose ion. The first direct evidence for the existence of ion pairs was the ESR studies by Weissman and associates (58Ada, 61Ath) in which hyperfine coupling constants from the cation were observed, and in which the ion pair was observed simultaneously with the free ion. Since that time a large number of studies have been carried out on a wide range of compounds. (see 72Szw for a review of the studies to that date.)

Rieke et al. (74Rie) attributed the changes observed in the ESR spectra of 2,3-DMN/K/DME to an ion pair which reverts to a free ion or a looser ion pair at low temperatures. Similarly Kirk's (75Kir) investigations of the methyl substituted naphthalene/K/DME systems were explained in terms of a loose ion pair at low temperatures and a tight ion pair at higher temperatures with interconversion between the two ion pairs at intermediate temperatures. Molecular orbital calculations by Goldberg and Bolton (70Gol) for naphthalene, Kirk (75Kir) for the symmetric dimethylnaphthalenes and von Borczykowski and Mobius (76von) for 1- and 2-phenylnaphthalenes have been used to determine the potential energy as a function of the position of the counter ion. When the counter ion is less than ca. 0.4nm above the plane of the molecule a potential energy minimum occurs when the counter ion is positioned above the centre of either six membered ring. It was postulated that the cation oscillated between the two potential minima. The effect of the steric and

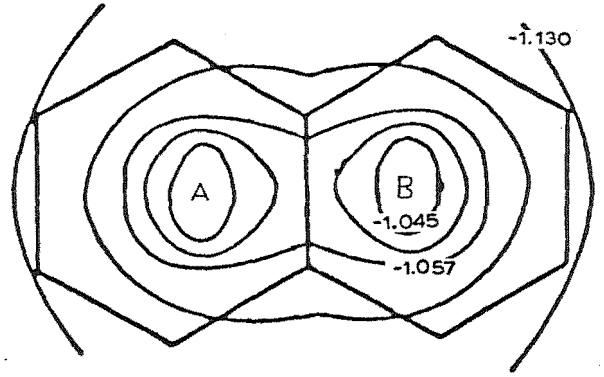

(a) naphthalene

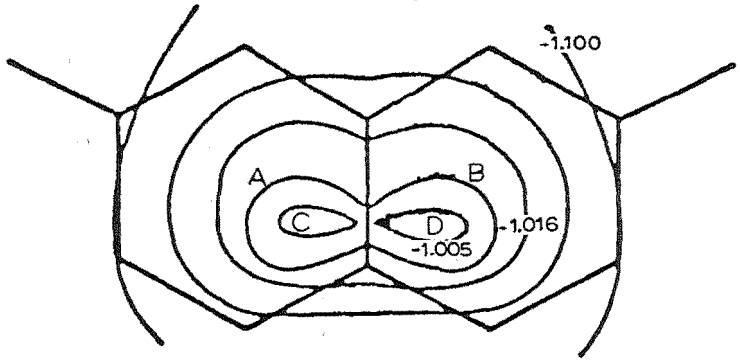

(b) 2,7-DMN

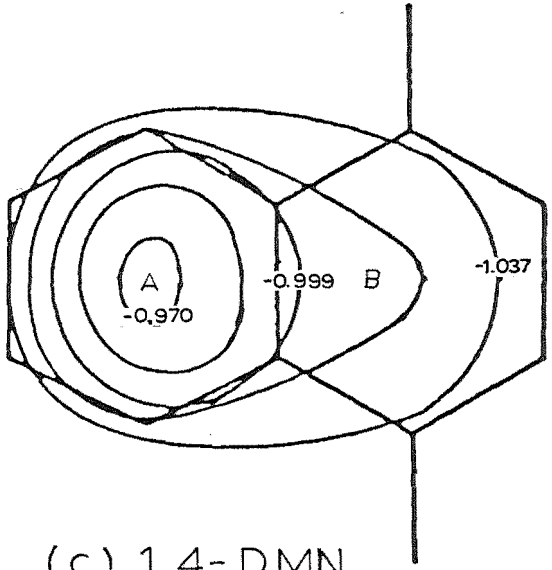

(c) 1,4-DMN

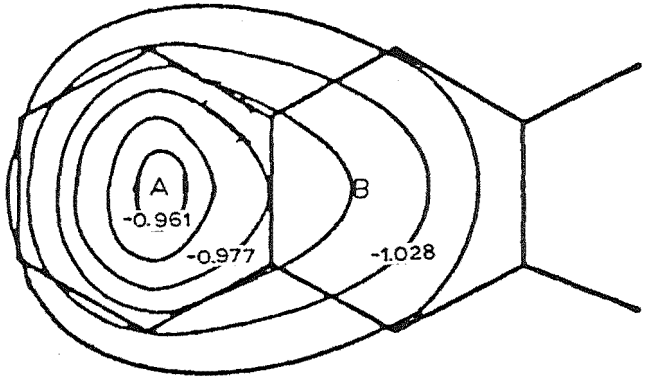

(d) 2,3-DMN

Figure 4.2 Ion Pair Potential Energy for some Methylnaphthalenes*

* Reproduced from 75Kir

electrostatic repulsion of a methyl substituent is to distort the potential energy minima; e.g in 2,7-DMN$^{\bar{\cdot}}$ the effect of the methyl substituents is to move the potential energy minima from positions A and B (Fig. 4.2b) to C and D. In 1,4-DMN$^{\bar{\cdot}}$ (Fig.4.2c) and 2,3-DMN$^{\bar{\cdot}}$ (Fig4.2d) the effect is to make the potential energy minimum at position B deeper than that at position A so that the cation would be at position B a greater proportion of the time than at position A. When the counter ion is more than 0.5nm above the plane of the molecule only one potential energy minima occurs, this is for the counter ion centred over the C_9-C_{10} bond.

1,2,3,4-tetramethylnaphthalene(1,2,3,4-TMN$^{\bar{\cdot}}$) was studied to determine if any ion pairing effects such as observed by Kirk (75Kir) in 1,4-DMN/K/DME, and Kirk and Rieke (74Rie) in 2,3-DMN/K/DME were occurring in this compound.

1,3,5,7-tetramethylnaphthalene (1,3,5,7-TMN) was not expected to yield unusual results and was studied as a matter of completeness, since samples of this compound were available. Similarly 1,2,3,4,5,8-hexamethylnaphthalene (1,2,3,4,5,8-HMN) and octamethylnaphthalene (OMN) were also expected to yield predictable results, although they were of some interest as no methylnaphthalene anion with more than four methyl substituents had been reported. Indeed Root and Rogers (69Roo) had reported that they were unable to form anions from OMN, 1,2,3,4,5,8-HMN or 1,2,3,4,6,7-HMN). OMN would also serve as an acyclic analog of tetracyclonaphthalene (see Chapter 6).

Brumby's work on the temperature dependence of the coupling constants of 1-and 2-methylnaphthalene in Na/THF and K/THF had raised some question of the assignments of the coupling constants

for these radicals. It was therefore decided to do a temperature dependence study for the 1- and 2-methylnaphthalene radicals in K/DME, which was the solvent system for which most results were available and consequently, for which the addivity relationships had been calculated.

Section 4.2
Experimental

Section 4.2.1 1-Methylnaphthalene^{-}

Samples of the 1-methylnaphthalene anion were prepared by exposing a solution of 1-methylnaphthalene to a potassium mirror. In all cases the solution turned an olive green colour. The solvents used were 1,2-dimethoxyethane(DME), 2-methyltetrahydrofuran(MTHF) and diethylether (DEE). A number of samples using sodium in tetrahydrofuran were also prepared. Spectra were collected using program COLLECT (section 2.4.1) from all these systems over a range of temperatures. Best fits to the ESR spectra were obtained for the DME, DEE and MTHF systems and are given in Appendix 4.1. No analysis of the sodium systems was carried out. All spectra were fitted using ESRCON, except for those of 1-MN in K/MTHF at temperatures above -44^{0}C for which the signal to noise ratio was too low for a satisfactory fit be produced. The results for 1-methylnaphthalene/K/DME at -88^{0}C agree well with those reported by Brumby (80Bru) for 1-methylnaphthalene/Na/THF at -76^{0}C. (see Appendix 4.1)

Section 4.2.2 2-Methylnaphthalene^{-}

The anion of 2-methylnaphthalene was prepared by reduction of 2-methylnaphthalene by potassium in DME, DEE, and MTHF, and by sodium in THF. Most samples turned the 'normal' olive green colour, but some turned orange (K/DME and K/MTHF) and one (Na/THF) turned a lemon yellow colour. The spectra obtained from the different coloured solutions was in all cases the same as that obtained from the olive green coloured solutions. The best fits to the collected ESR spectra, as calculated by ESRCON are given in Appendix 4.1. The fitted hyperfine coupling constants again agree well with those found by Brumby (80Bru) for 2-methylnaphthalene/Na/THF at -76^{0}C.

Section 4.2.3 1,2,3,4-Tetramethylnaphthalene^{-}

When reacted with potassium in DME, 1,2,3,4-tetramethylnaphthalene rapidly gave an olive green coloured solution. ESR spectra were collected over a range of temperatures from -88^{0}C to $+11^{0}$C. The form of the spectrum changed markedly, and reversibly with temperature. This linewidth effect prevented satisfactory simulation at all temperatures apart from -88^{0}C. ESRCON was used to fit the spectrum at -88^{0}C. The R value and the spectrum calculated from the fitted values both indicated that the fit was not very good. The values fitted at -88^{0}C are in reasonable agreement with those found by Gerson, Peake and Whitesides for 1,2,3,4-tetramethylnaphthalene/K/DME at -80^{0}C. The two sets of

hyperfine coupling constants are given in Appendix 4.1. The source of the linewidth effects is discussed in Section 4.3.3

Section 4.2.4 1,3,5,7-Tetramethylnapthalene^{-}

1,3,5,7-tetramethylnaphthalene reacted with potassium in DME. The resulting solution gave an ESR signal. The spectrum was readily fitted and the least squares fit to the experimental spectrum is given in Appendix 4.1

Section 4.2.5 1,2,3,4,5-Pentamethylnaphthalene^{-}

1,2,3,4,5-pentamethylnaphthalene gave an emerald green coloured solution when reacted with potassium in DME. A strong ESR signal was present but due to the large degree of overlap it was not possible to produce a satisfactory simulation of the experimental spectrum.

Section 4.2.6 1,2,3,4,5,8-Hexamethylnaphthalene

On reacting with potassium in DME 1,2,3,4,5,8-hexamethylnaphthalene gave the 'normal' olive green coloured solution and strong ESR signal. Over a period of 3-4 hours the colour of the solution slowly turned to lemon yellow, although no change in the ESR signal was seen. Spectra were recorded between $-87^{0}C$ and $-47^{0}C$, with no temperature variation being apparent. The fitted coupling constants are given in Appendix 4.1

Section 4.2.7 1,2,3,4,5,6,7,8-Octamethylnaphthalene

The one sample of octamethylnaphthalene gave an olive green coloured solution once the potassium mirror had been reformed by heating. A moderately strong ESR signal was present which was readily fitted and the fit refined using ESRCON. The coupling constants fitted are given in Appendix 4.1

Section 4.3
Discussion and Conclusions for Methylnaphthalene Anions

Section 4.3.1 Trends and Assignments in 1- and 2-Methylnaphthalenes

As can be seen from Appendix 4.1 the coupling constants found for the 1- and 2-methylnaphthalenes are in reasonable agreement with those found by Moss et al. (69Mos) under the same

Figure 4.3 1-Methylnaphthalene Anion* Coupling Constant Temperature Dependence

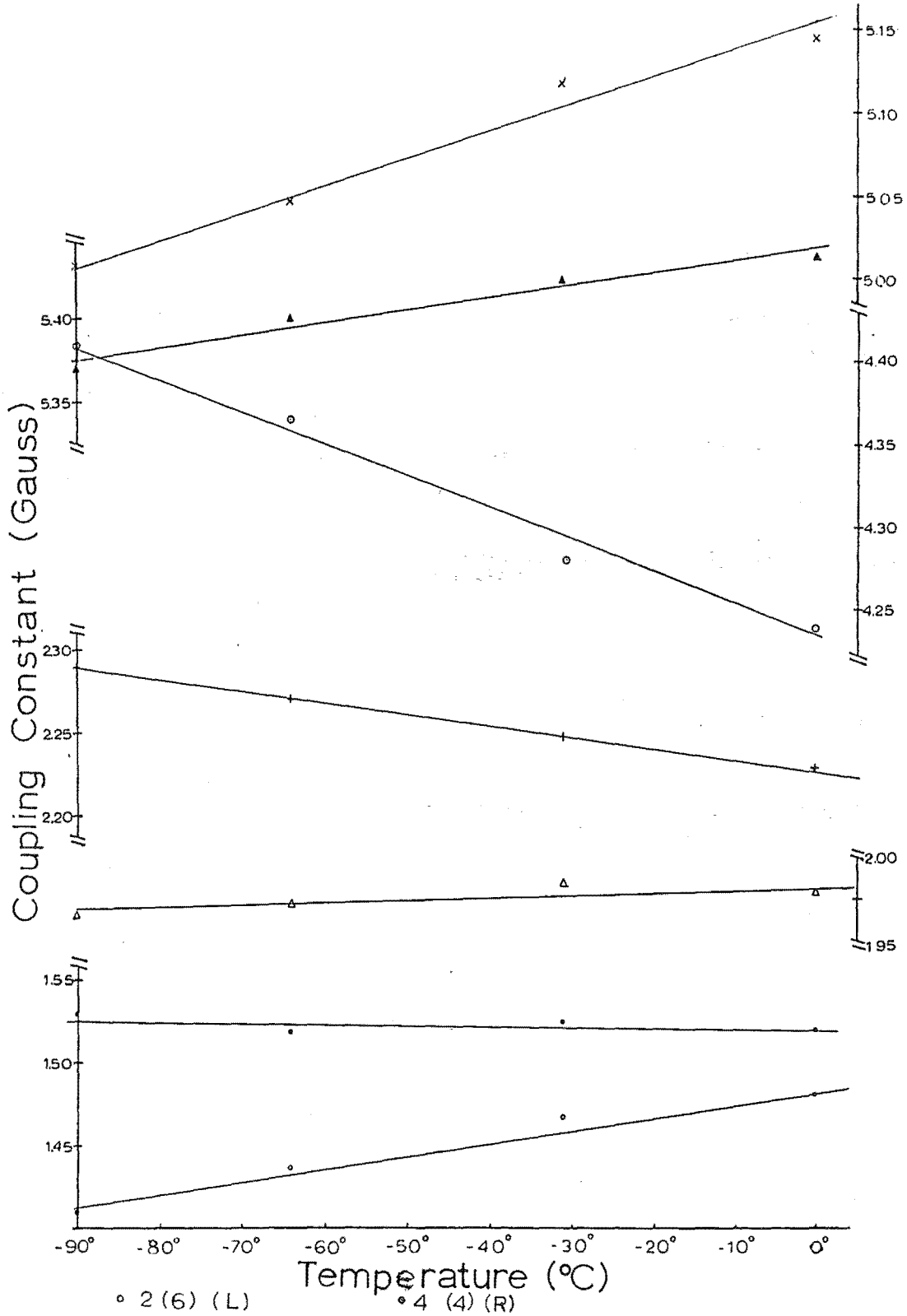

(L) indicates to use left-hand scale, (R) indicates right-hand scale
Brumby's assignments (80Bru) given in parenthesis
* 1-MN/K/DME

Figure 4.4 2-Methylnaphthalene Anion* Coupling Constant Temperature Dependence

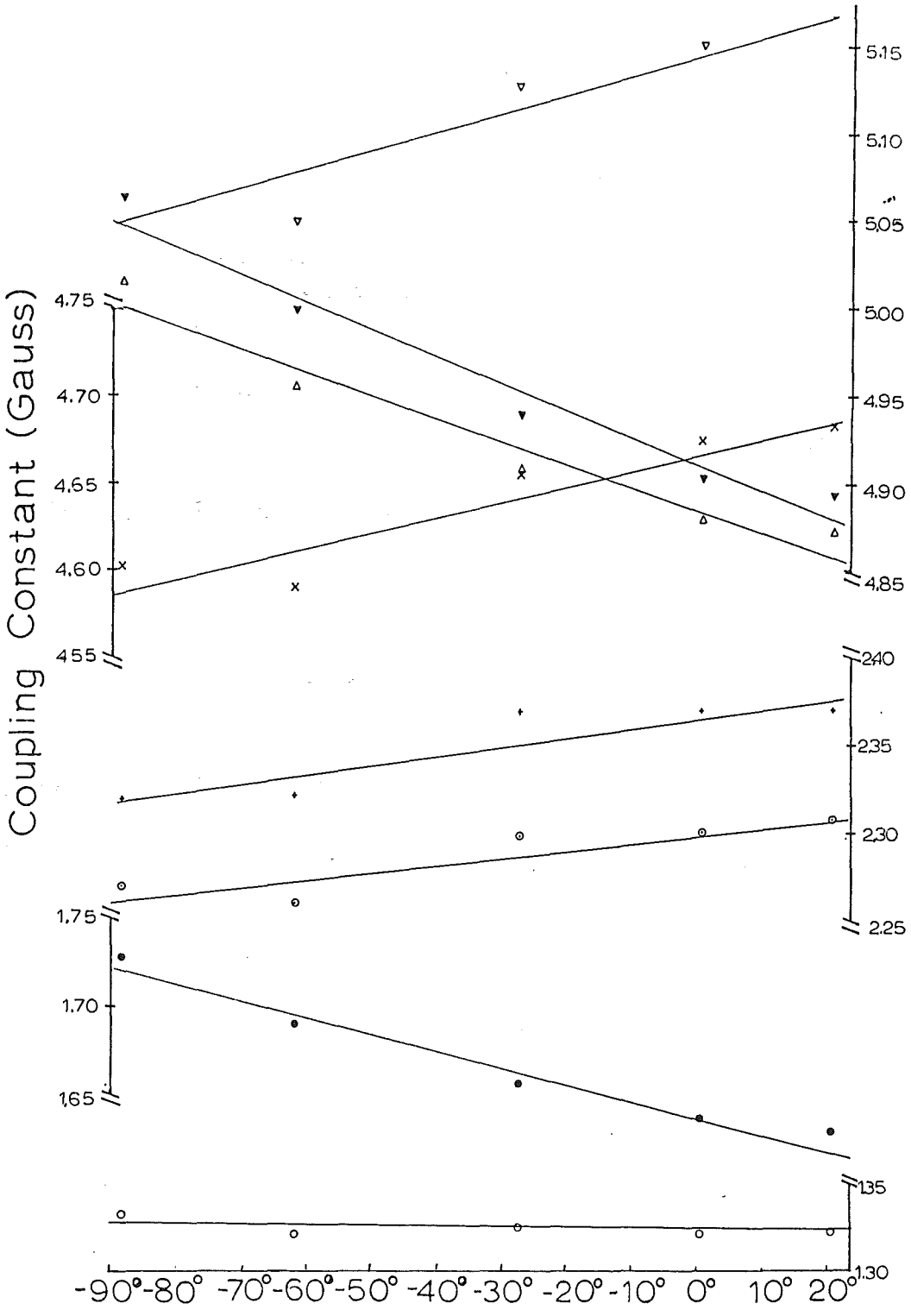

° 6 (6) (R) + 3 (7) (R) ▼4 (4) (R)
• 2 (2) (L) X 8 (8) (L) ▽5 (5) (R)
° 7 (3) (R) △ 1 (1) (L)

(L) indicates to use left hand scale, (R) indicates right-hand scale. Brumby's assignments (80Bru) given in parenthesis * 2-MN/K/DME

conditions and also with those found by Brumby (80Bru) in Na/THF. The temperature dependence of the coupling constants found in K/DME is given in Figs. 4.3 and 4.4 . The lines drawn are the least squares regression lines.

Calculations by Brumby (80Bru) for 1- and 2-methylnaphthalene^{-} indicate that the effect of decreasing the average distance between the counter ion and a given proton is to increase the coupling constant of that proton. Brumby calculated the difference in the proton coupling constants between the loose and tight ion pairs. Brumby made a number of assumptions, two of which require careful consideration. Brumby assumed that the cation was centred over either ring, and that the effective distance of the cation from the aromatic plane was the same whichever ring the cation was centred on. Kirk's (75Kir) calculations show clearly that the first assumption is not a good one, since the effect of the methyl substituent is to move the minimum in potential energy away from the centre of the ring. The second assumption cannot be evaluated directly, for methylnaphthalene anions in which the two rings are not equivalent it would be expected that the effective distance of the cation from the aromatic plane would not be the same for the two positions. However, given these reservations, Brumby's calculations do indicate that the changes in coupling constant with temperature can be correlated with changes in the proton-counter ion distance. A comparison between the temperature variation of the coupling constants reported by Brumby and those found in this study is given in Table 4.1.

Table 4.1 1- and 2-Methylnaphthalene Anion Coupling Constant Temperature Variation

1-Methylnaphthalene⁻				2-Methylnaphthalene⁻			
Position	Value (G)[1]	Temp. varia'n (mG/^{0}C)[2]		Position	Value (G)[1]	Temp. varia'n (mG/^{0}C)[2]	
1	3.854	-1.5	-2.4	1	4.764	-1.3	-1.7
2	1.529	+0.0	-0.0	2	1.729	-0.9	-0.9
3	2.290	-0.7	-0.4	3	2.322	+0.5	+0.8
4	4.408	-1.8	-2.5	4	5.063	-1.5	-2.3
5	5.372	+0.7	+1.3	5	5.063	+1.3	+1.2
6	1.409	+0.8	+0.9	6	1.331	-0.1	0.0
7	1.964	+0.2	+0.0	7	2.269	+0.4	+0.7
8	5.031	+1.6	+2.0	8	4.602	+0.9	+1.0

[1] $\pm$0.006

[2] left column this study $\pm$0.2mG/^{0}C, right column from (80Bru)

A portion of the differences apparent in Table 4.1 must be ascribed to the difference in counter-ion; potassium was used in the present study and sodium was used by Brumby. The combined errors are approximately $\pm$0.5mG/^{0}C, so that the differences between the two studies are probably not significant. The assignments given are considered in more detail in the following section where these assignments are compared with the assignments from the additivity relationship.

Moss et al. (69Mos) calculated an additivity relationship for methyl subsituted anions from the coupling constants for naphthalene$^{-\cdot}$, 1- and 2-methylnaphthalene$^{-\cdot}$, the symmetric dimethylnaphthalenes, and 1,4,5,8- and 2,3,6,7-tetramethylnaphthalenes. That is, a total of 17 α and 17 β coupling constants. Since that study, Kirk (75Kir) has fitted the asymmetric dimethylnaphthalenes and Gerson et al. (72Ger) have reported the coupling constants for 1,2,3,4-tetramethylnaphthalene$^{-\cdot}$.

In this study the work of Moss et al. on the 1- and 2-methylnaphthalenes, and that of Gerson et al. on 1,2,3,4-tetramethylnaphthalene$^{-\cdot}$, was repeated. Best fits for the spectra of 1,3,5,7-tetramethylnaphthalene$^{-\cdot}$, 1,2,3,4,5,8-hexamethylnaphthalene$^{-\cdot}$ and octamethylnaphthalene$^{-\cdot}$, which had not been reported, were found.

Taken altogether, this gave 32 equations in α coupling constants and 33 equations in β coupling constants. Least squares refinement of the additivity parameters gave the results tabulated in Table 4.2. The parameters determined by Moss et al. are included for comparison. The full least squares analysis is given in Appendix 4.2

There are a number of points to be made about the results given in Table 4.2. Firstly; this is the best fit, i.e. all the

TABLE 4.2

Additivity Parameters for Methylnaphthalene Anions

Proton Additivity Parameters

Parameter		Value (G)		Parameter		Value (G)	
1	2		3				3
α	α	-4.96±0.03	-4.97±0.05	β	β	-1.95±0.03	-1.93±0.05
A_B	a'	0.19±0.02	0.40±0.05	B_A	b	0.44±0.03	0.49±0.04
A_C	d'	-0.17±0.03	-0.08±0.05	B_C	c'	-0.40±0.03	-0.39±0.05
A_D	d	0.58±0.03	0.52±0.06	B_D	c	-0.05±0.03	-0.14±0.04
A_E	e	-0.37±0.03	-0.36±0.06	B_E	f	0.39±0.03	0.40±0.04
A_F	e'	-0.10±0.02	-0.12±0.05	B_F	f'	0.55±0.03	0.57±0.05
A_G	h'	0.36±0.02	0.20±0.05	B_G	g'	-0.38±0.03	-0.36±0.05
A_H	h	-0.12±0.02	-0.01±0.06	B_H	g	-0.32±0.03	-0.30±0.04
Overall σ		0.06	0.08			0.07	0.08

Methyl Additivity Parameters

Parameter		Value (G)		Parameter		Value (G)	
1	5		4				4
P	P	3.88±0.05	3.87	Q	Q	1.72±0.03	1.71
A_B	B	0.38±0.09	0.51	B_A	A'	0.22±0.05	0.23
A_C	C	-0.02±0.09	0.08	B_C	C'	-0.07±0.05	0.00
A_D	D	-0.60±0.09	-0.63	B_D	D'	0.08±0.05	0.16
A_E	E	0.49±0.09	0.52	B_E	E'	-0.36±0.05	-0.40
A_F	F	0.20±0.09	0.11	B_F	F'	-0.52±0.05	-0.49
A_G	G	-0.26±0.09	-0.38	B_G	G'	0.46±0.05	0.47
A_H	H	0.64±0.09	0.69	B_H	H'	0.51±0.05	0.47
Overall σ		0.12	-			0.06	-

Table 4.2 cont.

[1]standard nomenclature used in this work, [2]nomenclature used by Moss et al (69Mos), [3]values found by Moss et al, [4]values from Kirk, [5]nomenclature used by Moss et al and Kirk (75Kir)

---

assignments have been selected to give the best possible agreement between the additivity relationship and experiment. No account has been taken of the physical reasonableness or otherwise of the assignments. This has meant some changes in assignment from those used by Moss et al., which assignments were also based on the best least squares fit to the data then available. Specifically, the assignments for positions 1 and 5 in 2,3-DMN; 1 and 4 in 2,6-DMN; and positions 1 and 8 in 2-methylnaphthalene have been interchanged. These three changes have the effect of reducing the standard deviation for the α coupling constants. The least squares fit using Moss et al.'s assignment has a standard deviation of 0.0901G whereas the best least squares fit has a standard deviation of 0.0602G. The changes in assignment effectively interchange the values of parameters A_B and A_G (refer to Section 1.2 and appendix 4.2 for nomenclature). The only change made for the β subset is in the assignments for the 2 and 3 positions in 1,8-DMN; which have been interchanged, resulting in an improvement in the standard deviation from 0.0794G to 0.0735G. The full least squares analyses for the assignments used by Moss et al., and the best fit assignments are given in Appendix 4.2 Tables D and C respectively.

Secondly; the initial best fit least squares analysis of all the available data indicated that Kirk's (75Kir) coupling constants for 1,7-DMN⁻ were faulty. Specifically, Kirk reported that the α coupling constants were 4.540G, 4.883G and 4.883G, whereas the additivity relationship predicted coupling constants of 4.48G, 4.84G and 5.53G. A simulation using Kirk's values was in very poor agreement with Kirk's experimental spectra. Analysis of Kirk's original spectra gave the α coupling constants as 4.488G, 4.837G and 5.532G which not only gave a much better fit to Kirk's spectra, but are also in much better agreement with the additivity relationship. However since no computer record of Kirk's spectra existed, no least squares refinement of the coupling constant could be done, and hence the fit obtained was much inferior to that for the other compounds in this work.

The assignments for the monomethylnaphthalenes deduced from the additivity relationship, and listed in Appendix 4.1, are at variance with those determined by Brumby (80Bru) on the basis of temperature dependence and MO calculations (refer to Section 4.3.1). There is no conflict in the results found for the α coupling constants, but the assignments for the β coupling constants in 1-methylnaphthalene⁻ are totally different. Use of Brumby's assignments in the least squares refinement of the additivity relationship gave a standard deviation of 0.1067G. This set of assignments gave two calculated coupling constants which were 0.25G different from the experimental coupling constants, and 5 other calculated coupling constants which were more than 0.1G different from the corresponding experimental coupling constants. By comparison the best fit (that with standard

deviation of 0.0735G) had a largest difference of 0.14G and 4 other calculated coupling constants which were more than 0.1G different from the corresponding experimental coupling constants. The full least squares analysis using Brumby's assignments is given in Appendix 4.2, Table E. Brumby's assignments for positions 3 and 7 are exactly opposite those found from the additivity relationship as are the assignments for positions 2 and 6. The difference in temperature variation observed for these pairs of positions is sufficiently large that there is no doubt that the two assignment methods are at variance.

As has been indicated previously, Brumby's calculations are based on a model, which includes two questionable assumptions. It is impossible to determine, without further calculation, if this invalidates his results. Ideally, a number of different geometries would have been used to calculate the changes in coupling constant in going from one type of ion pair to the other. Further, the changes in coupling constant calculated by Brumby are differences between two MO calculations, and as such represent differences between two sets of inaccurate numbers. It would be anticipated that this difference would be less, not more, accurate than the calculated coupling constants themselves. On the other hand the additivity relationship is an empirical relationship and it is possible that due to the perturbing effects of the counterion it is not be precisely obeyed. Because of the uncertainities the assignment of the β coupling constants in 1-methylnaphthalene$^-$ can not be considered to be unequivocally established.

The number of methyl substituted naphthalene anions for which the coupling constants have been determined is now sufficiently large to allow the additivity relationship for the methyl coupling constants to be refined. There are 14 α and 13 β coupling constants reported. The least squares refined additivity parameters are given in Table 4.2 together with Kirk's parameters, which were derived from only the mono and dimethylnaphthalenes. The full least squares analysis is given in Appendix 4.3. There is no obvious pattern to the parameters derived, other than the observation that the additivity parameters for the methyl groups tend to be of opposite sign to the corresponding additivity parameters for the protons.

Section 4.3.3 Discussion of Linewidth Effects in 1,2,3,4-Tetramethylnaphthalene Anion

Kirk (75Kir) predicted that 1,2,3,4-tetramethylnaphthalene (1,2,3,4-TMN) in K/DME should show linewidth effects similar to those observed in 1,3-, 2,3-, and 1,4-DMN$^{\cdot-}$. Kirk observed that for 2,3- and 1,4-DMN$^{\cdot-}$ there was a temperature region for which linebroadening occurred and that above or below this temperature the lines again narrowed. In 2,3-DMN$^{\cdot-}$ the only lines to stay narrow are those for which $M_I(1)=M_I(5)=0,\pm1$. This condition requires that the change in A_1 (the coupling constant of the substituent at position 1) is equal and opposite to the change in A_5. In 1,4-DMN$^{\cdot-}$ the only lines to stay narrow are those for which $M_I(Me)=M_I(5)=0,\pm1$. This condition requires that the change in A_{Me} is equal and opposite to the change in A_5.

For a simple interconversion between a loose and a tight ion pair, (such as is postulated for methylnaphthalene/K/DME and other systems) Kirk predicted that the $M_I=\pm1$ lines should be broadened unequally for $M_I(1)$ and $M_I(5)$, since the changes in A_1 and A_5 were unequal. And, since these lines were equally broadened, ruled out such a simple interconversion. However Kirk assumed that the value of the coupling constants for the loose ion pair and the tight ion pair could be approximated by the observed coupling constants at low and high temperatures respectively. This assumption is valid only if the structures of both ion pairs do not vary significantly with temperature. However for the tight ion pair it would be expected that as the temperature increases the proportion of time spent at the energetically less favoured position (i.e the shallower energy minima, see Fig. 4.2) would increase thereby changing the value of the coupling constants of the tight ion pair. Similarly the coupling constants of the loose ion pair would also be expected to change with temperature. It is therefore possible that the changes in A_1 and A_5 are approximately equal and opposite which would imply that the $M_I=\pm1$ lines should be equally equally broadened. It was therefore felt that a model involving simply a loose ion pair and a tight ion pair, where the sum of A_1 and A_5 is kept constant, could adequately describe 1,4-DMN$^{\bullet-}$ and 2,3-DMN$^{\bullet-}$. If this was so then, it should also be possible to fit the spectra of 1,2,3,4-TMN$^{\bullet-}$ to such a model. Before any attempts were made to fit 1,2,3,4-TMN/K/DME it was decided that 1,4-DMN$^{\bullet-}$ should be fitted as a test of the model.

Using YKEXCH (Section 2.5.1), fits at high temperature, using a loose and a tight ion pair, were obtained. Similarly at low temperature it proved possible to obtain satisfactory fits. However no satisfactory fits could be obtained in the intermediate region. In this region the simulated spectra were extremely sensitive to small changes in rate, coupling constants and the ratio of the two species. At high and low temperatures the fits were not as sensitive to the rate and the coupling constants of the species present in smaller amount, or to the ratio of the two species. The fits at high temperature assumed a potassium hyperfine and at all temperatures it was assumed that the sum of the coupling constants from the methyl group and the proton at position 5 was constant.

It was found possible to fit 1,2,3,4-TMN⁻ using two species; the fitted parameters are given in Table 4.3, The experimental and simulated spectra are given in Fig. 4.5. It was found that no potassium hyperfine coupling was required to fit the experimental spectra. The plot of Log(K) versus 1/T is given in Fig. 4.6; ΔH is calculated to be -12 ± 6 kJ/mole , and ΔS -60J/K .mole. These values are similar to those found by Kirk for Na/THF systems.

Figure 4.5 Temperature Dependence of Spectra of 1,2,3,4-Tetramethyl-naphthalene Radical Anion*

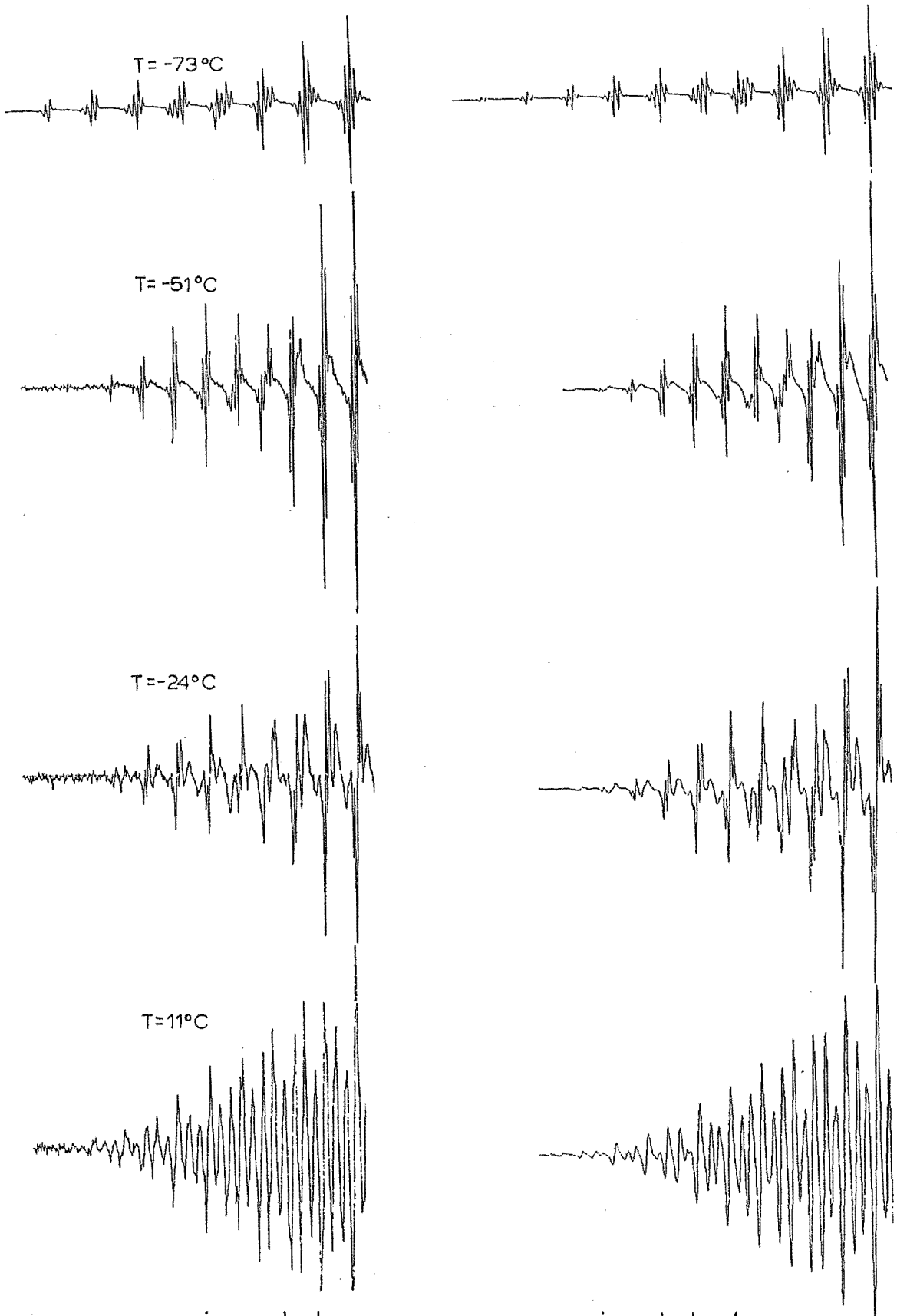

*1,2,3,4-TMN/K/DME

Figure 4.6 Plot of $Log_{10}(K)$ vs. 1/T for 1,2,3,4-Tetramethylnaphthalene*

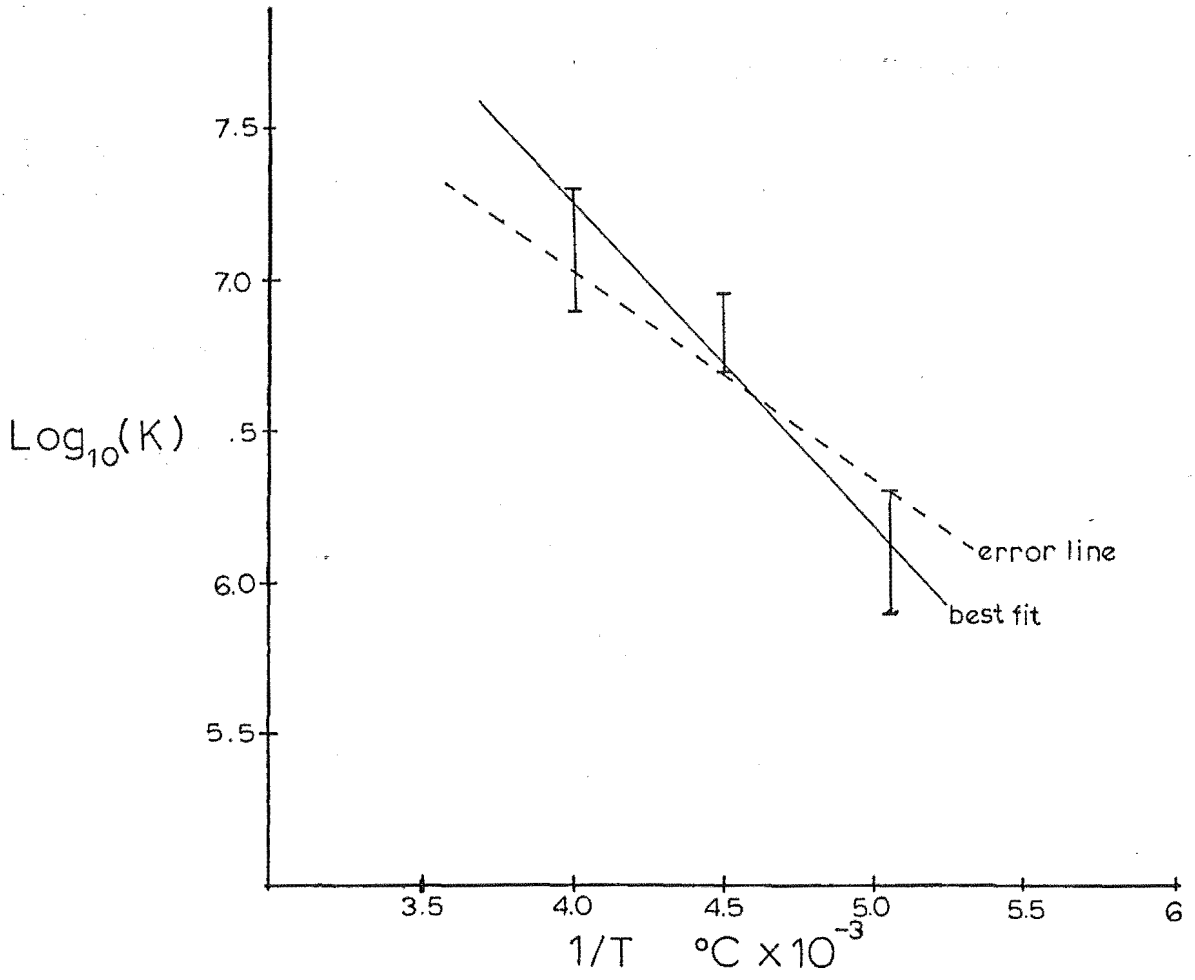

*1,2,3,4-TMN/K/DME

TABLE 4.3

Temperature Dependance of 1,2,3,4-Tetramethylnaphthalene/K^+/DME

Temp.	%A[1]	Rate[1] sec^{-1}		Coupling Constants[2] (G)			
				$A_{5,8}$	$A_{1,4}$	$A_{2,3}$	$A_{6,7}$
-73^0C	95%>90%>80%	$2x10^6<4x10^6<6X10^6$	A	5.201	3.680	1.923	1.72
			B	5.811	3.11	1.92	1.72
-75^0C	95%>90%>80%	$8X10^5<1X10^6<2X10^6$	A	5.136	3.654	1.916	1.704
			B	5.811	3.11	1.92	1.72
-51^0C	60%>50%>40%	$5x10^6<7x10^6<9x10^6$	A	5.081	3.64	1.92	1.72
			B	5.661	3.06	1.92	1.72
-24^0C	20%<30%<40%	$8x10^6<1x10^7<2x10^7$	A	5.031	3.69	1.92	1.72
			B	5.711	3.010	1.92	1.72
$+11^0C$	0%	-		5.611	3.06	1.92	1.72

[1]the middle figure given is the best estimate of the parameter, the other two figures are the error limits.[2] A and B are the two species present, A is presumed to be the loose ion pair and B the tight ion pair.

It appears likely that the data for the 1,3-, 2,3- and 1,4-DMNs and for 1,2,3,4-TMN$^{\cdot-}$ can be adequately explained in terms of an interconversion between a loose and a tight ion pair. In the loose ion pair the cation is centred at one position approximately over the centre of the molecule, and in the tight ion pair the cation oscillates between positions over the centre of the two rings. The mean position of the cation would be over the less substituted ring. There is however a degree of uncertainty because of the failure to produce satisfactory fits to the intermediate exchange region for 1,4-DMN$^{\cdot-}$. It is likely that only

with least squares fitting, such as employed by Barzaghi et al. (80Bar), would it be possible to fit these spectra adequately.

CHAPTER FIVE

STUDIES OF THE CATIONS OF SOME NAPHTHALENE DERIVATIVES

The introduction to this chapter is a review of monomer methyl substituted naphthalene cations. Section 5.2 contains details of the observations made and any comments on goodness of fit for the simulated spectra. The results in the form of the simulated coupling constants are given in Appendix 5.1 Tables A, B and C for normal monomer cations, methylnaphthalenedisulphides and miscellaneous other species respectively. Section 5.3 is a brief account of attempts made to prepare one of the dimethyl-naphthalenedisulphides observed. Section 5.4 contains the discussion of the results and any conclusions reached. It is subdivided into four subsections covering methylnaphthalene monomer cations, hindered rotation in 1,8-DMN^{+} and OMN^{+}, naphthalenedisulphide cations, and perylene cations. Section 5.5 is a brief discussion of suggestions for further investigations.

Section 5.1

Introduction to Methyl Substituted Naphthalene Cation Radicals

There is no series of compounds for which the set of additivity relationships for both the cations and anions has been reported. The comparison of the additivity relationships for a cation series and an anion series would be expected to give some insight into the difference in electron distribution between the cations and anions.

The additivity relationships for the methylnaphthalene radical anions were first calculated by Moss et al in 1969 (69Mos) and have been refined in Section 4.3.2. Prior to the present study there were not sufficient methyl substituted naphthalene cation results reported to allow the evaluation of the additivity relationship.

The first study of methyl substituted naphthalene cations was that carried out by Lewis and Singer (65Lew) in 1965. Using $SbCl_5$ in CH_2Cl_2 they produced the naphthalene dimer cation. This result was reproduced by Howarth and Fraenkel in 1969 (69How), who also reported the monomer cation of 1,4,5,8-tetramethylnaphthalene and the dimer of 2,3,6,7-tetramethylnaphthalene. In a 1969 study, octamethylnaphthalene+ and 1,2,3,4,5,8-and 1,2,3,4,6,7-hexamethylnaphthalenes were reported by Roots and Rogers (69Roo), using sulphuric acid as both oxidant and solvent. They reported the formation of the monomer cations only, for all three compounds. Yoshimi and Kuwata in 1972 (72Yos) used $SbCl_5$ in a mixture of CH_2Cl_2 and SO_2 to oxidise 1,4-, 1,5- and 1,8-dimethylnaphthalenes. They reported the monomer cation spectra for

all three, and a dimer spectrum for 1,4-dimethylnaphthalene. The most recent report of a methylnaphthalene radical cation in solution is that of Gerson, Peake and Whitesides in 1972 (72Ger), who oxidised 1,2,3,4-tetramethylnaphthalene with $AlCl_3$ in methylene chloride. A 1979 study of naphthalene in $SbCl_3/AlCl_3$(8%) melt (80Buc) reported the formation of perylene† from naphthalene. This is an example of a Scholl Condensation (65Bal). In the case of naphthalene the reaction procedes through 1,1'-binaphthyl. The precise mechanism for this condensation is still being disputed, but seems likely to include the formation of a cation followed by attack on neutral naphthalene and loss of hydrogen atoms. Whether hydrogen is lost as two hydrogen radicals, as two hydrogen cations or by some other means is not yet known. The appearance of this type of product from naphthalene and methylnaphthalenes was therefore considered a strong possiblity

As ESR spectra, attributed to dimer cation formation had been reported from a number of methyl substituted naphthalenes and other compounds it was also hoped to observe dimers for the methylnaphthalenes being studied.

Section 5.2

Experimental : Observations and Results

This section contains observations made and the results obtained. The method of sample prepartion used is that described in Section 2.2.2. The type of spectra observed for each compound is summarised in Table 5.1. The coupling constants fitted are given in Appendix 5.1, Table A for the methylnaphthalene cations, Appendix 5.1, Table B for the methylnaphthalenedisulphides and Appendix 5.1, Table C for any other compounds. As naphthalene gives typical spectra of all products, except the monomer cation, the reactions of naphthalene will be dealt with in greater detail. For the mono and dimethyl naphthalenes their reactions can be assumed to be similar unless stated otherwise. The best fits to all spectra were found using ESRCON unless stated otherwise.

Section 5.2.1 Naphthalene

After sealing the sample tube containing the naphthalene sample and evacuating it on the vacuum line, the $AlCl_3$ was sublimed. The naphthalene turned a faint pink, presumably due to formation of a complex with the $AlCl_3$. On addition of the CH_2Cl_2 the naphthalene dissolved to form a pale olive green solution typical of naphthalene ions. During the freeze/pump/thaw cycles the solution when frozen was red, returning to an olive

TABLE 5.1

Products of the Reaction of $AlCl_3/SO_2$ with Methylnaphthalenes

Compound	cation	dimer	Disulphide	Perylene	Other
Naphthalene	-	X	X	X	-
1-MN	-	-	X	-	X
2-MN	-	-	X	?	-
1,3-DMN	-	-	X	?	-
1,4-DMN	X	-	-	-	-
1,5-DMN	X	-	-	-	-
1,6-DMN	-	-	X	?	-
1,7-DMN	-	-	X	X	-
1,8-DMN	X	-	X	-	?
2,3-DMN	-	-	X	?	-
2,6-DMN	-	?	X	-	-
2,7-DMN	-	-	X	?	-
1,2,4-TriMN	X	-	-	-	-
1,2,3,4-TMN	X	-	-	-	-
1,3,5,7-TMN	X	-	-	-	-
1,2,3,4,5-PMN	X	-	-	-	-
1,2,3,4,5,8-HMN	X	-	-	-	-
OMN	X	-	-	-	-

X means that this product has been observed. ? means that what is believed to be this product is has been observed.

DMN = Dimethylnaphthalene, TMN = Tetramethylnaphthalene, PMN = Pentamethylnaphthalene, HMN = Hexamethylnaphthalene, OMN = Octamethylnaphthalene

green colour on thawing. Addition of SO_2 caused the solution to turn a pale brown colour, which colour deepened on mixing. The final solution when placed in the cavity was a dark, opaque brown. Generally, an ESR signal appeared within a couple of minutes of mixing. No correlation was found between signal strength, signal type, or colour. The gain settings used were generally one order of magnitude higher than that used with the methylnaphthalene anions, despite similar concentrations of both substrates being used.

The spectrum observed was the overlap of spectra from three separate species.(see Fig. 5.1) Two species gave spectra of linewidth ca. 0.1 Gauss and centred at g=2.008 and g=2.002 . The other species had a spectrum consisting of a single broad line of linewidth 15 to 20 gauss centred at g=2.004. The spectrum with g=2.0028 has, on the basis of g-value, and coupling constants, been identified as that of the perylene cation.The species with g=2.0083 will be shown to be the cation of naptho(1,8-cd)-1,2-dithiole (which will be referred to henceforth as naphthalenedisulphide).

A large number of naphthalene samples were prepared yielding various ratios of these three species plus also the naphthalene dimer and another species for which the ESR could not be satisfactorily fitted and therefore for which no identification is possible. The naphthalene dimer cation was observed simultaneously with the naphthalenedisulphide cation and with the perylene cation. Attempts to control the ratio of the various products by altering the amount of $AlCl_3$ and of SO_2 met with only modest success. The dimer was formed only when little or no

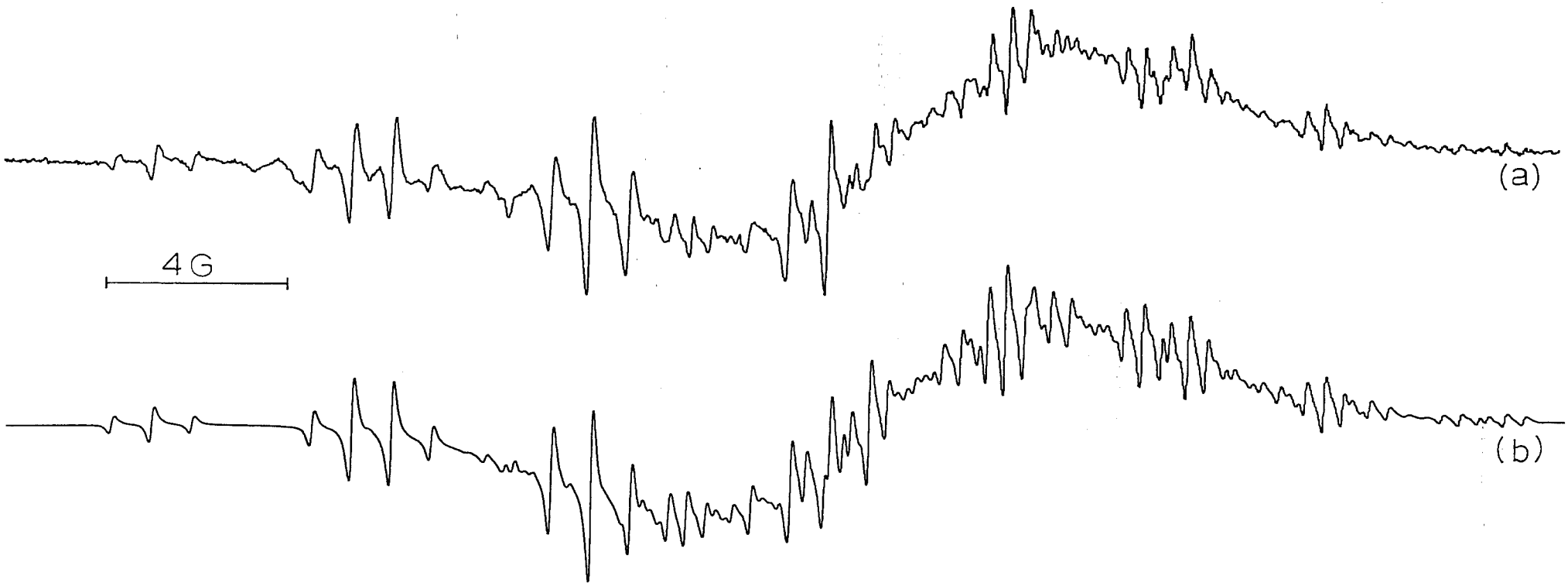

Figure 5.1
ESR Spectra of the Reaction Products of Naphthalene Cation at -60°C

(a) experimental
(b) simulated

SO_2 was used. Similarly no disulpide signal was seen in the absence of SO_2 and generally larger amounts of SO_2 (approximately $1\text{-}2x10^{-3}$ ml of liquid SO_2 in the sample arm) than would normally be used, were required to give satisfactory disulphide cation signal strength.

Often the sample required dilution and remixing to minimise the linewidth and maximise the signal strength. The maximum signal strength was found between -60^0C and -30^0C. At these temperatures the lifetime of the sample was approximately 12 to 18 hours. At higher temperatures (ca. 0^0C) the signal from the sample decomposed rapidly, with a lifetime of less than an hour.

Section 5.2.2 1-Methylnaphthalene

1-Methylnaphthalene readily gave a strong methylnaphthalenedisulphide cation signal. One sample intially gave a signal with linewidth of 70mG and g of approximately 2.006 . The g-value is approximate as it is measured relative to the quartz signal found in the quartz insert of the variable temperature controller. This g-value rules out the possiblity that this is the spectrum of the methylperylene cation from the Scholl Condensation of 1-methylnapathalene. The fitted coupling constants are 0.270G(2 hydrogens), 0.440G(4 hydrogens), 0.020G(two hydrogens), 2.306g(2 hydrogens), 4.770G(2 methyl groups) and imply a dimer of some form. This spectrum also shows evidence of another species with a lower g-value. After dilution

this sample showed a normal methylnaphthalenedisulphide cation spectrum with no broad curve and no other species present.

Section 5.2.3 2-Methylnaphthalene

2-Methylnaphthalene reacted readily to give a strong methylnaphthalenedisulphide cation signal, with dilution being required to give minimum linewidth. Spectra were obtained both with and without the presence of a of signal from a methyl-perylene cation. A baseline curve centred at g=2.0041 and linewidth of 7 Gauss was present in all samples.

Section 5.2.4 1,3-Dimethylnaphthalene

1,3-Dimethylnaphthalene gave a spectrum containing a strong tetramethylperylene cation signal in addition to the dimethyl-naphthalenedisulphide cation and baseline signals. Because of the interferring effect of the tetramethylperylene signal only the low field half of the spectrum could be fitted. The tetramethyl-perylene signal was however not sufficiently strong to be fitted.

Section 5.2.5 1,4-Dimethylnaphthalene

1,4-Dimethylnaphthalene gave samples which were initially pale green and deepened to dark green when mixed. Strong, well resolved spectra were observed with the outer most lines of the

being seen. On increasing temperature to -60^0C the colour changed to a deep radiant blue and the spectrum decayed quickly to be replaced by spectra from two species, one with g=2.015 the other with g=2.005 . The line at g=2.015 has two shoulders indicating unresolved hyperfine coupling. The signal at g=2.005 consists of nine groups of lines, but is not sufficiently well resolved to be fitted.

The observed coupling constants do not agree well with those observed by Yoshimi and Kuwata (72Yos). The spectra published by this group however, have poorer signal to noise ratios and are not as well resolved as those of the present study.

The signals with g=2.005 and g=2.015 must contain sulphur, beyond that however nothing can be said. Makekla et al. (84Mak) report the observation of a signal with similar g-value and produced by the reaction of hexahydropyrene in $HFSO_4$. This group attributes the signal to a sulfinyl .

Section 5.2.5 1,5-Dimethylnaphthalene

1,5-Dimethylnaphthalene gave an olive green solution which at -80^0C decayed within 2-3 hours. At higher temperatures decay was more rapid. Good spectra were obtained leading to satisfactory simulations. The spectra were of better signal to noise ratio and greater resolution than those of Yoshimi and Kuwata and the best fits consisted of coupling constants similar to those reported by Yoshimi and Kuwata (72Yos). The least

squares refined coupling constants are given in Appendix 5.1, Table A.

Section 5.2.6 1,6-Dimethylnaphthalene

1,6-Dimethylnaphthalene initially gave a spectrum consisting of the dimethylnaphthalenedisulphide cation and the tetramethylperylene cation spectra in approximately equal amounts. On dilution however the tetramethylperylene cation disappeared leaving a well resolved dimethylnaphthalenedisulphide cation spectrum.

Section 5.2.7 1,7-Dimethylnaphthalene

1,7-Dimethylnaphthalene initially gave a spectrum of the dimethylnaphthalenedisulphide cation and the tetramethylperylene cation in approximately equal amounts. Dilution resulted in the linewidth decreasing significantly and the proportion of the tetramethylperylene increasing. It proved possible to fit the tetramethylperylene spectrum directly by simulating the centre of the spectrum and to derive the four smallest coupling constants of the dimethylnaphthalenedisulphide cation from the low field portion of the spectrum where there were no tetramethylperylene cation lines. The large methyl coupling constant could also be obtained by inspection. It proved impossible however to pick out the remaining ring proton coupling constant directly. A value for this constant was found using the additivity relationship which

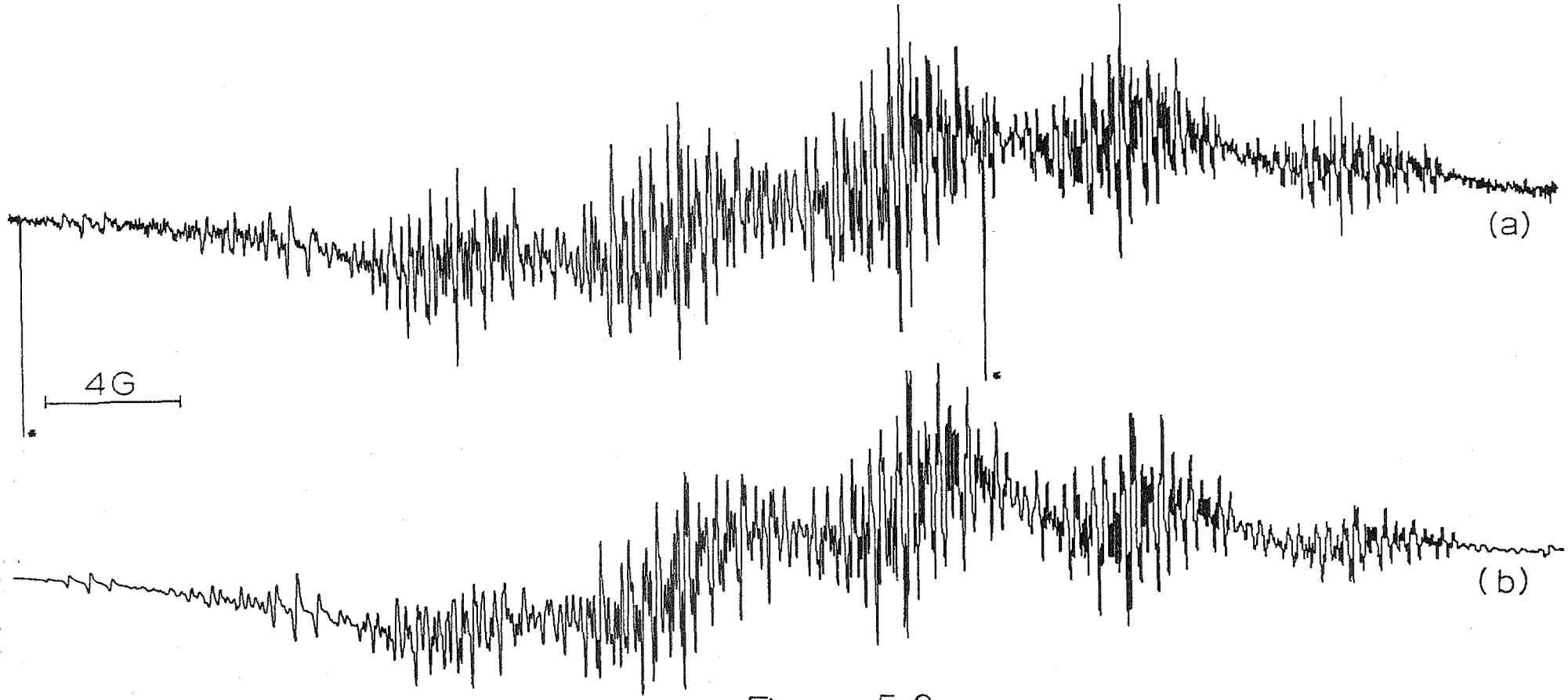

Figure 5.2
ESR Spectra of the Reaction Products of 1,7-Dimethylnaphthalene Cation at -60°C
(a) experimental
(b) simulated
* Field Marker

had been derived, and this set of coupling constants was used in ESRCON with satisfactory results. (see Fig. 5.2)

The tetramethylperylene formed is either 2,4,8,10-tetramethylperylene or 2,4,9,11-tetramethylperylene. It is not possible to decide between these two possibilities on the basis of the coupling constants.

Section 5.2.8 1,8-Dimethylnaphthalene

Most samples of 1,8-dimethylnaphthalene gave the spectrum of the monomer cation. One gave very weak spectra from the dimethylnaphthalenedisulphide cation and from a species with g=2.003 (measured relative to the quartz signal). This latter species had a methyl coupling constant of 6.5 Gauss and a quintet with coupling constant 0.33 Gauss. The signal to noise level of the spectra was too low to allow a complete analysis to be made. However 3,4,9,10-tetramethylperylene, which would be the expected product from the Scholl Condensation, can be ruled out as the spectra are too complex for this species.

Both the 1,8-DMN cation signal and the dimethylnaphthalene-disulphide cation signal decayed within 4-5 hours at -80^{0}C and decayed more rapidly at higher temperatures.

ESRCON was used to fit the calculated spectrum to the experimental spectrum. The fit was satisfactory for the positions of all lines. However for $M_I(Me)=\pm 3$ the calculated intensity of the lines was too low by an order of magnitude. This is shown in Figure 5.3 . There is little doubt that the calculated coupling

Figure 5.3
1,8-Dimethylnaphthalene^{+} Spectra at -84°C

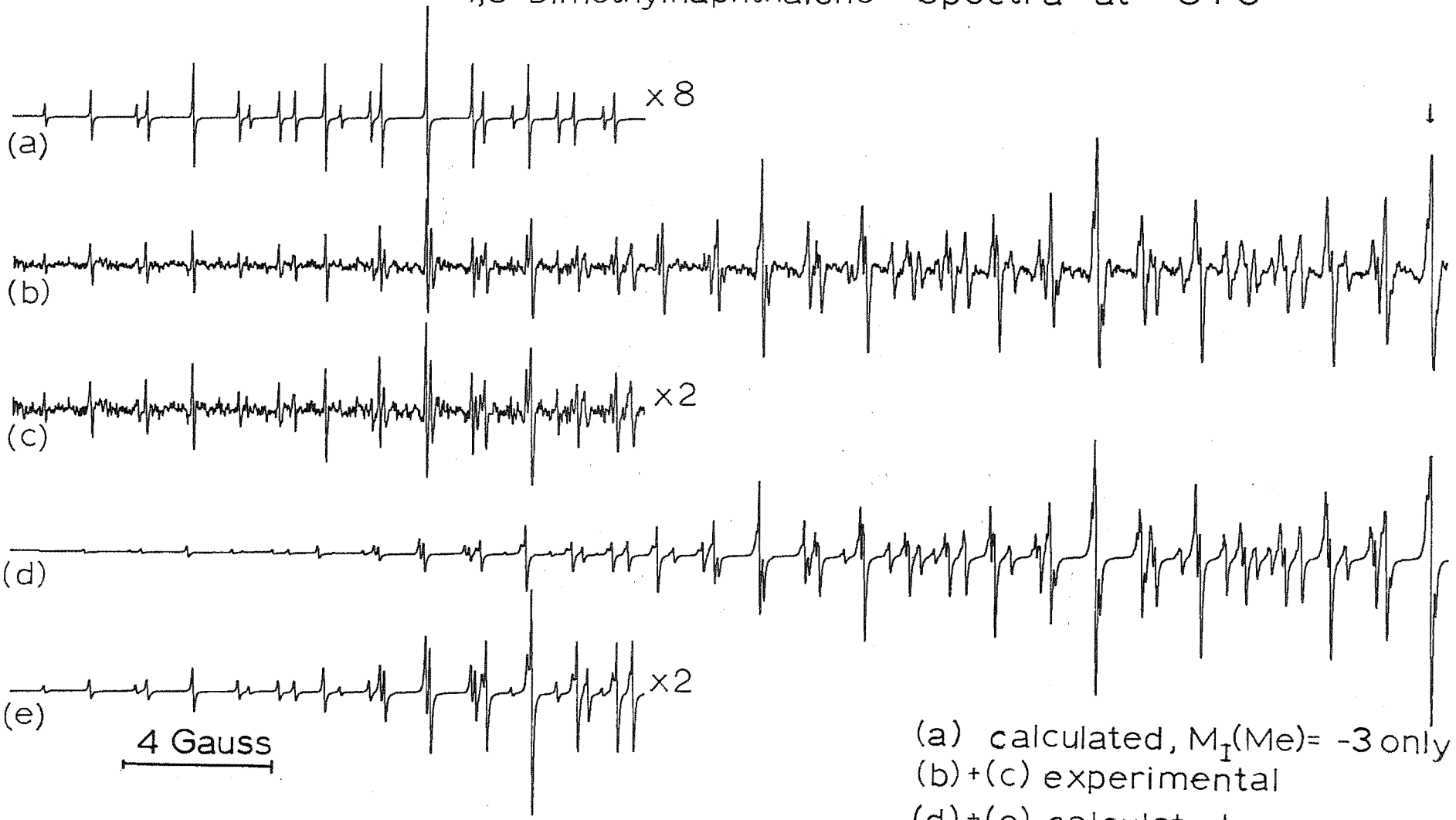

constants given in Appendix 5.1, Table A are correct, since the outer most lines of the spectrum were found, and the spectrum fitted from these lines. It was found that the spectrum could be fitted for $M_I(Me)=0,\pm1,\pm2$, with a linewidth of 40mG. However for $M_I(Me)=\pm3$ the amplitude needed to be increased by a factor of 8 and the linewidth reduced to 30mG.

Section 5.2.9 2,3-Dimethylnaphthalene

2,3-Dimethylnaphthalene readily yielded a strong, well resolved, dimethylnaphthalenedisulphide cation spectrum containing only a very minor tetramethylperylene cation component.

Section 5.4.10 2,6-Dimethylnaphthalene

2,6-Dimethylnaphthalene initially gave a dark green solution with a weak, poorly resolved spectrum due to a species with g=2.0026 . Mixing and dilution gave a dimethylnaphthalene-disulphide cation spectrum with no tetramethylperylene cation signal present.

The best fit found to the initial spectrum is 0.117G(12 hydrogens), 2.572G(8 hydrogens), 4.888G(4 hydrogens). The fit 0.117G(12 hydrogens), 2.572G(4 hydrogens), 4.888G(8 hydrogens) is only slightly worse. These results suggest the formation of a dimer cation with the methyl coupling constant 0.117 Gauss. The second fit, of 0.117G(12 hydrogens), 2.572G(4 hydrogens), and 4.888G(8 hydrogens), appears more reasonable as this would allow

the 4.888G coupling constants to be assigned to the eight α coupling constants. The alternative would require four α coupling constants to be the same as the β coupling constant. The poor signal to noise ratio of the spectrum make this a very tentative identification.

Section 5.2.11 2,7-Dimethylnaphthalene

Initially 2,7-dimethylnaphthalene showed only a very weak signal, but after remixing a strong dimethylnaphthalenedisulphide cation signal was present as well as a weaker tetramethylperylene cation signal.

Section 5.2.12 1,2,4-Trimethylnaphthalene

A sample of crude 1,2-dimethylnaphthalene gave a strong well resolved spectrum with g=2.0027 . There was also a broad baseline curve with wavelength 14-20 Gauss. No other species were present. A simulation with the parameters given in Table 5.2 fitted very well, showing clearly the presence of a trimethyl-naphthalene cation. The presence of an impurity was confirmed by both NMR and HPLC, although no identification of the impurity could be made.

The spectrum was assigned to 1,2,4-trimethylnaphthalene$^+$ on the basis of a least squares refinement of the β subset of the

additivity parameters for the methylnaphthalene cations. The best fit for 1,2,4-trimethylnaphthalene$^+$ had a standard deviation of 0.1023G. The best fit for 1,2,5-trimethylnaphthalene$^+$ had a standard deviation of 0.1578G . The best fit for 1,2,8-trimethylnaphthalene$^+$ had a standard deviation of 0.1659G. Any other trimethylnaphthalenes can be excluded on the basis of the methyl coupling constants, since the coupling constants of 9.87G and 8.97G must belong to α methyl groups.

The methyl coupling constants were assigned on the basis of an INDO calculation which gave coupling constants of 10.92G and 9.59G for the methyl groups at 1 and 4 respectively. On this evidence the 9.87G coupling constant was assigned to the 1 position and the 8.97G constant to the 4 position.

Section 5.2.13 1,2,3,4-Tetramethylnaphthalene

1,2,3,4-Tetramethylnaphthalene when reacted with $AlCl_3/SO_2$ gave a bright green solution and a strong well resolved signal with g=2.0030. The fitted coupling constants are similar to those found by Gerson at el. (72Ger)

Section 5.2.14 1,3,5,7-Tetramethylnaphthalene

1,3,5,7-Tetramethylnaphthalene gave a very intense olive green solution which gave a very strong signal, g-value 2.0027. Carbon-13 satellite peaks were visible, but the resolution was insufficient to allow these coupling constants to be determined. The simulated spectra indicated the presence of one very small

coupling constant and one coupling constant which was the difference between two other coupling constants. A further sample was prepared which yielded better resolved spectra in which the small coupling constant was clearly resolved and where the other coupling constants were not sum and difference. The coupling constants that give the best fit to the experimental spectrum are given in Appendix 5.1, Table A.

Section 5.2.15 1,2,3,4,5-Pentamethylnaphthalene

1,2,3,4,5-Pentamethylnaphthalene gave a clear green sample and medium strong signal. However the signal was not sufficiently strong for the outside lines of the spectrum to be observed and so it did not prove possible to analyse this spectrum.

Section 5.2.16 1,2,3,4,5,8-Hexamethylnaphthalene

1,2,3,4,5,8-Hexamethylnaphthalene readily gave an orange solution with a medium/weak ESR signal when only $AlCl_3$ was used as oxidant. The spectra has a g-value of 2.0030. The fitted coupling constants are substantially the same as those found by Root and Rogers (69Roo).

Section 5.2.17 1,2,3,4,5,6,7,8-Octamethylnaphthalene

Octamethylnaphthalene gave a golden orange solution and weak signal. At higher temperatures (above $-60^{0}C$) the spectrum (see Fig. 5.4) could be fitted in terms of the coupling constants determined by Root and Rogers (69Roo), although it is only the position of the lines and not their intensities that is correct. The lines for $M_I=\pm3,\pm6$ are much higher in the experimental spectra than in the calculated spectra. As the temperature is lowered this discrepency worsens until at $-87^{0}C$ the spectrum has collapsed to 5 groups of 13 lines. Both the linewidth and intensity have dropped dramatically as compared to the higher temperature spectra. This temperature effect was reversible. This change in the spectrum with change in temperature is discussed in Section 5.4.2.

Section 5.3

Attempts at Preparation and Separation of Products of the Reaction of $AlCl_3/SO_2$ with 2-Methylnaphthalene

An attempt was made to prepare and characterise the products of the reaction of sulphur dioxide with 2-methylnaphthalene. A number of procedures were explored in the attempt to separate the aluminium trichloride from the organic products, but no satisfactory method was found.

Figure 5.4 Temperature Dependence of Octamethylnaphthalene Radical Cation Spectra

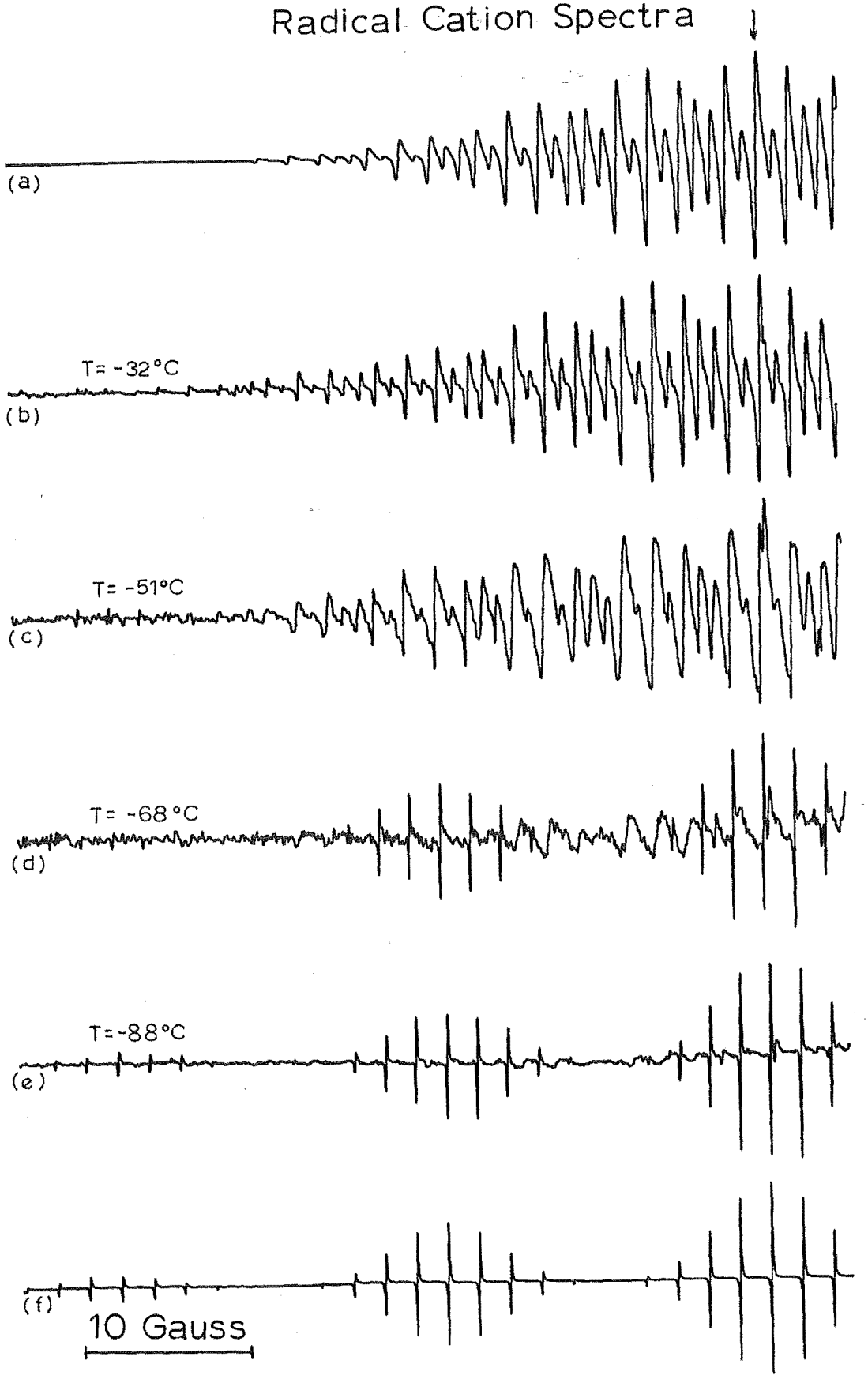

(b),(c),(d) and (e) experimental (a) and (f) simulated

The reaction was carried out using a scaled-up form of the technique used for sample preparation for ESR studies. 2-Methylnaphthalene (200mg) was placed in a 2cm glass tube and aluminium trichloride (ca. 500mg)was placed in a side arm of this tube which was then sealed and placed on a vacuum line. The aluminium trichloride was purified by sublimation along the side arm. Dichloromethane (ca. 50ml) was then distilled in, and any oxygen present removed by freeze/pump/thawing the solvent. Sulfur dioxide (ca. 10ml) was then added and after sealing, the sample tube was shaken and allowed to stand for 1 hour.At the end of this period part of the sulfur dioxide was removed by leaving the sample tube open to air for four hours. The resulting solution was dark green-black in colour, and was subjected to the following procedures.

(a) A 2ml aliquot of the sample was evaporated to yield a brick red solid.

(b) A second aliquot left exposed to air went the same red colour within hours.

(c) A third aliquot washed with saturated aqueous sodium bicarbonate again gave a brick red precipitate which was insoluble in water, dichloromethane, benzene chloroform, and ethanol. A component was soluble in acetone.

(d) Addition of hexane to a fourth aliquot resulted in a green precipitate forming which when dried became a brick red in colour.

(e) According to Schmidt et al (78Sch) addition of sodium sulphate should result in the precipitation of aluminium sulphate which can then be filtered off.

Addition of sodium sulphate dexahydrate (10mg) dissolved in dichloromethane (50ml) to an aliquot (5ml) of the reaction mixture resulted in the deposition of a dark black-green precipitate, leaving a deep green solution. Over a period of an hour the solution turned red. The solution was filtered and addition of hexane to the filtrate did not produce any further precipitation. Removal of the solvent yielded small red needles(ca.1mg). Use of anhydrous sodium sulphate gave a similar result.

(f) When sodium sulphate decahydrate was added to the remaining reaction mixture (ca.20ml), the mixture filtered and the filtrate evaporated, a dark red , acrid smelling compound(ca.5mg) was produced. ^{1}H NMR did not reveal the presence of any aromatic protons, and the absence of well resolved peaks indicated the the sample contained a number of different compounds.

From the observations above it appears that the products formed are both air and water sensitive.

Section 5.4

Discussion and Conclusions for E.S.R of methyl substituted naphthalene/$AlCl_3/SO_2$ systems

Section 5.4.1 Monomer Methylnaphthalene Cations

The spectra of the methylnaphthalene cations were collected and analysed with the aim of evaluating the additivity parameters for this series and comparing them with those in the anion series. In most of the systems studied perylene cations and/or disulphide cations were formed in preference to the monomer cation. This has meant that there are very few observations on which to base any evaluation of the additivity relationship for monomer cation. It has however proved possible to make some estimates of most of the parameters of interest, which appear in Tables 5.2, 5.3 and 5.5

Table 5.2 shows the additivity parameters for the effect of a methyl group on a hydrogen coupling constant. The β subset (i.e. the hydrogens in the β position) has been evaluated from 13 independent equations, with all parameters being defined from at least two equations. The α subset has been evaluated from 8 equations in 8 variables, where the variables α, A_D, A_E, and A_H were inseparable.(see Section 1.2 for the nomenclature used for additivity relationship parameters) By defining three variables Z1, Z2, and Z3 to be $\alpha+A_D+A_E$, $\alpha+A_D+_H$ and $\alpha+A_E+A_H$ repectively it was possible to reduce this to 8 equations in 7 variables with

TABLE 5.2

Additivity Parameters for Methylnaphthalene Cations

Proton Coupling Constants : Experimental cf Calculated

Parameter		Value (in Gauss)				
		Exptl.	Sharma1[1]	Sharma2[2]	INDO1[3]	INDO2[4]
α	α	(-5.40±0.30)[5]	-5.33	-5.18±0.16[7]	-5.40	-5.39±0.10
A_B	a'[6]	-0.47±0.11	-1.44	-1.15±0.14	-0.86	-0.73±0.08
A_C	d'	-0.12±0.13	0.88	0.75±0.13	0.13	0.20±0.08
A_D	d	(-0.79)	-1.37	-1.37±0.14	-0.97	-0.92±0.08
A_E	e	(0.46)	0.95	0.90±0.13	0.56	0.55±0.07
A_F	e'	0.59±0.07	1.53	0.95±0.13	0.97	0.86±0.07
A_G	h'	-0.33±0.07	-0.34	-0.50±0.13	-0.32	-0.31±0.07
A_H	h	(1.00)	1.79	1.46±0.13	1.13	1.05±0.07
σ		0.12		0.34		0.14
β	β	-1.82±0.08	-1.24	-1.14±0.11	-1.20	-1.07±0.06
B_A	b	-0.55±0.05	-1.10	-0.86±0.10	-0.67	-0.80±0.05
B_C	c'	1.20±0.08	1.31	1.01±0.10	1.33	1.06±0.05
B_D	c	0.22±0.05	-0.40	0.22±0.09	0.56	0.42±0.05
B_E	f	0.51±0.06	0.69	0.61±0.10	0.64	0.45±0.04
B_F	f'	-0.65±0.06	-1.05	-0.72±0.09	-0.76	-0.80±0.05
B_G	g'	0.66±0.06	1.08	0.60±0.09	1.07	0.80±0.05
B_H	g	-0.07±0.06	-0.15	-0.34±0.08	-0.07	-0.23±0.04
σ		0.08		0.23		0.09

[1] additivites calculated by Sharma and Boyd from calculations of 1- and 2-methylnaphthalene using Q=-25 Gauss

[2] additivities from Least Squares fit to UHFAA calculations of Sharma and Boyd.(79Sha1)

Table 5.2 cont.

[3]additivity constants calculated by INDO method from 1- and 2-methylnaphthalene assuming α is -5.4 G and β is -1.2 G.

[4]additivity constants calculated from Least Squares fit to INDO calculations.

[5]values derived using the value of α for naphthalene found in powder (720we)

[6]nomenclature used by Sharma and Boyd (79Sha1)

[7]estimated parameter standard deviation

all variables being refined. This allowed A_B, A_C, A_F and A_G to be evaluated. By using the value of α found for naphthalene cation in crystalline naphthalene (i.e. from a powder spectrum) by Owen and Vincow (710we) an estimate of A_D, A_E and A_H can be made as is shown in Table 5.2 . The other columns of this table show calculations of the additivity parameters made by a number of methods. Sharma and Boyd (79Sha1) calculated the additivity parameters for the methylnaphthalene cations using the unrestricted Hartree-Fock after annihilation method (UHFAA) with the methyl group being treated as a hetero-atom. In the column labelled Sharma1 are values for the addivity parameters calculated from the coupling constants calculated for naphthalene[†] and 1 and 2 methylnaphthalene[†]. The column labelled Sharma2 contains the additivity parameters calculated by applying least squares regression analysis to the coupling constants calculated by Sharma and Boyd for a number of mono-, di-, tri- and tetramethylnaphthalenes. This gave 40 independent equations in each subset. The columns labelled INDO1 and INDO2 were calculated similarly using the Intermediate Neglect of Differential Overlap

method. The INDO calculations were done over a number of years by Kirk, Claridge, and the author. The observations for 1,8 DMN^{+} were omitted as significantly different geometry was used in this case as compared to the other dimethylnaphthalenes and the mono and trimethylnaphthalene. 30 equations in each subset were used.

The agreement between the experimental and calculated values, while not very good, is none the less encouraging with the signs being correct in all but one case for the INDO and all but two cases for the UHFAA method. The INDO calculations are generally in better agreement with the experimental results, than the UHFAA calculations, as is to be expected since the INDO calculations make fewer assumptions. The self-consistency of the calculations, as indicated by the standard deviation is also consistent with the INDO calculations yielding better results.

The agreement between experiment and theory indicates that no dramatic error has been made either in assigning the coupling constants or in calculating the additivity parameters.

The additivity parameters for the anions and cations are shown in Table 5.3. There does not appear to be any relationship between the two sets of additivity parameters. This would indicate that the effect of a methyl group on the molecular orbitals of the naphthalene system is considerably different for cations and anions.

The value for β calculated is consistent with the pairing theorem ($59M^{C}L$) which predicts that for even-alternate

TABLE 5.3

Additivity Parameters for Methylnaphthalene Ions

Comparison of Anion and Cation Proton Coupling Constants

Parameter	Value (Gauss)	
	Anion	Cation
α	-4.96 ± 0.03[2]	(-5.40 ± 0.30)[1]
A_B	0.19 ± 0.02	-0.47 ± 0.11
A_C	-0.17 ± 0.03	-0.12 ± 0.13
A_D	0.58 ± 0.03	(-0.79)
A_E	-0.37 ± 0.03	(0.46)
A_F	-0.10 ± 0.02	0.59 ± 0.07
A_G	0.36 ± 0.02	-0.33 ± 0.07
A_H	-0.12 ± 0.02	(1.00)
Over-all σ	0.06	0.12
β	-1.95 ± 0.03	-1.82 ± 0.08
B_A	0.44 ± 0.03	-0.55 ± 0.05
B_C	-0.40 ± 0.03	1.20 ± 0.08
B_D	-0.05 ± 0.03	0.22 ± 0.05
B_E	0.39 ± 0.03	0.51 ± 0.06
B_F	0.55 ± 0.03	-0.65 ± 0.06
B_G	-0.38 ± 0.03	0.66 ± 0.06
B_H	-0.32 ± 0.03	-0.07 ± 0.06
Over-all σ	0.07	0.08

[1]values in brackets are calculated using powder value of α from 710we [2]estimated parameter standard deviation

---

hydrocarbons such as naphthalene the coupling constants for the cation and anion will be approximately the same. The value is

also consistent with the coupling constants in the series anthracene, tetracene and pentacene where the β coupling constant is less in the cation than the anion and rises with the decrease in the number of rings. As is shown in Table 5.4

TABLE 5.4

"β" Coupling Constants for Naphthalene and related Polycenes

Compound	cation (G)	anion (G)	Ref
Naphthalene	1.82±0.16	1.93	This study,69Mos
Anthracene	1.38	1.51	67Rey,70Red
Tetracene	1.03	1.16	67Rey,65Mob
Pentacene	0.76	0.87	67Bol

The additivity parameters for methyl group coupling are shown in Table 5.5. The additivity parameters for a methyl at an α position were found by least squares regression on 12 equations in 8 variables. The two β additivity parameters shown were calculated from comparison of the coupling constants in 1,2,4-trimethyl and 1,4-dimethylnaphthalene[†] and by comparing octamethylnaphthalene[†] and 1,2,3,4,5,8-hexamethylnaphthalene[†]. Taken, as they are, from the difference between only two observations, they must be regarded as indicative rather than definitive.

The methyl proton splitting for the methyl group attached to a carbon atom is proportional to the spin density on that

TABLE 5.5

Additivity Parameters for Methylnaphthalene Ions

Comparison of Cation and Anion Methyl Coupling Constants[1]

Parameter	Value (Gauss)	
	Anion	Cation
P	3.88±0.05[3]	8.60±0.15
A_B	0.38±0.09	0.46±0.16
A_C	-0.02±0.09	-0.44±0.16
A_D	-0.60±0.09	0.95±0.17
A_E	0.49±0.09	-1.50±0.15
A_F	0.20±0.09	-1.07±0.34
A_G	-0.26±0.09	-0.21±0.31
A_H	0.64±0.09	-0.29±0.15
Over-all σ	0.12	0.19
Q	1.72±0.03	4.07[2]
B_A	0.22±0.05	
B_C	-0.07±0.05	-1.47[2]
B_D	0.08±0.05	
B_E	-0.36±0.05	
B_F	-0.52±0.05	
B_G	0.46±0.05	
B_H	0.51±0.05	
Overall σ	0.06	

[1] values from Appendix 4.1

[2] these values were determined from only one equation

[3] estimated parameter standard deviation

carbon atom. The proportionality constant Q_{CCH3} is a positive constant (58M^cC). For methyl-substituted condensed benzenoids

Q_{CCH3} is 44G for cations and 21G for anions (79Sha2). The pairing theorem states that the unpaired electron density distribution is the same in cations and anions of even-alternant hydrocarbons. This would therefore predict that the methyl coupling constants in the cation should be twice the value of the corresponding coupling constants in the anion. Experimentally, it is found that P and Q, the methyl coupling constants in 1- and 2-methylnaphthalene, are 3.87G and 1.71G respectively in the anion. In the cation the values of P and Q found from the additivity relationships, are 8.60G and 4.07G respectively, i.e. the values of P and Q for the cations, are approximately twice that found for the anions.

As was found for the hydrogen additivity parameters, there is no obvious relationship between the methyl additivity parameters in the cations and the anions. There is, however, an observable pattern to the additivity parameters. For a methyl group at position 1 in the cation, addition of a methyl to the other ring or at position 3 will reduce the methyl coupling constant, whereas substitution of a methyl at position 2 or position 4 will increase the methyl coupling constant. This trend is consistent with the electron donating character (+I, 76Ste) of the methyl group. The 2 and 4 positions are directly conjugated with the 1-methyl and so would tend to draw the positive charge and the spin-density onto that ring. Similarly a methyl group on the other ring would tend to disperse the charge over both rings and so decrease the spin density at the 1 position.

Section 5.4.2 Hindered Methyl Rotation

There is little doubt that the linewidth effects seen in the OMN cation are due to the hindered rotation of the alpha methyl groups. At the lowest temperature obtainable ($-89^{0}C$) an alternating linewidth effect is seen, (see Fig. 5.4) although in this case it is every third, rather than every second line, that remains unbroadened (64Fre). At higher temperatures the lines broaden, although the averaged spectrum is still not reached by the highest temperature in this study ($-31^{0}C$). At this temperature, the $M_I=\pm 6$ set of lines are still proportionally higher than expected for a group of 12 equivalent hydrogens.

This same effect is observed for the 1,8-DMN cation where the $M_I=\pm 3$ groups are also much higher than expected for 6 equivalent methyl protons.

Observations of hindered methyl rotation by ESR in solution have not previously been reported. Studies of hindered rotation of other groups such as amide (80Bar) and phenyl (76von) by ESR are quite common. Observations of methyl rotation, hindered or otherwise, using NMR are quite common (72Sai, 72Sch, 76Lad) and there have also been reports of ESR in solid state at low temperatures in which the rotation of the methyl group has been stopped.(62Miy, 62Hor)

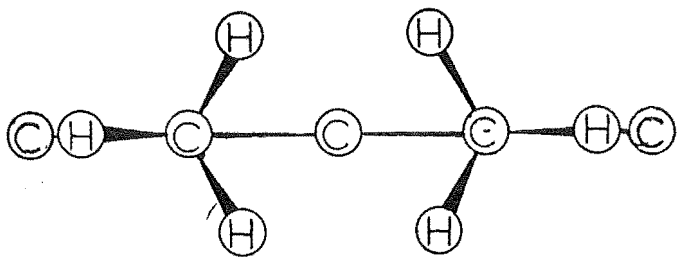

Figure 5.5 1,8-DMN viewed down C_9-C_{10} bond

Intuitively, it would be expected that the lowest energy configuration in 1,8-DMN would be that in which the hydrogens of the two methyl groups are interleaved. Rotation of one methyl group would then be expected to lead to an exactly opposite rotation in the other methyl group. E.g. if one group rotates 120^0 clockwise the other group would rotate 120^0 anti-clockwise. This type of rotation is an example of correlated motion. The alternative, where the two methyl groups rotate independently, is an example of uncorrelated motion. It is possible to have rotation intermediate between these two extremes, where due to, for example, quantum mechanical tunnelling, slippage occurs. This would be partially correlated rotation.

An X-ray study of 1,8-DMN by Bright, Maxwell and de Boer (73Bri) indicates that, in the solid state, rather than having the hydrogen atoms interleaved, they are in fact opposed, with one hydrogen of each methyl group lying in the plane of the molecule.(see Fig. 5.5) These two hydrogens point away from each other so that the other hydrogens are pointed towards each other. The strain of the opposing hydrogens is relieved by distortions in the naphthalene ring and in the ring carbon-methyl carbon bond angle. Strain energy calculations indicate that this is indeed the minimium energy configuration and that it is the result of intra rather than intermolecular forces. This implies that 1,8-DMN would be expected to have substantially the same geometry in solution.

It was also observed that the spectrum became asymmetric as the temperature was lowered, indicating that the high and low temperature forms have different g-values. This observation tends

to suggest that the rotation of the methyl groups distorts the molecular skeleton.

It should be possible, using the data available, to calculate approximate values for the variable parameters required to simulate the spectra of 1,8-DMN‡ and OMN†at low temperatures.

The coupling constant for a hydrogen on a β carbon can be calculated from the relationship proposed by M^{c}Connell and Heller (60Hel, see Section 3.1 and Equation 3.1). The constant B_2 can be found from the requirement that $\langle B_1+B_2\cos^2(\theta)\rangle$ must equal the average coupling constant at the fast exchange limit. Using the value of 8.25G for the averaged methyl coupling constant in 1,8-DMN†and assuming that $B_1=0$ a value of 0G, 12.37G and 12.37G can be found for the three hydrogen coupling constants.

Ladner et al. in 1976 (76Lad) used ^{13}C NMR to determine the rate of relaxation. They found E_a to be 2.8 kcal/mol and a pre-exponential factor of 8.8×10^{-10} jumps per second. Saika et al.(72Sai) used proton NMR and found E_a to be 3.0 kcal/mol and a pre-exponential factor of 3.6×10^{-3} seconds. The second figure converts to 100 jumps per second. The difference between the two figures makes any prediction of the methyl rotation rate at $-84^{0}C$ meaningless.

Simulations using YKEXCH (Section 2.5.1) on a range of coupling constants and rates for a correlated methyl rotation indicated that the observed linewidth and intensity effects in

1,8-DMN†could not be explained on this basis. No attempt was made to use an uncorrelated model due to the scale of computation required.

For 1,8-DMN†a 3-jump model corresponding to correlated motion required 30 minutes CPU time on the fastest computer available. If the other coupling constants had been added in it would have required 27 times as much time i.e. 13.5 hours.

Neglecting the other coupling constants is not a serious flaw as it is still possible to extract the required information from the principal lines (to which all the other coupling constants make no contribution). However the lines are sufficiently narrow that second order broadening of the lines is visible. Including this effect would quadruple the computation time to 2 hours. This would not present a serious problem (just an expensive one!) were it not that preliminary simulations have shown clearly that this correlated model is not correct. A correlated model gives heights at intermediate exchange of 1:8:1 whereas measurements on 1,8-DMN†spectra indicate that this ratio is too high. An uncorrelated model in the form which YKEXCH presently requires would correspond to a set of nine different states. This would give a 35-jump model and require 20 hours computing time. OMN†would require 81 states, 3321 jumps and approximately 200,000 hours. It is clear that the algorithm used must be substantially improved if this problem is to be soluble.

Freed and Fraenkel in 1964 (64Fre) used the relaxation matrix method (63Fre) to do a theoretical study of rotating methyl groups. The relaxation matrix method applies only to systems with rates at or above intermediate exchange rate. It is in this

region that both 1,8-DMN†and OMN†at the temperatures under study fall. For 1,8-DMN†the peak heights at intermediate exchange are predicted to be 1:8:1 for correlated rotation and 1:2:1 for uncorrelated rotation. The second observation of 1:2:1 peak heights is closer to what is found experimentally for 1,8-DMN† For OMN†the same ratios are 1:64:216:64:1 and 1:4:6:4:1 respectively. Experimentally the ratios for OMN†at the lowest temperature are 1:5:8:5:1 indicating that the system is undergoing uncorrelated rotation. It is expected that a program based on this algorithm would be substantially faster.

Section 5.4.3 Discussion and Conclusions for Methylnaphthalenedisulphides

The reaction of $AlCl_3/SO_2$ with methylnaphthalenes in 10 cases yielded a species with g of 2.008 . The identity of this species will now be discussed.

The first observation to be made is that this species was not formed for all compounds. In all cases where this species was not produced, the spectrum found was that of a normal monomer cation. Further, except for 1,2-DMN, which, because of the presence of an impurity, gave a monomer cation spectrum of 1,2,4 trimethylnaphthalenene, all these compounds were substituted at the 1 and 4 or 1 and 5 positions.

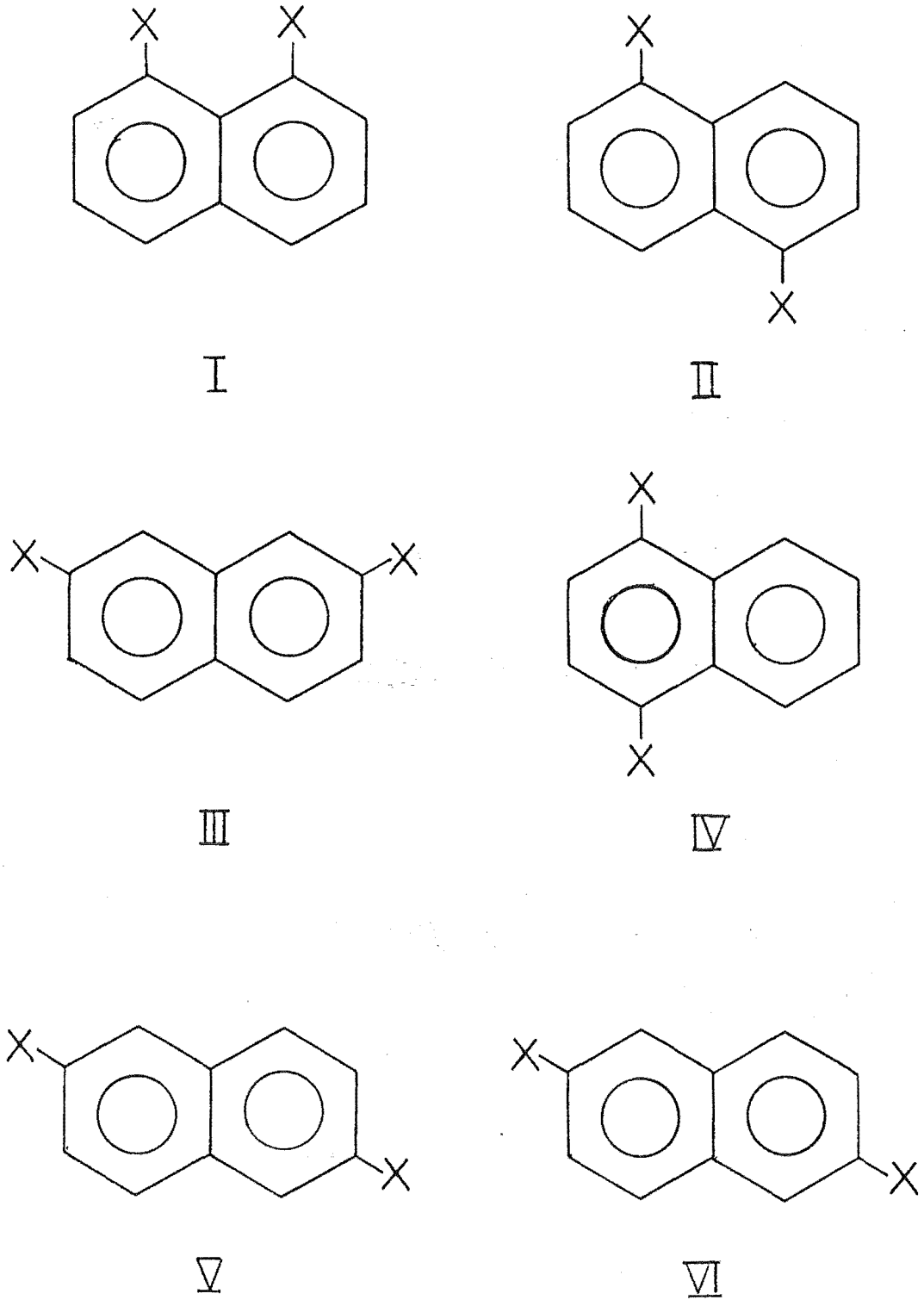

Figure 5.6
Symmetric Di-substitution Products
from Naphthalene

Secondly; all examples of this type of spectra show no more than six coupling constants, while that derived from naphthalene itself shows only three doublets. These observations require a symmetric substitution at two positions. The six possiblities are shown in Fig 5.6

Thirdly; 1,8-DMN gives a spectrum consisting of two doublets and one sextet. This implies that the compound formed must have either mirror symmetry or a centre of inversion. If there is no methyl migration then structures II, IV, V, and VI can be ruled out. The assumption of no methyl migration rules out III as a possiblity since 2,3-DMN, 2,6-DMN and 2,7-DMN all yield spectra of this type. This elimination of β substitution is also supported by the absence of this type of spectra from 1,4-DMN and 1,5-DMN and the tri- and tetramethylnaphthalenes. This absence also supports the assumption of no methyl migration as methyl migration followed by substitution would mean that 1,4-DMN and 1,5-DMN would also be expected to yield this type of spectra. Further invoking methyl migration in some cases requires explaining why there is no methyl migration in other cases. As will be seen, substitution at the 1 and 8 positions is completely consistent with all the experimental data and gives a satisfactory additivity relationship.

Having determined the substitution pattern, it is now possible to assign the coupling constants and hence the structure. The coupling constants for the compound derived from 1-methyl-naphthalene are 0.588G, 0.759G, 4.002G, 4.286G, 4.978G and 6.001G(methyl group). Since the methyl must be at the 4 position (see Fig. 5.6 I) this means that the 0.588G and 0.759G coupling

constants must belong to the hydrogens at 2 and 7 or those at 3 and 6. For 1,3-DMN where the coupling constants are 0.495G, 0.716G, 3.655G, 5.833G, 4.308G(methyl) and 5.107G(methyl), the 0.495G and 0.716G coupling constants must be assigned to the 3 and 6 positions. The particular assignment of 0.716G to the 3 position and 0.495G to the 6 position can be made by using the additivity relationship with 2,7-DMN, 2,3-DMN and 2,6-DMN all of which give unambiguous values for the 3 and 6 positions (the full least squares analysis is given in Appendix 5.2). From there the assignments given in Appendix 5.1, Table A follow. Of particular interest are 2-methylnaphthalene and 2,7-DMN where addition occurs at the sterically hindered 1 rather than the more open 4 position.

From the available evidence it should be possible to identify the substituent(s). The species present in solution contain only carbon, chlorine, sulphur, oxygen, aluminium and/or hydrogen. Of these six chlorine, aluminium and hydrogen can be ruled out because of the absence of any coupling from ^{35}Cl, ^{37}Cl, ^{27}Al or ^{1}H. Carbon on its own can be ruled out because no aromatic carbon compound has a g-value in the vicinity of 2.008, most falling between 2.002 and 2.003. Similarly most oxygen containing aromatics fall between 2.003 and 2.004 (77Lan). Given that no ESR spectrum is seen in the absence of SO_2, incorporation of SO_2 must be suspected.

The only suitable sulphur containing compound for which the

Figure 5.7
Sulphur bridged Naphthalenes

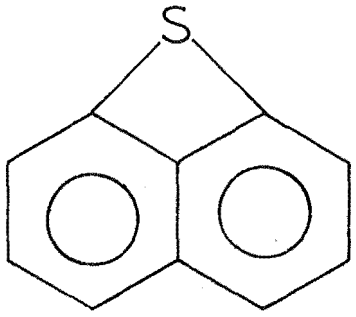

VII

naphtho(1,8-bc)thiete

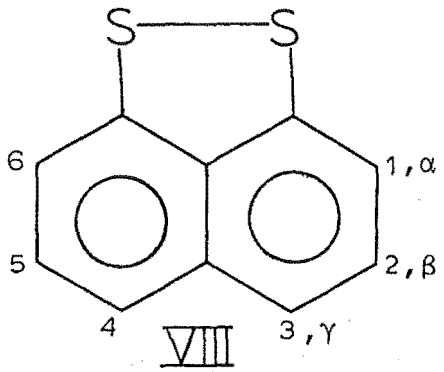

VIII

naphtho(1,8-bc)-1,2-dithiole
(naphthalene-1,8-disulphide)

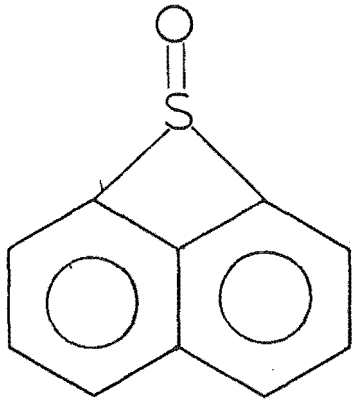

IX

naphtho(1,8-bc)thiete-
1-oxide

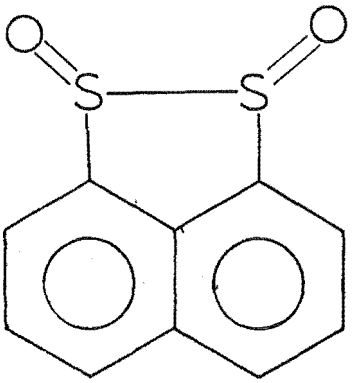

X

naphtho(1,8-bc)-1,2-
dithiole-1,2-dioxide

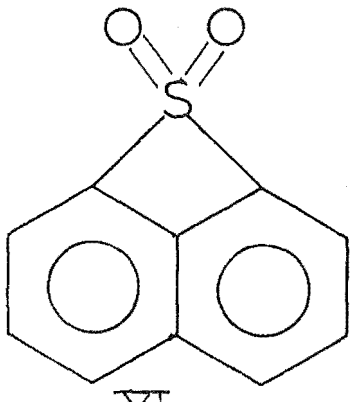

XI

naphtho(1,8-bc)thiete-
1,1-dioxide

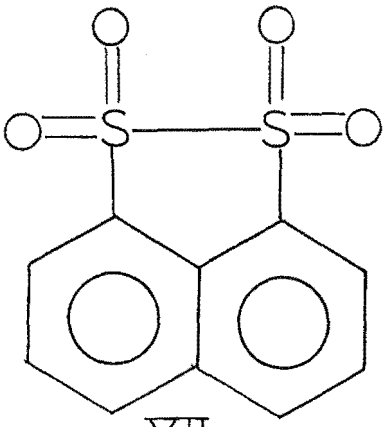

XII

naphtho(1,8-bc)-1,2-
dithiole-1,1,2,2-tetraoxide

ESR spectrum of the cation has been reported is naphtho-[1,8-cd]-1,2-dithiole (see Fig. 5.7 I), otherwise known as naphthalene-1,8-disulphide. The ESR spectrum has been published by four different groups. Zweig and Hoffman (65Zwe) reported 5.30G, 4.44G and 0.88G with g=2.0081, Stepanov et al (71Ste) 5.20G, 3.85G and 0.70G, Bramwell et al (78Bra) 5.52G, 4.56G and 0.96G with g=2.0079, and Bock et al in 1981 (81Boc) reported 5.25G, 4.32G and 0.96G with g=2.0086. This compares with 5.26G, 4.42G and 0.88G with g=2.0086 for the unknown. The agreement is reasonable given the spread in the reported coupling constants and g-value. This result is indicative, rather than definitive, as there are several related compounds which would be expected to have similar g-values and coupling constants. These other compounds (see Fig. 5.7) are naphtho[1,8-bc]thiete (VII), naphtho[1,8-bc]thiete 1-oxide (VIII), naphtho[1,8-bc]thiete 1,1-dioxide (IX), naphtho[1,8-bc]-1,2-dithiole 1,2-dioxide (X) and naphtho[1,8-bc]-1,2-dithiole 1,1,2,2-tetraoxide (XI)

Ionisation potentials (81Boc) indicate that $AlCl_3$ should not be able to oxidise VII, so this structure is unlikely. Further it would be expected that the ionisation potentials for sulphoxides would be higher than those of the corresponding sulphides and that the ionisation potentials of the corresponding sulphones would be higher still. This is the pattern that is found in both diethyl and diphenyl sequences as is shown in Table 5.6. It is therefore possible to eliminate VIII and IX as possiblities.

Table 5.6

Ionisation Potentials of Sulphides, Sulphoxides and Sulphones

Compound	Ionsiation Potential	Ref.
$(C_2H_5)_2S$	8.44eV	72Tom
$(C_2H_5)_2SO$	8.76eV	72Boc
$(C_2H_5)_2SO_2$	9.96eV	75Eva
$(C_6H_5)_2S$	7.93eV	77Dom
$(C_6H_5)_2SO$	8.58eV	74Boc
$(C_6H_5)_2SO_2$	9.37eV	75Sol

Work by Delamar, Lacaze and Dubois (80Dub) indicates that $AlCl_3$ reacts with SO_2 to form $SOCl^+$ and $AlOCl_2^-$ so that what is occurring might be an electrophilic attack by $SOCl^+$ on neutral naphthalene. These authors reacted $AlCl_3/SO_2$ with benzene to produce C_6H_5SOCl. Their work was carried out in liquid SO_2 rather than dichloromethane, but this does not diminish the relevance of their work as the ESR samples prepared were usually strong in SO_2, being perhaps one tenth SO_2 by volume.

The formation of a sulphur bridge of some form is supported by work by Villars (59Vil) on the Friedel Crafts reactions of sulphur monochloride (S_2Cl_2), thionyl chloride ($SOCl_2$), sulphuryl chloride (SO_2Cl_2) and sulphur dichloride (SCl_2) with aromatic compounds. These reactions gave sulphur bridged coupling products as seen in Eqn 5.1

$$2p\text{-}ClC_6H_6 + SOCl_2 \longrightarrow p\text{-}ClC_6H_5\text{-}S(O)\text{-}C_6H_5\text{-}pCl + 2HCl \quad \text{Eqn 5.1}$$

There is, however, evidence suggesting that the pathway does not involve electrophilic attack on neutral naphthalene. The substitution of 2-methylnaphthalene and 2,7-DMN were shown to occur at the 1 rather than the 4 position. Electrophilic substitution by SO_3 in nitromethane (79Lam) has been shown to yield mainly products from attack at the 4 position, while nucleophilic attack of CN^- on electrochemically generated naphthalene cation (79Yos) has been shown to yield predominantly 1 substitution.

The picture is further complicated by the observation that ESR gives spectra of radicals only. Further, under the given reaction conditions ESR will not show the presence of any species having ionisation potentials above 8eV, since such species will not be ionised by $AlCl_3$ (81Boc). Further, if there is not sufficient $AlCl_3$ present to ionise all the products formed then charge transfer will result in only the most stable species being seen. The ionisation potential of naphthalene-disulphide is 7.14eV (81Boc), that of perylene is 7.45eV (72Dew) and that of naphthalene 8.12eV (66Ved), so that the disulphide would be expected to be seen rather than the perylene or the monomer cation. The observation that the overall gain settings used to collect the spectra were an order of magnitude higher for the disulphides than in other cases, suggests that the disulphide is probably a minor reaction product.

Figure 5.8

Some Methylperylenes

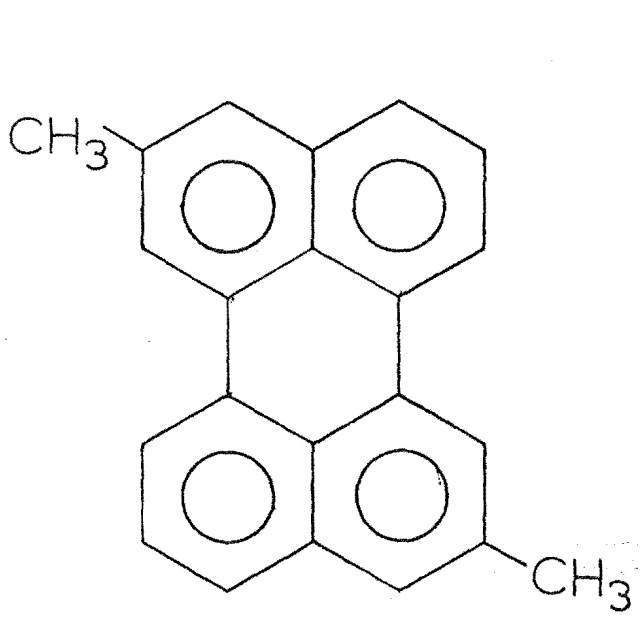

2,4-dimethylperylene

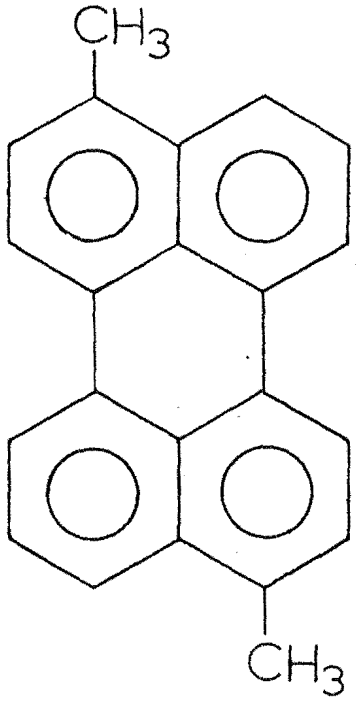

3,9-dimethylperylene

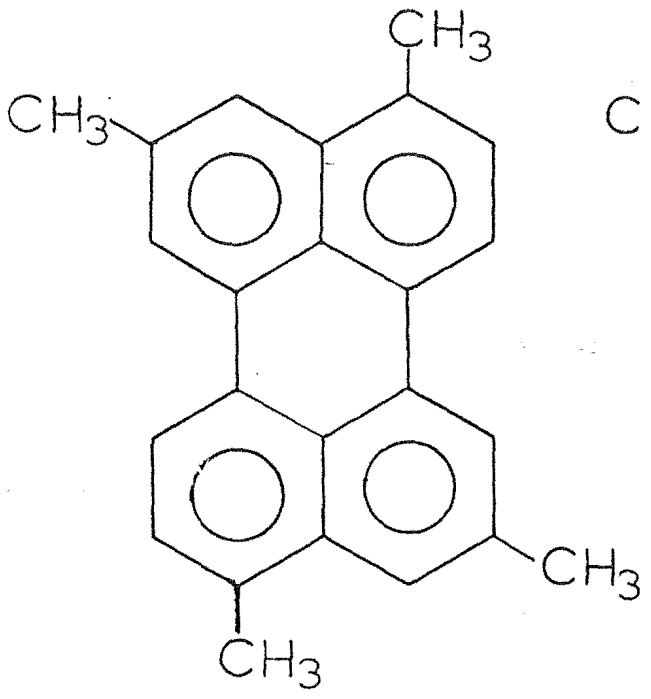

2,4,8,10-tetramethyl-perylene

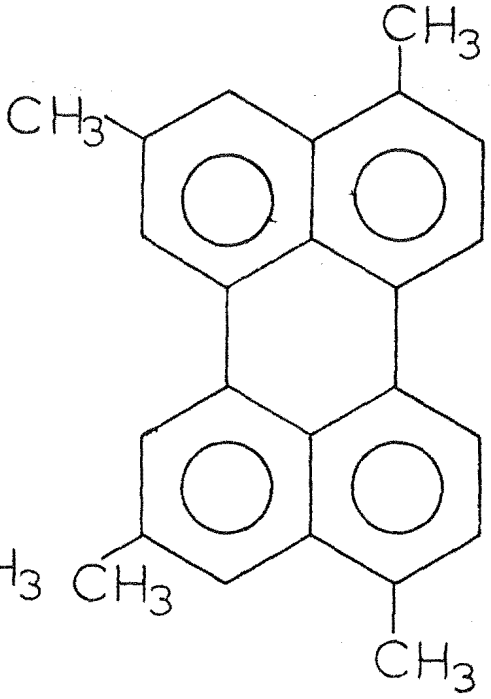

2,4,9,11-tetramethyl-perylene

Section 5.4.4 Discussion and Conclusions for Perylenes Formed

After fitting the spectrum from the cation of the tetramethylperylene formed from 1,7-DMN, an attempt to determine the structure was made by collecting and solving the spectra of authentic samples of 2,8-dimethylperylene and 3,9-dimethylperylene (Fig. 5.8). It was reasoned that, given the correct assignment of the coupling constants, it should be possible to produce an additivity relationship for trans-dimethylperylenes. If the perylene from 1,7-DMN fitted this additivity relationship it must therefore be the trans-tetramethylperylene and hence it could be shown to be 2,4,8,10-tetramethylperylene (Fig. 5.8). If it did not fit the additivity relationship it must therefore be 2,4,9,11-tetramethylperylene.

Strong, well resolved spectra for the cation from 3,9-dimethylperylene yielded a satisfactory fit of 0.235G, 0.395G, 2.818G, 2.905G, 3.877G and 4.389G(methyl). The spectra from an authentic sample of 2,8-dimethylperylene were not as well resolved and the best fit of 0.464G, 2.635G, 3.135G, 4.069G, 4.202G and 0.299G(methyl) was not very satisfactory. Confidence can be placed only in 0.299G, 0.464G and 2.635G as coupling constants. Due to the poor resolution and poor fit 3.135g, 4.069G and 4.202G, though reasonable, can not be considered certain.

Failure to produce a satisfactory fit to 2,8-dimethylperylene means that no definite conclusion as to the structure of the perylene from 1,7-DMN can be made. The additivity relationship produced from the coupling constants found indicates that the coupling constants found for the perylene from 1,7-DMN are

incompatible with any additivity relationship from 2,8-dimethyl- and 3,9-dimethylperylenes. This suggests either that the spectrum is that of 2,4,9,11-tetramethylperylene, or that the spectrum does not belong to a tetramethylperylene cation at all. The second alternative is considered less likely because of the g-value and the satisfactory fit obtained.

Section 5.5

Suggestions for Further Investigations

There are clearly a number of areas in which further work would be fruitful, or is required. The most important of these is probably to prove conclusively that the signals seen at g=2.008 are in fact from naphtho[1,8-cd]-1,2-dithiole. The most direct method of doing this would be to use isotopic labelling. Use of ^{33}S labelled SO_2 would unequivocally give the number of sulphurs present, since ^{33}S has spin 1/2 and so would produce an extra coupling constant. The magnitude of the observed coupling constant would also be a good indicator of the oxidation state of the sulphur. Since the ^{33}S coupling constant is already known (81Boc, 78Bra) any deviation from this value would indicate whether there are oxygen(s) attached to the sulphur(s). Use of ^{17}O labelled SO_2 would definitively establish the number of oxygens present since ^{17}O has a spin of 5/2. Another approach to the problem, which would definitely eliminate the oxides as possiblities, would be to use thionyl chloride and sulphur

dichloride instead of sulphur dioxide. If the same ESR spectrum is seen, and Villar's results suggest that it might be, then naphtho[-1,8-cd]-1,2-dithiole and naphtho[-1,8-cd]thiete would remain as the only possiblities. The absence of the expected ESR spectrum would, however not rule any of the possiblities out. A third possibility would be the synthesis of the other possiblities, followed by the collection of their ESR spectra.

A recent report by Tan and Brownstein (83Tan) describing NMR measurements on the complexes formed between $AlCl_3$, acetylchloride and aromatics such as benzene in sulphur dioxide, offers hope of a more quantative sample preparation method. These authors purified their aluminium chloride and transferred it in a dry box, into an NMR sample tube closed with a Teflon high vacumm stopcock. The mass of the $AlCl_3$ added could then be determined and the appropriate amounts of the other reagents added by distillation on a vacuum line. Such a procedure, applied to the reactions of the methylnaphthalenes, would facilitate the production of spectra from one species only, be it monomer, dimer, perylene, disulphide or other. It would also remove the uncertainity about the mode of the reaction. Because the $AlCl_3$ is sublimed into the sample tube, there is a considerable period of time during which solid methylnaphthalene is in contact with the aluminium trichloride, giving rise to the possibility that the perylenes are formed in the solid phase, rather than in solution. An improvement in the preparative technique would resolve this.

The study of these other products would be of some interest. The conformation of the methylperylenes formed as a function of methyl substitution would give some information as to the

mechanism of the Scholl Condensation, about which very little is at present known. Similarly very little work has been done on dimers from aromatics and a systematic study would yield insight into the conformation of such dimers and the delocalisation of charge within the dimer. It is unlikely that such an improvement in technique will lead to monomer cations of those methyl-naphthalenes for which the cations have not already been seen. The ease of condensation indicates that the monomer cation is a very short lived species and it seems likely that only flow techniques would be able to study the ESR spectrum of e.g. naphthalene^{+}. There is however a report by Saunders, Cox and Lloyd (79Sau) which offers some hope of obtaining solutions of unstable radicals, by reacting the parent hydrocarbon with SbF_6 in the gas phase and then condensing on a cold finger. Given the instablity of the monomer cations, the best chance of determining the remaining additivity parameters, using the methods employed in this study, would probably be from 1,2,3-trimethylnaphthalene, 1,2,3,6-tetramethylnaphthalene or 1,2,3,6,7-pentamethyl-naphthalene. These would all give the required information, while forming more stable cations, which are also more hindered to attack at the 1 position.

The last area which would yield interesting results is the hindered rotation in 1,8-DMN^{+}and octamethylnaphthalene^{+}. Use of a Freon such as Freon12 (CCl_2F_2), which has a freezing point of $-158^{0}C$, as solvent, would allow study of OMN^{+}in the region between intermediate exchange and the slow exchange limit. 1,8-DMN^{+}cation could also be studied from the fast exchange limit

in CH_2Cl_2 and down to intermediate exchange in Freon. The Freed and Fraenkel relationship is probably sufficient to give the barrier height in OMN†and to show that the linewidth effects in 1,8-DMN†are the result of hindered rotation. It would not be applicable below intermediate exchange and so an efficient algorithm based on the Bloch equations would need to be produced.

CHAPTER 6

TETRACYCLOPENTANAPHTHALENE

Section 6.1 Introduction

Tetracyclopentanaphthalene (TCPN, Fig. 6.1 I) contains four five-membered rings attached to a naphthalene moiety. Because of the strain involved in having three sp^3 hybridised carbons all in the same plane, it would be expected that each of the five-membered rings is puckered. The γ carbon of each five-membered ring can then be either above or below the plane of the molecule. From the results obtained for HP, DP and other similar compounds, it would be expected that each ring would interconvert between the two possible positions. Bauld and Farr (74Bau) in 1974 observed an alternating linewidth affect in the spectrum of the Indan anion (Fig. 6.1 II) which they ascribed to such an interconversion. Rieke et al(74Rie) did not observe any such affect in 5,6-benzindan (Fig. 6.1 III). When a sample of TCPN became available from Professor R. P. Thummel (81Thu) it was decided to investigate this interconversion in both the cation and anion of TCPN.

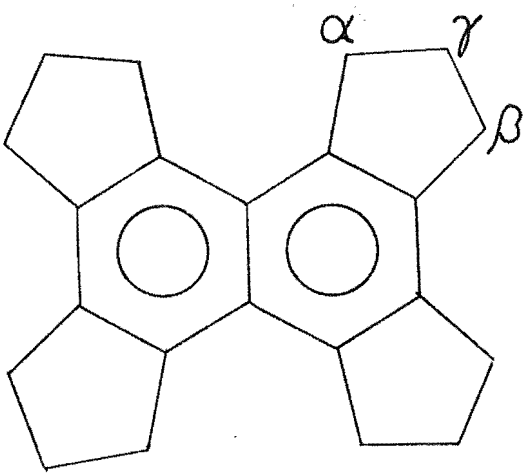

I

tetracyclopentanaphthalene

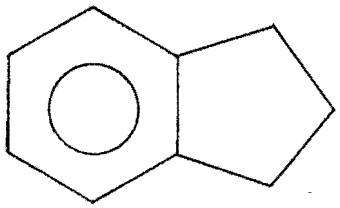

II

indan

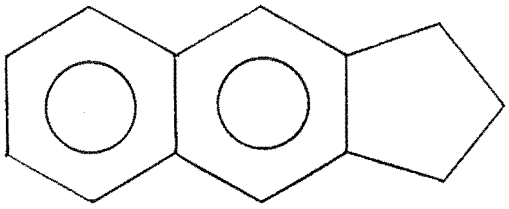

III

5,6-benzindan

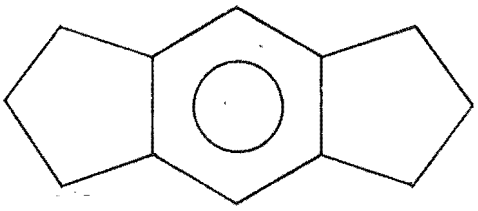

IV

sym-hydrindacene

Figure 6.1 Some Alkyl Ring containing Compounds

Figure 6.2
Tetracyclopentanaphthalene: Spectra at -85°C

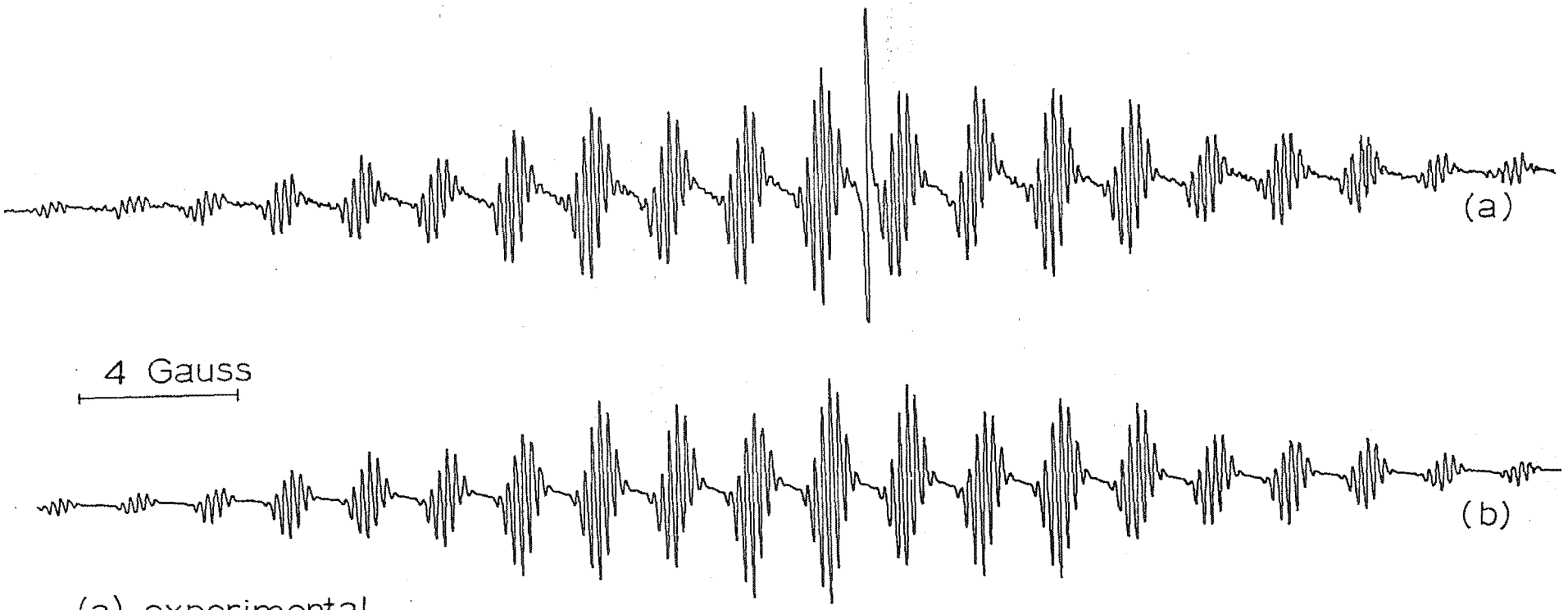

(a) experimental
(b) simulated

Section 6.2 Experimental

TCPN reacted slowly with potassium in DME. The potassium needed to be reheated a number of times, and as much as 1 hour was required for the signal to grow to a maximum. The solutions produced were a very pale sky blue colour, and stable for 3-4 hours at low temperatures. The signal ascribed to the TCPN anion, was slowly replaced by a line due to solvated electrons. The spectra were generally not well resolved, with a linewidth of 90mG being found. A satisfactory fit to the experimental spectrum was given by the coupling constants 5.891G, 1.983G and 0.207G, and linewidth of 90mG. The experimental and calculated spectra are given in Fig 6.2 a and b respectively.

TCPN reacted readily with $AlCl_3/SO_2$ to give a pale red solution and strong well resolved spectrum which we ascribed to TCPN cation. Because of drift in the microwave frequency, ESRCON (Section 2.4.4) gave a very poor fit. The best fit found by simulation was 11.637G, 4.387G and 0.062G with linewidth of 37mG., The resulting spectrum is shown in Fig 6.3.

Section 6.3 Discussion and Conclusion

In neither anion nor cation is there any indication of line-broadening due to oscillation. Further, in both cases satisfactory fits are obtained by the use of only three coupling

constants. This indicates that oscillation is so rapid that the pairs of α, β and γ coupling constants are each totally averaged.

The assignment of the 0.207G and 0.062G coupling constants to the γ protons in the anion and cation respectively is selfevident. The assignment of the larger, 5.891G and 11.637G coupling constants to the α hydrogens is based on the coupling constants for octamethylnaphthalene cation, where the larger coupling constant is assigned to the 1 methyl group (69Roo). The large value of 11.637G in the cation is not unexpected as Dessau and Shih (72Des) found a value of 19.2G for the cation of symhydrindacene (Fig. 6.1 IV). The value of 11.637G found represents an average of α_{eq} and α_{ax} and is much larger than the average values found for $HP^{\dagger}$ of 8.5G and $DP^{\dagger}$ of 6.5G.

CHAPTER SEVEN

SUMMARY

This study was undertaken with three major objectives. These objectives were;

(1) to improve the understanding of conformational interconversion.

(2) to extend the range and improve understanding of additivity relationships.

(3) because objectives (1) and (2) required the fitting of very complex ESR spectra, it was necessary that the methods of fitting such spectra be improved.

(1) The Study of Conformational Interconversion

It had been envisaged that the study of intramolecular motions would be limited to the ring oscillations in the peri-alkylnaphthalenes. However, extensions of the study to 1,2,3,4-TMN$^-$ (Section 4.3.3), 1,8-DMN and OMN cations (Section 5.4.2), and TCPN (Chapter 6) became desirable.

The computing problems resulting from the scale of computation required to simulate conformational interconversion

in peri-alkylnaphthalenes, 1,8-DMN†and OMN‡ show clearly the need for more efficient algorithms in simulating the spectra of systems undergoing such exchange processes. For 1,8-DMN and OMN cations the high symmetry involved offers hope of such improved algorithms. For the peri-alkylnaphthalenes the out-look is somewhat bleak, although use of Fourier Transforms (81Bru) does offer the possiblity of decreasing the computing effort required to simulate spectra where some coupling constants are not modulated.

(2) Additivity Relationships

As discussed in Section 1.2 the concept of an additivity relationship has been applied successfully to a wide range of compounds. In this study it has enabled the assignment of coupling constants to be made unequivocally in naphthalene-disulphides (Section 5.4.3), peri-alkylnaphthalenes (Section 3.3.1), methylnaphthalenes (Section 4.3.2, and Section 5.4.1), and others (Section 1.2). It would appear from the results on methylnaphthalene anions (Chapter 4) that assignments on the basis of an additivity relationship are more accurate, and certainly more self-consistent, than those based on Molecular Orbital calculations.

In Chapter 5 additivity relationships were successfully used to determine the structure of the naphthalenedisulphides produced, and to indicate which of two tetramethylperylenes had been formed in the Scholl Condensation of 1,7-DMN. The number of coupling constants required to determine an additivity relationship

is certainly a drawback, however once an additivity relationship has been calculated for a series, the method has considerable predictive power and the remaining members of a series can be quickly solved. As was shown in the case of 1,7-DMN anion where the error made in the coupling constants for this compound was quickly noticed and rectified.

The absence of any relationship between the additivity parameters in the naphthalene cation and anion is certainly a disappointment, but there is no a reason, a priori, why a methyl group in a cation should produce a similar effect to a methyl group in an anion.

In view of the success of additivity relationships in this study, it would be interesting to determine the accuracy with which such relationships can be established. This would require the precise measurement of the coupling constants of a series of compounds under precisely the same conditions. Previous studies have either been insufficiently precise, or the complete set of coupling constants can only be determined by pooling the results from a number of groups.

The use of an additivity relationship with the peri-alkyl-naphthalenes in Section 3.3.1 suggests that the additivity relationship could well be applied to different substituents on the same substrate. e.g. given the additivity parameters for methyl and ethyl substituents on naphthalene it should be possible to determine the effect of having both ethyl and methyl substituents on naphthalene.

In the course of this study a number of different avenues for improving the fitting of ESR spectra were explored. It is clear that for complex spectra least squares fitting is much superior to the older, visual techniques. Although the initial set of coupling constants must still be determined by the application of human pattern recognition skills.

Least squares fitting is, however, very sensitive to faults in the experimental data caused by drift of microwave frequency or magnetic field.

Attempts to overcome this problem by use of an interface between the computer and a microwave frequency counter, with subsequent correction of the spectrum for drift in the microwave field, were at best only partially successful. It is clear that further testing and development of this approach is required before it will yield satisfactory results. An alternative approach to the problem of microwave drift not requiring a Field Frequency Lock is the application of auto-correlation techniques (83Jac), although this has the drawback of requiring computing resources much larger than those employed in the present study.

The use of a dedicated system for the simulation of spectra was extremely successful, allowing the rapid production of the initial coupling constants for input to the least squares fitting.

APPENDIX 1.1

Least Squares Refinements for some Additivity Relationships

Table A Deuterobenzene Radical Anions[1]

Parameter	Value (G)	Error[2] (G)
A	-3.802	0.011
$A+A_B$	-0.190	0.007
$A+A_C$	-0.190	0.009
$A+A_D$	0.352	0.012

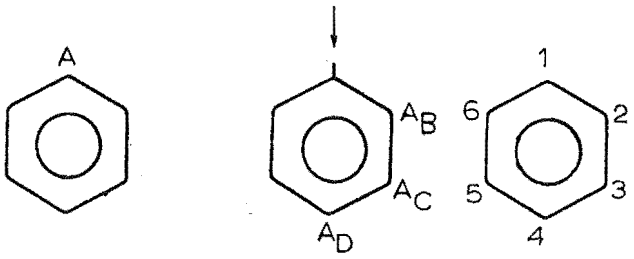

Compound	Position	Equation	Expt. (G)	Calc. (G)	Diff. (G)
benzene⁻	1	A	-3.807	-3.802	-0.005
d-benzene⁻	1	$A+A_B$	-3.984	-3.991	0.007
	3	$A+A_D$	-3.454	-3.450	-0.004
1,2-d-benzene⁻	3	$A+A_B+A_C$	-4.163	-4.182	0.019
1,3-d-benzene⁻	2	$A+2A_B$	-4.192	-4.181	-0.011
	4	$A+A_B+A_D$	-3.628	-3.639	0.011
	5	$A+2A_C$	-4.192	-4.183	-0.009
1,2,5-d-benzene⁻	3	$A+2A_B+A_D$	-3.836	-3.829	-0.007

Standard Deviation 0.015 Gauss

[1] from 67Law, [2] estimated parameter standard deviation

Table B Methylbiphenyls Radical Anions; Para Coupling Constants[1]

Parameter	Value (G)	Error[3] (G)
A	-5.486	0.075
A_B	0.233	0.105
A_C	0.299	0.058
A_D	0.032	0.058
A_E	0.063	0.105
A_F	0.079	0.156

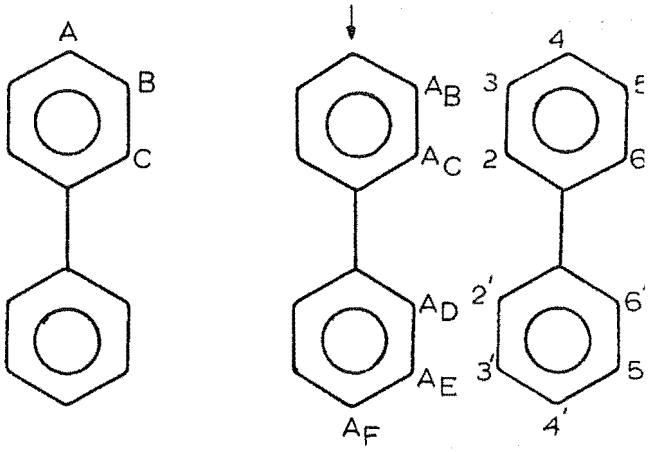

Compound	Position	Equation	Expt. (G)	Calc. (G)	Diff. (G)
biphenyl$^-$	4,4'	A	-5.310	-5.486	0.176
2-MB$^-$ [2]	4	$A+A_C$	-5.300	-5.191	-0.109
	4'	$A+A_D$	-5.440	-5.454	0.014
4-MB$^-$	4'	$A+A_F$	-5.410	-5.408	0.002
3-MB$^-$	4	$A+A_B$	-5.220	-5.254	0.034
	4'	$A+A_E$	-5.390	-5.423	0.033
2,2'-DMB$^-$	4,4'	$A+A_C+A_D$	-5.210	-5.158	-0.052
3,3'-DMB$^-$	4,4'	$A+A_B+A_E$	-5.220	-5.190	-0.030
2,6-DMB$^-$	4	$A+2A_C$	-4.990	-4.895	0.010
	4'	$A+2A_D$	-5.580	-5.422	0.158
2,6,2',6'-TMB$^-$	4,4'	$A+2A_C+2A_D$	-4.660	-4.831	0.171
3,5,3',5'-TMB$^-$	4,4'	$A+2A_B+2A_E$	-4.900	-4.895	-0.006
Standard Deviation					0.137 Gauss

[1] from 77Ish, 73Chr, 75Ish1, 75Ish2, 75Nem, 65Ish

[2] MB = methylbiphenyl, DMB = dimethylbiphenyl, TMB = tetramethylbiphenyl, [3] estimated parameter standard deviation

Table C Methylbiphenyls Radical Anions; Meta Coupling Constants

Parameter	Value (G)	Error (G)
B	-0.477	0.034
B_A	-0.157	0.059
B_C	0.232	0.049
B_D	-0.052	0.049
B_E	0.136	0.085
B_F	0.121	0.059
B_G	0.137	0.068
B_H	-0.034	0.049
B_I	-0.030	0.049
B_J	0.067	0.068

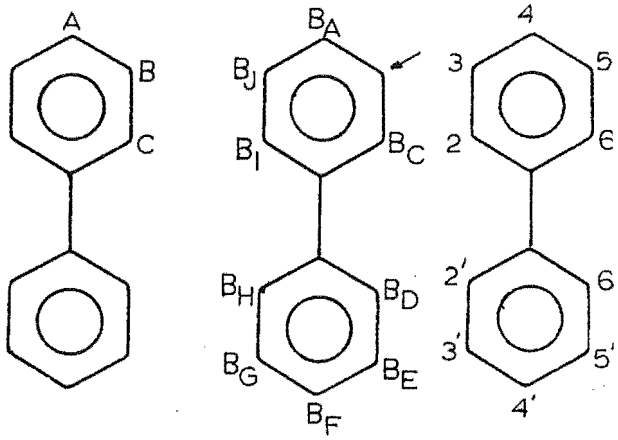

Compound	Position	Equation	Expt. (G)	Calc. (G)	Diff. (G)
biphenyl$^-$	5,3,3',5'	B	-0.410	-0.476	0.066
2-MB$^-$	3	$B+B_C$	-0.330	-0.244	-0.086
	3'	$B+B_D$	-0.610	-0.528	-0.082
	5'	$B+B_H$	-0.610	-0.510	-0.100
	5'	$B+B_I$	-0.610	-0.506	-0.104
4-MB$^-$	3,5	$B+B_A$	-0.570	-0.635	0.065
	3',5'	$B+B_F$	-0.290	-0.355	0.065
3-MB$^-$	5	$B+B_J$	-0.410	-0.409	-0.001
	5'	$B+B_G$	-0.340	-0.339	-0.001
	3'	$B+B_E$	-0.340	-0.340	0.000

Table C cont.

2,2'-DMB⁻	3,3'	$B+B_C+B_D$	-0.260	-0.296	0.036
	5,5'	$B+B_H+B_I$	-0.510	-0.540	0.030
3,3'-DMB⁻	5,5'	$B+B_G+B_J$	-0.270	-0.272	0.002
4,4'-DMB⁻	3,5,3',5'	$B+B_A+B_F$	-0.490	-0.513	0.023
3,5-DMB⁻	3',5'	$B+B_C+B_I$	-0.210	-0.274	0.064
2,6,2',6'-TMB⁻	3,5,3',5'	$B+B_C+B_D+B_H+B_I$	-0.330	-0.361	0.031
2,4,2',4'-TMB⁻	3,3'	$B+B_A+B_F+B_H+B_I$	-0.610	-0.578	-0.032
	5,5'	$B+B_A+B_F+B_C+B_D$	-0.390	-0.334	-0.056
2,4,6,4'-TMB⁻	3,5	$B+B_A+B_F+B_C+B_I$	-0.300	-0.312	0.012
	3',5'	$B+B_A+B_F+B_D+B_H$	-0.610	-0.600	-0.010

Standard Deviation 0.078 Gauss

see footnotes p158

Table D Methylbiphenyls Radical Anions; Ortho Coupling Constants with Literature Assignments

Parameter	Value (G)	Error (G)
C	-2.682	0.082
C_A	-0.172	0.149
C_B	-0.076	0.163
C_D	0.032	0.125
C_E	0.153	0.163
C_F	0.098	0.149
C_G	-0.068	0.155
C_H	0.050	0.121
C_I	0.396	0.126
C_J	0.112	0.155

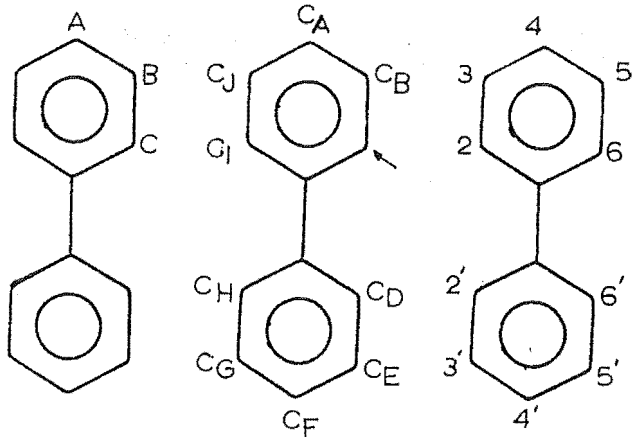

Table D cont.

Compound	Position	Equation	Expt. (G)	Calc. (G)	Diff. (G)
biphenyl$^-$	2,6,2',2'	C	-2.660	-2.682	0.022
2-MB$^-$	6	$C+C_I$	-2.200	-2.285	0.085
	6'	$C+C_H$	-2.860	-2.633	-0.227
	2'	$C+C_D$	-2.860	-2.651	-0.209
4-MB$^-$	2,6	$C+C_A$	-2.830	-2.855	0.025
	2',6'	$C+C_F$	-2.560	-2.585	0.025
3-MB$^-$	2	$C+C_J$	-2.430	-2.570	0.140
	6'	$C+C_G$	-2.610	-2.750	0.140
	2'	$C+C_E$	-2.560	-2.529	-0.031
	6	$C+C_B$	-2.790	-2.759	-0.031
2,2'-DMB$^-$	6,6'	$C+C_H+C_I$	-2.270	-2.236	-0.034
3,3'-DMB$^-$	6,6'	$C+C_G+C_J$	-2.810	-2.638	-0.172
4,4'-DMB$^-$	2,6,2',6'	$C+C_A+C_F$	-2.730	-2.757	0.027
2,6-DMB$^-$	2',6'	$C+C_D+C_H$	-2.340	-2.601	0.261
2,4,2',4'-TMB$^-$	6,6'	$C+C_A+C_F+C_H+C_I$	-2.310	-2.310	0.000
3,5,3',5'-TMB$^-$	2,2',6,6'	$C+C_B+C_E+C_G+C_J$	-2.530	-2.561	0.031
2,4,6,4'-TMB$^-$	2',6'	$C+C_A+C_F+C_D+C_I$	-2.380	-2.328	-0.052

Standard Deviation 0.189 Gauss

see footnotes p158

Table E Methylbiphenyls Radical Anions; Best fit to Ortho Coupling Constants

Parameter	Value (G)	Error (G)
C	-2.694	0.067
C_A	-0.168	0.122
C_B	-0.066	0.125
C_D	0.037	0.102
C_E	0.294	0.125
C_F	0.102	0.122
C_G	-0.021	0.125
C_H	0.056	0.100
C_I	0.400	0.103
C_J	-0.079	0.125

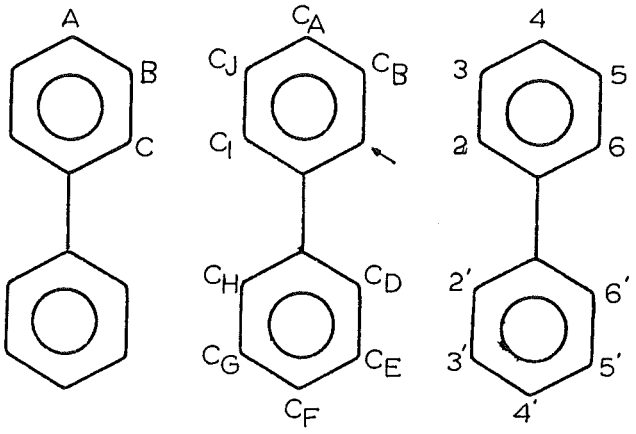

Compound	Position	Equation	Expt. (G)	Calc. (G)	Diff. (G)
biphenyl$^-$	2,6,2',2'	C	-2.660	-2.694	0.034
2-MB$^-$	6	$C+C_I$	-2.200	-2.294	0.094
	6'	$C+C_H$	-2.860	-2.637	-0.222
	2'	$C+C_D$	-2.860	-2.656	-0.204
4-MB$^-$	2,6	$C+C_A$	-2.830	-2.862	0.032
	2',6'	$C+C_F$	-2.560	-2.592	0.032
3-MB$^-$	2	$C+C_J$	-2.710	-2.773	0.063
	6'	$C+C_G$	-2.610	-2.673	0.063
	2'	$C+C_E$	-2.430	-2.400	-0.030
	6	$C+C_B$	-2.790	-2.760	-0.030
2,2'-DMB$^-$	6,6'	$C+C_H+C_I$	-2.270	-2.238	-0.032

Table E cont.

3,3'-DMB$^-$	6,6'	$C+C_G+C_J$	-2.810	-2.752	-0.058
	2,2'	$C+C_B+C_E$	-2.430	-2.466	0.036
4,4'-DMB$^-$	2,6,2',6'	$C+C_A+C_F$	-2.730	-2.760	0.030
2,6-DMB$^-$	2',6'	$C+C_D+C_H$	-2.340	-2.600	0.260
2,4,2',4'-TMB$^-$	6,6'	$C+C_A+C_F+C_H+C_I$	-2.310	-2.306	-0.006
3,5,3',5'-TMB$^-$	2,2',6,6'	$C+C_B+C_E+C_G+C_J$	-2.530	-2.524	-0.006
2,4,6,4'-TMB$^-$	2',6'	$C+C_A+C_F+C_D+C_I$	-2.380	-2.323	-0.057

Standard Deviation 0.154 Gauss
see footnotes p158

Table F Methylbenzene Radical Anions[1]

Parameter	Value (G)	Error[2] (G)
A	-3.574	0.185
A_B	-1.603	0.137
A_C	-2.006	0.137
A_D	3.883	0.185

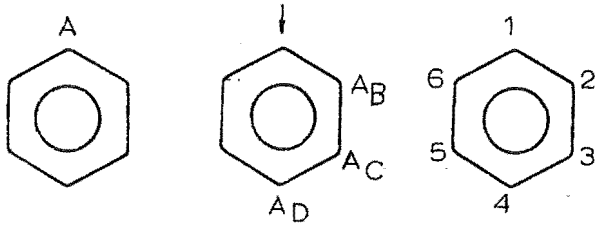

Compound	Position	Equation	Expt. (G)	Calc. (G)	Diff. (G)
Benzene$^-$	1	A	-3.807	-3.574	-0.233
Toulene$^-$	2	$A+A_B$	-5.120	-5.176	0.056
	3	$A+A_C$	-5.450	-5.580	0.130
	4	$A+A_D$	0.590	0.310	0.280
1,3-DMB$^-$	2	$A+2A_B$	-6.850	-6.779	-0.071
	5	$A+A_B+A_D$	-1.460	-1.293	-0.167
	4	$A+2A_C$	-7.720	-7.586	-0.134

Table F cont.

1,2-DMB$^-$	3	$A+A_B+A_C$	-6.930	-7.182	0.252
	4	$A+A_C+A_D$	-1.810	-1.696	-0.114
Standard Deviation					0.237 Gauss

DMB = Dimethylbenzene

[1] from 61Bol, 64Bol, [2] estimated parameter standard deviations

Table G Cyano-Benzene Radical Anions[1]

Parameter	Value (G)	Error[2] (G)
A	-3.153	0.770
A_B	0.144	0.503
A_C	1.845	0.503
A_D	-4.456	0.893

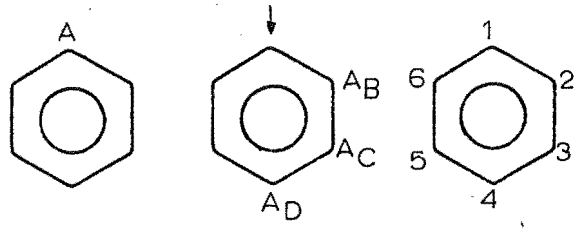

Compound	Position	Equation	Expt. (G)	Calc. (G)	Diff. (G)
Benzene$^-$	1	A	-3.807	-3.154	-0.653
Cyanobenzene$^-$	3	$A+A_C$	-0.300	-1.308	1.008
	2	$A+A_B$	-3.630	-3.010	-0.620
	4	$A+A_D$	-8.420	-7.610	-0.810
1,4-DCB$^-$	3	$A+A_B+A_C$	-1.590	-1.165	-0.425
1,2-DCB$^-$	3	$A+A_B+A_C$	-0.420	-1.165	0.745
	4	$A+A_C+A_D$	-4.130	-5.764	1.634
1,3-DCB$^-$	2	$A+2A_B$	-1.440	-2.866	1.426
	4	$A+A_B+A_D$	-8.290	-7.466	-0.824
	5	$A+2A_C$	-0.080	0.537	-0.617
1,2,4,5-TCB$^-$	3	$A+2A_B+2A_C$	-0.040	0.824	-0.864
Standard Deviation					1.179 Gauss

DCB = Dicyanobenzene, TCB = Tetracyanobenzene

[1] from 63Rei, [2] estimated parameter standard deviation

Table H Assignments for t-Butylacenaphthene According to Huffadine et al[1]

Parameter	Value (G)	Error[3] (G)
A	1.460	0.351
B	2.390	0.351
C	4.218	0.314
A_B	0.840	0.405
A_C	0.640	0.536
A_D	1.180	0.536
A_E	-0.940	0.405
A_F	0.540	0.536
B_A	0.475	0.405
B_C	-1.388	0.536
B_D	-0.988	0.536
B_E	-0.938	0.536
B_F	-0.765	0.405
C_A	0.081	0.391
C_B	-0.265	0.391
C_D	0.052	0.512
C_E	-0.115	0.391
C_F	0.151	0.391

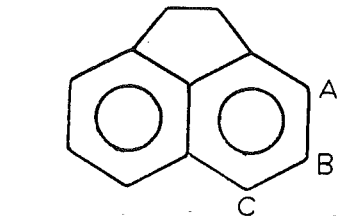

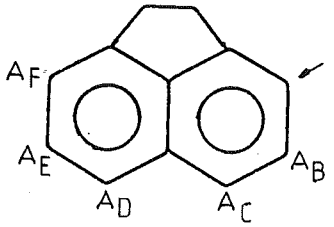

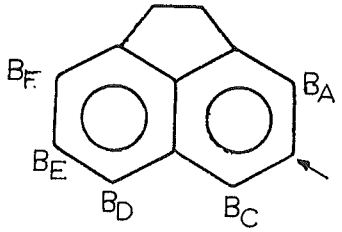

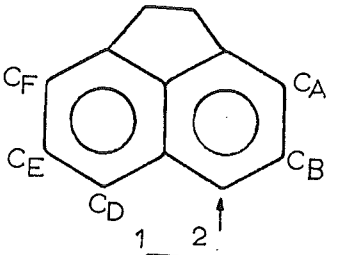

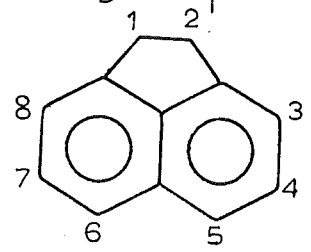

Table H cont.

Compound	Position	Equation	Expt. (G)	Calc. (G)	Diff. (G)
ACN[2]	3,8	A	1.090	1.460	-0.370
	4,7	B	2.390	2.238	0.153
	5,6	C	4.140	4.218	-0.078
3-TACN	8	$A+A_F$	2.000	2.000	0.000
	5	$C+C_A$	4.330	4.299	0.031
	6	$C+C_F$	4.400	4.369	0.031
	7	$B+B_F$	1.320	1.473	-0.153
	4	$B+B_A$	2.560	2.713	-0.153
4-TACN	7	$B+B_E$	1.300	1.300	0.000
	5	$C+C_B$	4.000	3.953	0.047
	6	$C+C_E$	4.150	4.103	0.047
	3	$A+A_B$	2.670	2.300	0.370
	8	$A+A_E$	0.890	0.520	0.370
5-TACN	3	$A+A_C$	2.100	2.100	0.000
	4	$B+B_C$	0.850	0.850	0.000
	6	$C+C_D$	4.270	4.270	0.000
	7	$B+B_D$	1.250	1.250	0.000
	8	$A+A_D$	2.640	2.640	0.000
3,8-DTACN	4,7	$B+B_A+B_F$	2.100	1.948	0.153
	5,6	$C+C_A+C_F$	4.420	4.451	-0.031
4,7-DTACN	3,8	$A+A_B+A_E$	0.990	1.360	-0.370
	5,6	$C+C_B+A_E$	3.790	3.837	-0.047
Standard Deviation					0.405 Gauss

[1] from 75Huf, [2]ACN = acenaphthene, TACN = T-butylacenaphthene, DTACN = di-t-butylacenaphthene, [3]estimated parameter standard deviation

Table I Best Fit Assignments for t-Butylacenaphthenes

Parameter	Value (G)	Error[2] (G)
A	1.118	0.061
B	2.407	0.061
C	4.218	0.055
A_B	0.155	0.071
A_C	-0.268	0.093
A_D	0.132	0.093
A_E	-0.255	0.071
A_F	0.202	0.093
B_A	-0.425	0.071
B_C	-0.308	0.093
B_D	0.233	0.093
B_E	0.263	0.093
B_F	0.135	0.071
C_A	0.081	0.068
C_B	-0.265	0.068
C_D	0.052	0.089
C_E	-0.115	0.068
C_F	0.151	0.068

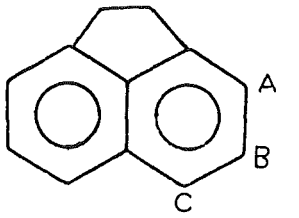

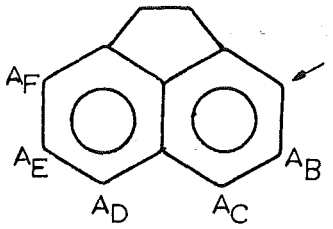

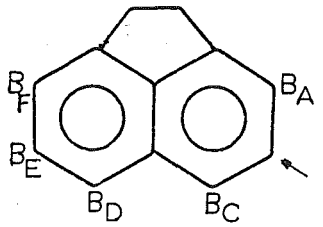

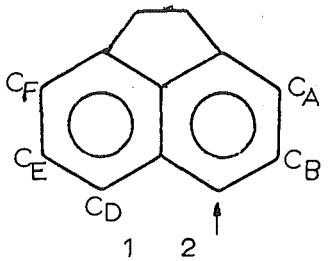

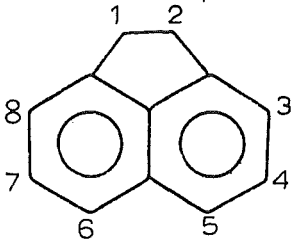

Table I cont.

Compound	Position	Equation	Expt. (G)	Calc. (G)	Diff. (G)
ACN[1]	3,8	A	1.090	1.118	-0.028
	4,7	B	2.390	2.401	-0.019
	5,6	C	4.140	4.218	-0.078
3-TACN	8	$A+A_F$	1.320	1.320	0.000
	5	$C+C_A$	4.330	4.299	0.031
	6	$C+C_F$	4.400	4.369	0.031
	7	$B+B_F$	2.560	2.542	0.018
	4	$B+B_A$	2.000	1.982	0.018
4-TACN	7	$B+B_E$	2.670	2.670	0.000
	5	$C+C_B$	4.000	3.953	0.047
	6	$C+C_E$	4.150	4.103	0.047
	3	$A+A_B$	1.300	1.272	0.028
	8	$A+A_E$	0.890	0.862	0.028
5-TACN	3	$A+A_C$	0.850	0.850	0.000
	4	$B+B_C$	2.100	2.100	0.000
	6	$C+C_D$	4.270	4.270	0.000
	7	$B+B_D$	2.640	2.640	0.000
	8	$A+A_D$	1.250	1.250	0.000
3,8-DTACN	4,7	$B+B_A+B_F$	2.100	2.118	-0.018
	5,6	$C+C_A+C_F$	4.420	4.451	-0.031
4,7-DTACN	3,8	$A+A_B+A_E$	0.990	1.018	-0.028
	5,6	$C+C_B+C_E$	3.790	3.837	-0.047
Standard Deviation					0.071 Gauss

[1]ACN = acenaphthene, TACN = T-butylacenaphthene, DTACN = di-t-butylacenaphthene, [2]estimated parameter standard deviation

Appendix 2.1

Description of Computer to Spectrometer Interface

The circuit diagram of the interface constructed by Mr. J. Sheriff of this department is shown in the accompanying diagram. The interface is connected to the parallel port of the SBC-100 CPU board. The signals 'direction input', 'scan input', and 'external enable are produced by the computer. The signals 'left limit', 'right input' and 'high freq. error' are signals from the interface to the computer. The interface is designed to produce a carriage return in either direction by providing a series of pulses to cause the plotter to step. When a limit error occurs, indicating that the plotter has reached either the right or left margin, the sequence of pulse finishes. The high frequency error signal was implemented to prevent a sequence of steps of frequency greater than the greatest possible stepping frequency being input. The error is generated by a timing circuit rather than any physical limitation of the plotter.

The interfaced is addressed by outputting a byte of value 00H to output port 7EH followed by a byte that contains the required command. The values of the various commands are as follows;

07H Disable the Y-axis; give control of the plotter Y-axis to the Spectrometer.

0FH	Set Direction to Right; causing the plotter to scan from left to right, i.e. towards increasing magnetic field.
09H	Raise the pen.
0DH	Return the plotter to the margin. The margin returned to is in the opposite direction to the scan command.
0EH	Set Direction to Left; causing the plotter to scan from right to left
0AH	Lower the pen.
08H	Enable the Y-axis; this results in the input for the Y-axis of the plotter coming from the computer

There are no constraints to prevent a command being given before a previous command has been executed, so that software timing routines are used to determine when commands are complete.

Further details are given in the documentation accompanying the computer, particularly in comments in the programs that operate this interface.

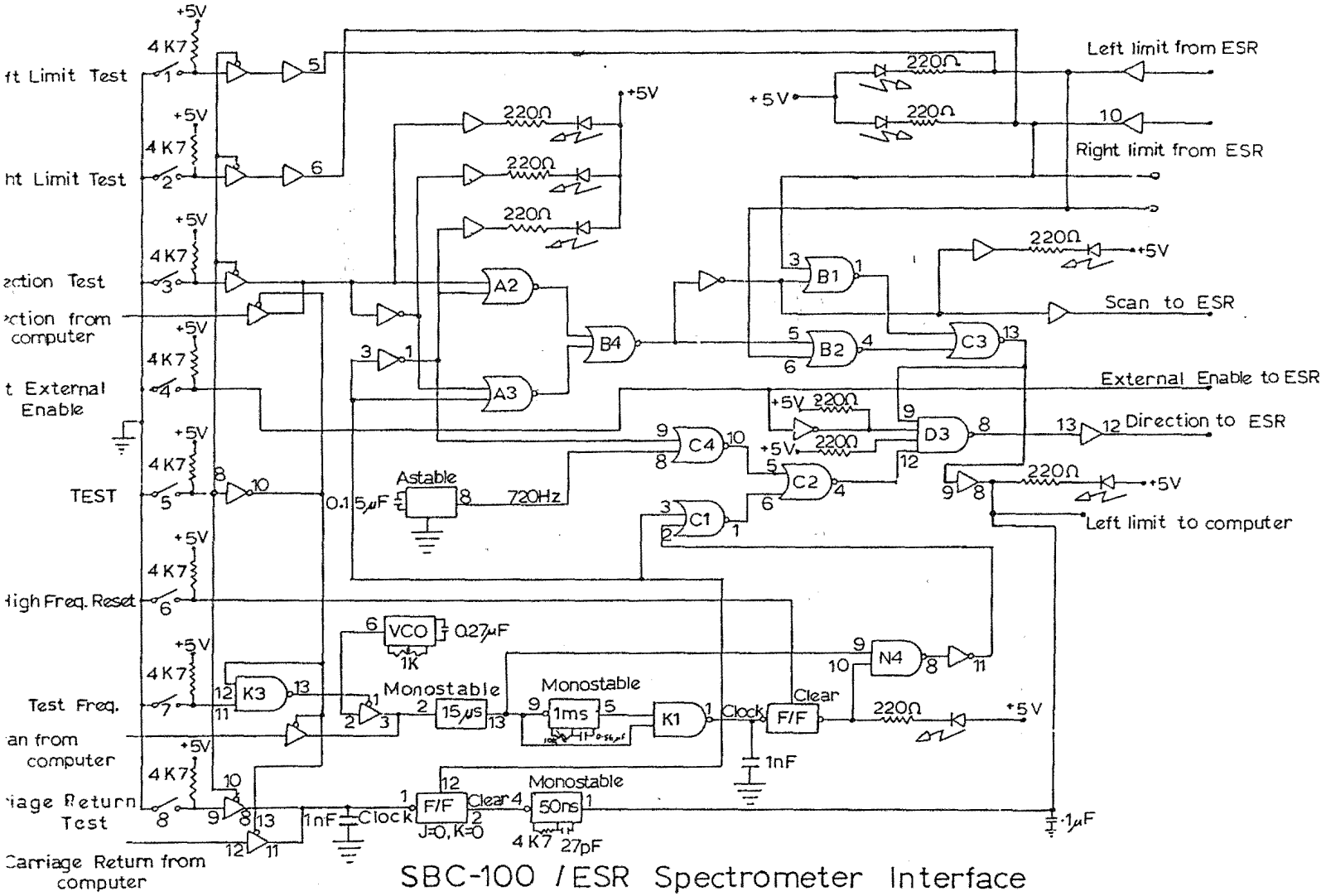

SBC-100 / ESR Spectrometer Interface

Appendix 2.2

Description of Computer-Frequency Counter Interface

The interface board can be divided into four separate units ; Address decoding, Digital Input, Digital Output, and Interrupt Servicing.

The first of these functions is handled by ICs U1 to U8. These ICs decode the address presented by the CPU and select the addressed IC. The base address of the group of addresses handled by the board can be selected by switches S1, S2, and S3.

Address Select			
S1	S2	S3	Base Address
Open	Open	Open	D8H
Open	Open	Closed	F8H
Open	Closed	Open	C8H
Open	Closed	Closed	E8H
Closed	Open	Open	D0H
Closed	Open	Closed	F0H
Closed	Closed	Open	C0H
Closed	Closed	Closed	E0H

Digital Input is performed by ICs V1 to V5 which are 8-bit latches. The four ICs V1 to V2 are split so that the four bits of one IC controlled by the low active control line are coupled with the corresponding four bits of another IC to produce one eight bit word. e.g. the Input Port with an address Base Address+2 is produced from the four bits of V3 and the four bits of V4 that are controlled by the high active control line.

Digital Output is performed by ICs R1, R2, and R3. R3 is a driver, required to control the A-60 Plotter. Because of the length of cable required between the computer and this plotter a

high powered driver was required. R5 is a tri-state buffer used to read from the A-60 plotter into the computer.

The Interrupt processing is performed by R4 which is a pulse-shaping circuit required to sharpen the pulses produced by the push button to which this circuit is connected.

In normal operation S1, S2, and S3 are all closed so that the base address selected is E0H. The input from the counter appears therefore at Input Ports E0H to E4H, control of the counter is through Output Port 0EH, and the A-60 plotter is controlled Input E7H and Output Port E7H.

Detailed examples of the use of this board are given in the listings of the programs MACHOL and ESRCON. Listings of which are kept with the computer.

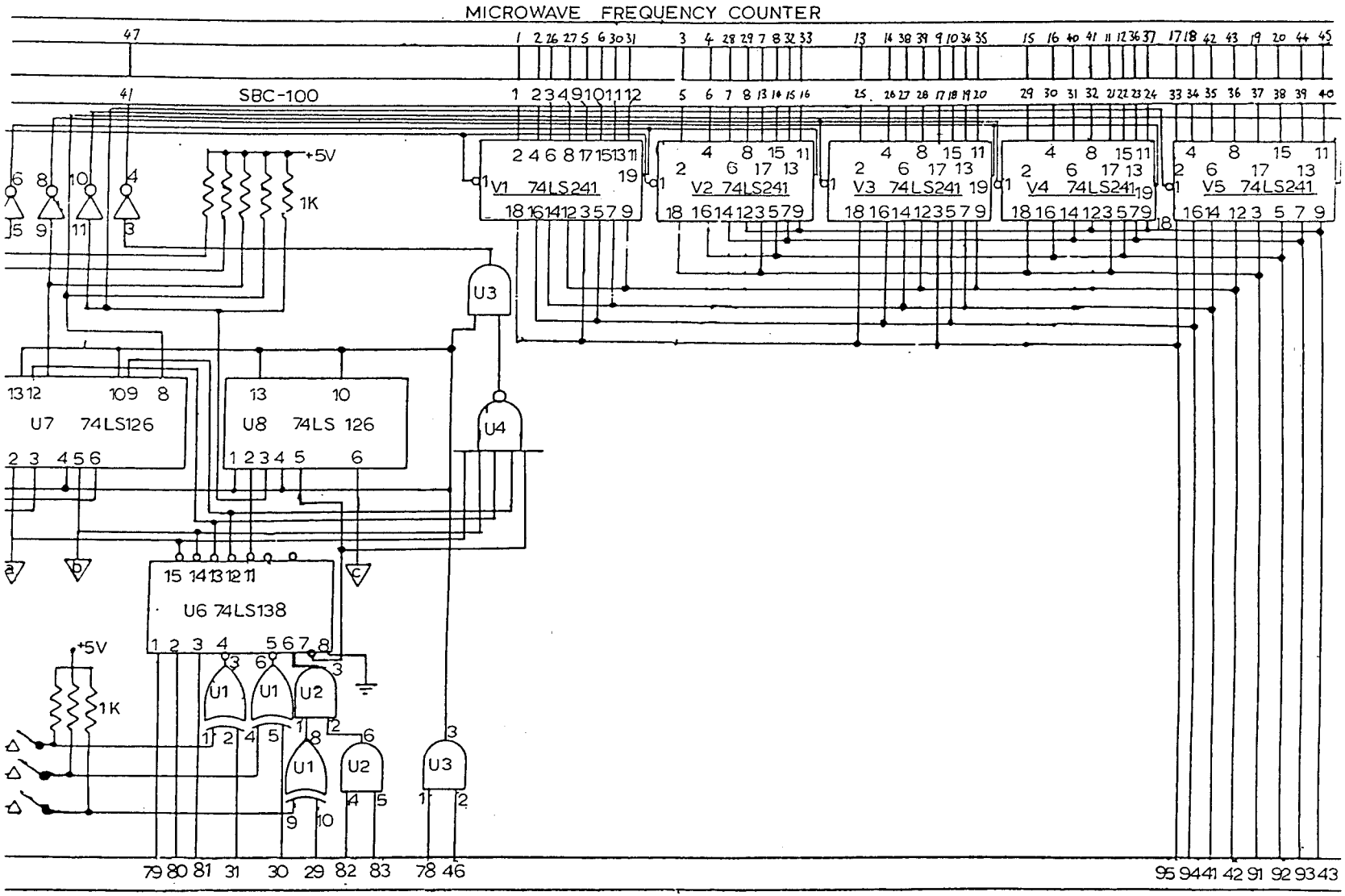

SBC-100 / FREQUENCY COUNTER INTERFACE

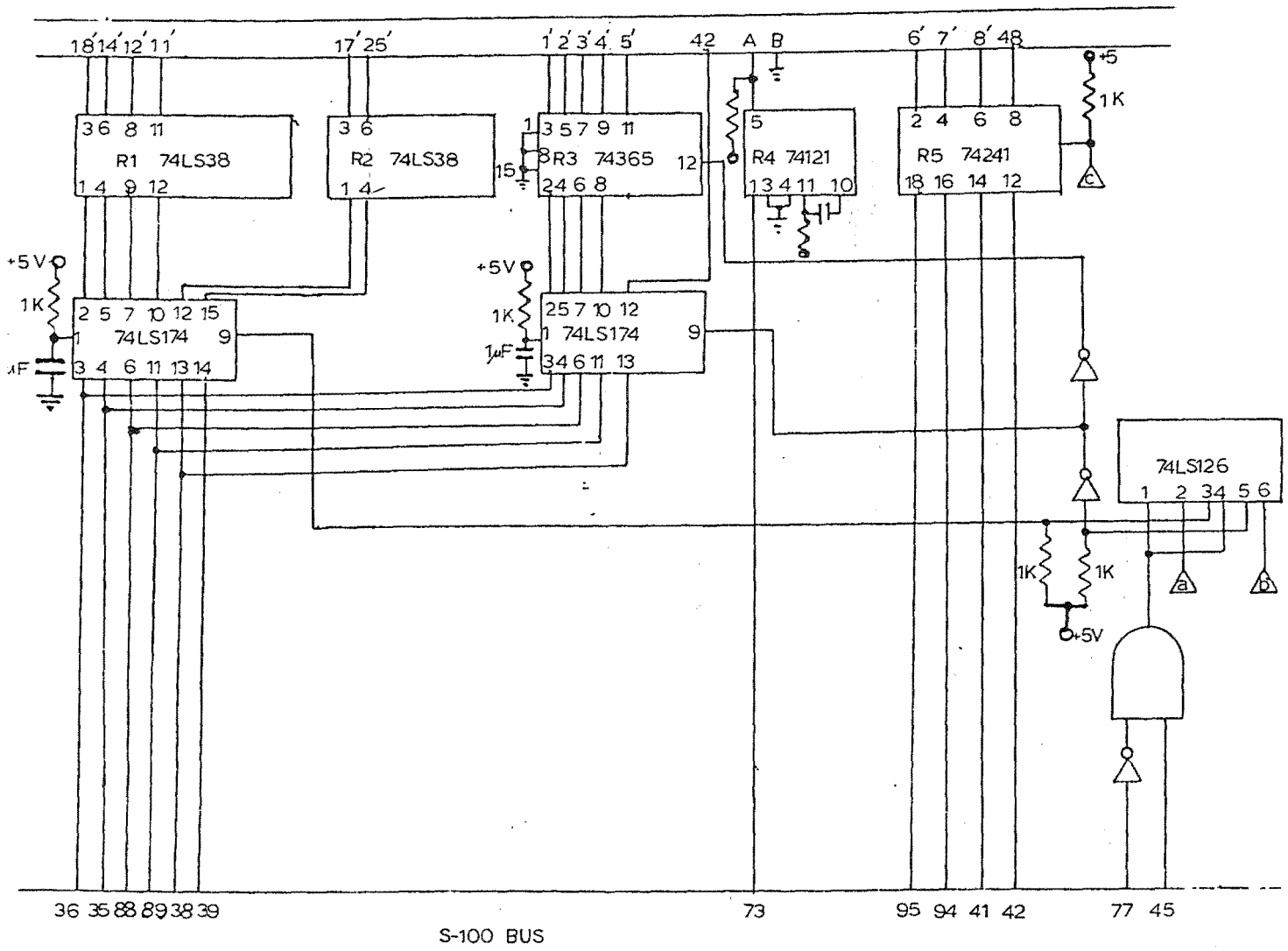
18 14 12 11
17 25
1 2 3 4 5
42
A B
6 7 8 48
+5
1K
3 6 8 11
R1 74LS38
1 4 9 12
3 6
R2 74LS38
1 4
1 3 5 7 9 11
R3 74365
2 4 6 8
12
15
5
R4 74121
13 4 11 10
2 4 6 8
R5 74241
18 16 14 12
+5V
1K
2 5 7 10 12 15
1 74LS174 9
3 4 6 11 13 14
1μF
+5V
1K
2 5 7 10 12
1 74LS174 9
3 4 6 11 13
74LS126
1 2 3 4 5 6
1K
1K
+5V
a
b
36 35 88 89 38 39
73
95 94 41 42
77 45
S-100 BUS

cont.

Appendix 2.3

File Formats

For all file types, the first number in the file is an I6 integer, called the file control word, which indicates the type of file that follows. If bit 14 is set, (bits read 0-15 least to most significant), then the file is a Lineshape file (i.e. a file produced by program LINESHA), if bit 6 is set then the file is a Stick file (i.e. a file produced by programs STICK and SORT). If bits 14, 11 and 9 are set then the file is a collect file. The various programs check the file control word and will indicate an error if the wrong file type is found.

Section 1 Stick Files

The file control word for Stick files is 64 (i.e. bit 6 set) for unsorted Stick files, and 65 (bits 6 and 0 set) for sorted files. The file control word, being followed directly by a carriage return and linefeed, is on a single line. The next line contains a comment line of 80 characters. The third line contains the center of the spectrum in F13.6 format. The fourth line contains the number of coupling constants in I3 format. The fifth, and subsequent lines contain the coupling constants, the number of nuclei with each coupling constant and the spin of the nuclei. There is one set per line. The format is; coupling constant: F12.6, number of nuclei: I4, spin: F12.6. A coupling constant calculated to second order is indicated in the file header has having a spin of 1000.5. The line after the last

coupling constant contains the number of (position, intensity) pairs in the file in I5 format. The file header is ended by a series of blanks. The number of blanks provided is enough to make the total length of the file header a multiple of 128 characters long. The remainder of the file contains the (position, intensity) pairs stored in core image format. The pairs are read/written in blocks of 16 using an unformatted read/write.

Section 2 Lineshape Files

The file control word contains information about the options used in creating a Lineshape file. If bit 0 is set then a gaussian curve was used. If bit 1 is set then a lorentzian curve was used. Bits 3 and 4 are coded for the derivative used. If neither is set then an absorption curve was used, if bit 3 only is set, 1st derivative, and if both 2nd derivative. The second line of the file header contains an 80 character comment. The third line contains the maximum and minimum amplitudes of the spectrum calculated, written in E13.6 format. The fourth line contains the upper and lower bounds, and scan range. The format used is 1X,3F12.6. The fifth line contains the number of species present in the file, written in 1X,I2 format. Normally this number is 1, but when LNLOAD is used to merge files it will be some other number. The sixth line contains the phase, linewidth and centre of the spectrum. The format is 28X,F12.6,I2,F10.4. The 28X contains a number 1.00002 to make the file header compatible with an earlier form of LNLOAD. The seventh line contains the number of coupling constants, in I2 format. The following lines

contain the sets of coupling constant, number of nuclei and spin in 1X,F12.6,I4,F12.6 format. The file header is padded with blanks to the next multiple of 128 characters. The data in the file follows in core image format.

Section 3 Collect Files

The only extra bit of the file control word used in Collect files is bit 5 which is set if the scan was aborted, so that only part of the scan was completed.

The file header of a Collect file is almost the same as that for a Lineshape file for the first six lines. The only differences are that the phase of a Collect file is set to zero. The seventh line of a Collect file contains the number of scans, and the number of samples per channel, both in I6 format. The file header is padded with blanks to the next multiple of 128 characters. The data is input/output using unformatted read/writes.

Appendix 2.4

Example Dialogue for SBC-100 Programs.

All responses made by the user are underlined. (cr) will be used to denote a carriage return entered by the operator.

Section 1 COLLECT

```
A>COLLECT(cr)
SCAN TIME IN SECONDS=?25.(cr)
RANGE OF SCAN=?10.(cr)
CENTRE OF SPECTRUM =?3250.(cr)
LOWER BOUND OF SPECTRUM=?3245.(cr)
UPPER BOUND OF SPECTRUM=?3255.(cr)
DO YOU WANT THE SPECTRUM ECHOED ON PLOTTER?Y(cr)

MICROWAVE CORRECTION(Y/N)?Y(cr)

MINIMUM SAMPLE/CORRECTION RATIO=  200
RATIO=?200.(cr)

MICROWAVE OVERRIDE THRESHOLD=20000.(cr)

ENABLE INTERRUPT FOR MAGNETIC FIELD MEASUREMENT (Y/N)?Y(cr)
COMMENT =
?SN107A/HP+17,HP/ALCL3/CH2CL2/SO2,-34C,1E4,1E-2, .25SEC,.2MW,100K
HZ(cr)
OUTPUT FILENAME=?SN107A(cr)
OUTPUT FILE DRIVE=?2(cr)

NAME OF OUTPUT FILE=SN107A  .DAT
COMMENTS:
SN107A/HP+17,
HP/ALCL3/CH2CL2/SO2,-34C,1E4,1E-2,.25SEC,.2MW,100KHZ
ACTUAL SCAN TIME=  24.58SECONDS
NUMBER OF SCANS=    1 TOTAL ELASPED TIME=   79.64 SECONDS
NUMBER OF SAMPLES PER CHANNEL =     2
CENTRE AT   3250.000000 GAUSS,RANGE IS    10.000000 GAUSS
UPPER BOUND AT 3255.00000 GAUSS,CHANNEL NUMBER  4982
LOWER BOUND AT 3245.00000 GAUSS,CHANNEL NUMBER     1
ECHO ENABLED
MICROWAVE CORRECTION AT    200 POINTS
INTERRUPT ENABLED FOR MAGNETIC FIELD MEASUREMENT
DO YOU WISH TO MAKE ANY CHANGES?N(cr)

DO YOU WANT SPECTRUM PLOTTED?Y(cr)
```

```
(the program here returns the plotter to the left hand margin)
INPUT "Y" WHEN OSCILLOSCOPE MODULATION IS TURNED OFFY(cr)

INPUT "Y" WHEN FREQUENCY COUNTER SWITCHES ARE OUTY(cr)
(the program nows scans the spectrum)
HIT RETURN TO PLOT SPECTRUM(cr)
(the collected spectrum is now plotted back, and output to disk)
```

Section 2 Simulation Programs

```
A>STICK(cr)
INPUT FILE EXISTS?(Y/N)N(cr)

NAME OF OUTPUT FILE=?S7P1(cr)
OUTPUT FILE DRIVE=?2(cr)
TITLE OF FILE?(IN 80 CHAR OR LESS)
CALCULATION TO 6,7+ AT -90C(cr)
CENTRE OF SPECTRUM=?50.(cr)

OUTPUT TO DISK?N(cr)
COUPLING CONSTANT=?1.5(cr)
NUMBER OF THIS TYPE OF NUCLEUS=?2(cr)
SPIN OF NUCLEUS=?.5(cr)
ORDER=?2(cr)
DO YOU WANT LINES PRINTED?(Y/N)N(cr)

OUTPUT TO DISK?Y(cr)
COUPLING CONSTANT=?1.(cr)
NUMBER OF THIS TYPE OF NUCLEUS=?1(cr)
SPIN OF NUCLEUS=?.5(cr)
ORDER=?1(cr)
DO YOU WANT LINES PRINTED?(Y/N)N(cr)

WHICH PROGRAM NEXT?(0-5)2(cr)

A>ERA B:S7P1.DAT
NO FILE
A>REN B:S7P1.DAT=B:S7P1.$$$
A>A:SORT

NAME OF FILE TO BE SORTED IS?S7P1(cr)
DRIVE=?2(cr)

SUM LINES WITH SAME POSITIONS?Y(cr)


WHICH PROGRAM NEXT?(0-5)3(cr)
A>ERA FORT??.DAT
NO FILE
A>ERA B:S7P1.DAT
A>REN B:S7P1.DAT=S7P1.$$$
A>A:LINESHA

NAME OF INPUT FILE?S7P1(cr)
INPUT FILE DRIVE=?2(cr)
```

```
OUTPUT FILENAME=?S7PL(cr)
OUTPUT FILE DRIVE=?2(cr)
LOWER BOUND OF SPECTRUM=?45.(cr)
UPPER BOUND OF SPECTRUM=?55.(cr)
SCAN RANGE(IN GAUSS)=?20.(cr)
GAUSSIAN(G) OR LORENTZIAN(L)?L(cr)
SPECTRUM TYPE?;"0"=ABSORPTION
               "1"=FIRST DERIVATIVE
               "2"=SECOND DERIVATIVE1(cr)
LINEWIDTH=?.05(cr)
PHASE=(1./-1.)?-1.(cr)


WHICH PROGRAM NEXT?(0-5)4(cr)
A>ERA B:S7PL.DAT
NO FILE
A>REN B:S7PL.DAT=B:S7PL.$$$
A>A:GRAPH

INPUT FILENAME=?S7PL(cr)
INPUT FILE DRIVE=?1(cr)

SCAN RANGE=     20.000
STEPS PER POINT (AS *N. OR /N.)?*2.(cr)

>>>LOWER BOUND=   45.0000 <<<
PLOT LOWER BOUND=?45.(cr)

>>> UPPER BOUND=   55.0000 <<<
PLOT UPPER BOUND=?55.(cr)
HORIZONTAL OFFSET=?0.(cr)
SCALING OPTIONS:
(1) DEFAULT=MAXIMUM AND MINIMUM VALUES FROM FILE,SCALED TO GIVEN
HEIGHT
(2) LOCAL DEFAULT = MAXIMUM AND MINIMUM VALUES IN REGION PLOTTED,
SCALED TO GIVEN HEIGHT
(3) ABSOLUTE VALUES INPUT
WHAT IS YOUR CHOICE?1(cr)

WHAT IS THE HEIGHT (IN CM) OF THE SPECTRUM?5.(cr)
OFFSET REQUIRED(Y/N)?Y(cr)
OPTIONS;(1) OFFSET IN CM
        (2) REQUIRE FIRST POINT TO BE AT A GIVEN HEIGHT?2(cr)
REQUIRED HEIGHT=?12.(cr)

FINE TUNE PEN POSITION(Y/N)?Y(cr)

LINEARISE PLOT(Y/N)?N(cr)

WRITE TO OUTPUT FILE?(Y/N)N(cr)

WHICH PLOTTER:0=E-12
              1=A-60:?1

COMMANDS:
R=RIGHT,L=LEFT,U=UP,D=DOWN,E=BEGIN PLOTTINGUUUUUUUUURRRRRE
```

SECTION 3 LNLOAD

```
A>LNLOAD(cr)
NAME OF INPUT FILE 1?C1M6L(cr)
INPUT FILE 1 DRIVE=?2(cr)
NAME OF INPUT FILE 2?C1M6L(cr)
INPUT FILE 2 DRIVE=?2(cr)

NAME OF OUTPUT FILE?C1M7L(cr)
OUTPUT FILE DRIVE=?2(cr)
HORIZONTAL OFFSETS REQUIRED(Y/N)?Y(cr)
HORIZONTAL OFFSET FILE 1 (IN GAUSS)=?5.3(cr)
HORIZONTAL OFFSET FILE 2 (IN GAUSS)=?0.(cr)
SET BOUNDS(Y=SET,N=DEFAULT SETTING)?Y(cr)
OUTPUT FILE LOWER BOUND=?40.(cr)
OUTPUT FILE UPPER BOUND=?50.(cr)
LOWER BOUND OF FILE 1 =?40.(cr)
UPPER BOUND OF FILE 1 =?60.(cr)
LOWER BOUND OF FILE 2 =?40.(cr)
UPPER BOUND OF FILE 2 =?60.(cr)
VERTICAL OFFSET FILE 1 (IN CM)=?.(cr)
VERTICAL OFFSET FILE 2 (IN CM)=?.(cr)
FILE 1 UNDEFINED TO LOWER BOUND;
FILL OPTIONS:
(1)ZERO
(2)AVERAGE OF MAX AND MIN VALUES
(3)VALUE INPUT
?1(cr)
FILE TITLE=? CAL TO 1-METHYL NAP-, 7 COUPLING CONSTANTS(cr)
DO YOU REQUIRE:(1)ABSOLUTE SCALING
               (2)RELATIVE SCALING
               (3)EXPERIMENTAL SCALING?1(cr)
WEIGHT OF FILE 1=?.5(cr)
WEIGHT OF FILE 2=?.5(cr)
SUBTITLE FOR SPECIES IN INPUT FILE 1 ?(cr)
SUBTITLE FOR SPECIES IN INPUT FILE 2 ?(cr)

WHICH PROGRAM NEXT?(0-5)0(cr)

A>ERA B:C1M7L.DAT
NO FILE
A>REN B:C1M7L.DAT=B:C1M7L.$$$
A>
```

The effect of the above is to add a singlet, 5.3 Gauss coupling constant to the existing six coupling constants that have been simulated. Adding a coupling constant in this fashion is considerably faster than adding one via STICK, SORT, and LINESHA.

```
A>LNLOAD(cr)
NAME OF INPUT FILE 1?SN107A(cr)
INPUT FILE 1 DRIVE=?2(cr)
NAME OF INPUT FILE 2?SN107B(cr)
INPUT FILE 2 DRIVE=?2(cr)

NAME OF OUTPUT FILE?SN107T1(cr)
```

```
OUTPUT FILE DRIVE=?2(cr)
HORIZONTAL OFFSETS REQUIRED(Y/N)?Y(cr)
HORIZONTAL OFFSET FILE 1 (IN GAUSS)=?0.03(cr)
HORIZONTAL OFFSET FILE 2 (IN GAUSS)=?0.(cr)
SET BOUNDS(Y=SET,N=DEFAULT SETTING)?Y(cr)
OUTPUT FILE LOWER BOUND=?3241.397(cr)
OUTPUT FILE UPPER BOUND=?3260.98725(cr)
LOWER BOUND OF FILE 1 =?3241.367(cr)
UPPER BOUND OF FILE 1 =?3250.0(cr)
LOWER BOUND OF FILE 2 =?3250.03(cr)
UPPER BOUND OF FILE 2 =?3260.98725(cr)
VERTICAL OFFSET FILE 1 (IN CM)=?.(cr)
VERTICAL OFFSET FILE 2 (IN CM)=?.(cr)
FILE 1 UNDEFINED TO UPPER BOUND;
FILL OPTIONS:
(1)ZERO
(2)AVERAGE OF MAX AND MIN VALUES
(3)VALUE INPUT
?1(cr)
FILE 2 UNDEFINED TO LOWER BOUND;
FILL OPTIONS:
(1)ZERO
(2)AVERAGE OF MAX AND MIN VALUES
(3)VALUE INPUT
?1(cr)
FILE TITLE=? SN107A&B/HP+, HP/ALCL3/SO2, -90C(cr)
DO YOU REQUIRE:(1)ABSOLUTE SCALING
                (2)RELATIVE SCALING
                (3)EXPERIMENTAL SCALING?3(cr)
WEIGHT OF FILE 1=?.5(cr)
WEIGHT OF FILE 2=?.5(cr)
SUBTITLE FOR SPECIES IN INPUT FILE 1 ?SN107A(cr)
SUBTITLE FOR SPECIES IN INPUT FILE 2 ?SN107B(cr)

WHICH PROGRAM NEXT?(0-5)0(cr)

A>ERA B:SN107T1.DAT
NO FILE
A>REN B:SN107T1.DAT=B:SN107T1.$$$
A>
```

The above is an example of the concatenation of two collect output files.

Details of Programs Written

Section 1 COLLECT

The FORTRAN section of the program is called COLLECT.F80. It is compiled using the F80 FORTRAN compiler, and linked with the required operating system subroutines using LINK or L80. When linking, it is necessary to leave the region of memory from 100H to 800H free for the assembly language routines. This can be done by using /:P800. The source code for the assembly language section of COLLECT is in file MACHOL.ZSM. This file is assembled by the S.D. Sales Z-80 Assembler and loaded by LOAD to produce an executable file. The interfacing of the assembly language subroutines with the linked FORTRAN code is done by using ZSID, the debugger provided with the operating system. The linking of the two sets of routines involves placing JMP <address> instructions at the beginning of the dummy subroutines GO, INITAL, PEND, MOVE and PENUP provided in the FORTRAN code. Where <address> is the start location of the corresponding subroutines START (address 103H), INITAL, SPEND, MOVE and SPENUP in the assembly language section. There is one further JMP required, this is JMP 800H at 100H, which means that the program begins executing the FORTRAN code first.

The normal mode used is :

(1) Scan time. This is the time to be spent on scanning the spectrum. From this time is calculated the number of samples (A to D conversions) to be taken at each point.

(2) single scan. An option exists to do multiple scanning summing the spectra as they are recorded. This option is not compatible with doing a microwave correction. Because of the incompatibility, the multiple scanning option is rarely used. In this study the average linewidth was 50mG and, for a number of compounds, linewidths of ca. 20mG were recorded. Clearly microwave drifts of 30-40mG or more mean that multiple scanning would cause the resultant spectrum to be 'smeared' with an apparent linewidth much larger than the actual linewidth and a consequent loss of resolution.

(3) from one edge of the plotter to the other : The operator is prompted to input the field and scan range set, and then asked the value of the magnetic field to start scanning at, and the value at which to stop.

(4) echo set : This results in the pen being down and the Y-axis linked to the ESR Spectrometer during the scan, so that a normal ESR spectrum is produced.

(5) microwave correction set : The spectrum output to the disk file, but not the spectrum echoed on the plotter, is corrected for microwave drift.

(6) The ratio Sample/Correction set to the minimum possible value. This ratio is the number of points (also referred to as channels) between successive readings of the frequency counter.

The maximum value possible is 3, which corresponds to 1660 readings of the microwave field. This is the maximum number of microwave readings that can be stored.

(7) Microwave override set to approximately 20000.0 - 50000. depending upon the time spent scanning. This option allows for the possiblity of an incorrect reading of the counter by the computer. When the program is correcting for changes in the microwave frequency (at the end of each scan), the program compares successive readings and, if the difference is more than the value input, it halts processing, displays the two microwave readings, and asks the operator whether or not the second reading is to be ignored. The precise value for this variable is a matter of trial and error as it depends on the length of time the scan will take and upon the stablity of the variable temperature controller.

(8) The interrupt would be enabled so that a marker can be placed in the output file and on the echoed spectrum. When the interrupt is enabled, pushing the push button on the console will cause the program to halt data collection, switch the frequency counter to radio frequency, and read the frequency of the Systron Donner frequency counter. The radio frequency input of this counter is normally attached to the output from the NMR Gaussmeter, so that it is this frequency that is read. The program expects this to be a valid frequency marker, calculating the value of the magnetic field at the marker, and adjusting the boundaries of the file accordingly.

(9) The resulting spectrum would normally be plotted back. This means that at the end of the scan, when the program is outputting

the collected spectrum to the disk file and making the microwave correction, the pen would be down, and the Y-axis controlled by the computer so that the spectrum plotted out would be the same one as is being output to the disk file.

Once all the required input parameters have been entered, the program prints them back, together with a number of derived parameters such as the number of samples to be taken at each point. It then gives the operator an opportunity to make any changes to the input parameters that might be required. Once the plotter has returned to the left hand margin, the program prompts the operator to check that all the range and selection switches on the frequency counter are off, and that the modulation of the oscilloscope is off. The program then proceeds to scan the spectrum.

There are also a number of options which will modify the data collection and which are used during the scan. The first is an option to abort the data collection. Pushing the Esc(Escape) key will abort the data collection. The program will then ask if the data collected before the abort instruction is to be saved to the disk file. Pressing key 'H' during a data collection will halt the data collection, and pressing key 'R' will cause the data collection to resume. Pressing key 'C', at any time, will cause the data collection to continue until either the right hand edge of the plotter is reached or until Esc is used.

Section 2 Transfer of Data and Control Between Programs

Data is transferred between programs using one of two file formats. These file formats are respectively Stick format and Lineshape format. Stick format files are used as both input and output files by STICK, SORT and LNLOAD, and as input file by LINESHA. The file header contains a file control word which indicates what operations have been performed.

Control is passed from one program to the next by use of a implied form of the CP/M SUBMIT command. When CP/M does a cold start, such as would occur when the power is first turned on, CP/M checks to see if a file named $$$.SUB is present on disk. If this file is present it reads and executes the contents precisely as if they had been keyed in by the operator. Before the STOP command is executed at the end of each program, the program concerned creates a file $$$.SUB, which contains the details of any file erase and rename commands, and the name of the next program to run. The instructions are written into the $$$.SUB file, one line per block and in the opposite order to which they are processed.

Because of an error in the FORTRAN-80 used, when random access files are being used, closing a random access output file will corrupt a random access input file. This problem is overcome by calling a subroutine called ESCAPE, in STICK, SORT, LINESHA and LNLOAD. ZSID is used to add a JMP 0000 (i.e. return to the operating system.) at the start of subroutine ESCAPE.

It should also be noted that much of the input read from the keyboard uses F format, and therefore requires the use of a decimal point, otherwise the value of the number read by the program is likely to be some power of ten too large or too small.

Section 3 STICK.

STICK accepts input from the console to generate a Stick file. STICK will also accept Stick output files as an input file and generate further Stick files. If it is not given an input file, STICK asks for a comment line of up to 80 characters and the centre of the spectrum. STICK then asks if the output file is to be closed after the next coupling constant is generated. STICK next asks for the coupling constant, the number of nuclei with that coupling constant, their spin, and whether to use a first or second order approximation. If second order is requested for any but spin 1/2 nuclei, STICK calculates a first order spectrum. If the output file is to be closed, the next program is selected, otherwise the next coupling constant is requested. STICK is able to buffer 1500 lines internally, but once this number is exceeded automatically outputs to the output file. A temporary file <filename>.$$$ is used, which STICK changes to <filename>.DAT, before passing control to the next program selected. If the input and output files have the same name STICK changes the name of the input file to <filename>.DBK. Since each coupling constant is generated separately the maximum waiting time would be 3-4minutes. The number of lines that STICK can buffer internally is dependent upon the FORTRAN used. FORTRAN-80 will only load

programs into the bottom 32K of core, so that the 16K up to the operating system area is free. This could easily be accessed by using a small assembly language handler in M-80 code, to set up an array in this area. This would add a further 4000 lines to the buffer.

Section 4 SORT

SORT sorts the Stick files produced by STICK into ascending positional order. Because of the size of the program, SORT requires a special linking procedure. When LINK issues the first prompt for a command line /P: and /D: are used to place the program and data areas well apart. The program is then linked normally. Once the library routines have been linked in, the length of the program and data segments can be calculated. /R is then used to reset the linker. /P: and /D: are then used to control the linking, where, contrary to normal practice, the program origin is placed above the data origin.

Files with less than 1900 lines can be handled internally, using the sorting routine of Peake (71Pea). Files larger than this are sorted by splitting them into groups of 1900 lines. These groups are then written alternately into files FORT06.DAT and FORT07.DAT on A: drive. A merge sort of the groups is then done into files FORT08.DAT and FORT09.DAT. Further merge sorts are done between these two pairs of files, until the sort is completed. Once the merge sort is complete the sorted file is rewritten into the output file. A command to remove all

FORT??.DAT files from A: drive is included in the submit file produced.

Section 5 GRAPH

GRAPH consists of two sections, the FORTRAN section which does the calculations and disk input, and an assembly language section which drives the plotters. The assembly language section is written in M-80, and so can be directly linked with the FORTRAN code using L-80. The assembly language source code is file ESRCON.M80. The FORTRAN code is linked first followed by the assembly language module.

The plotting options available with GRAPH are; the X-axis (the magnetic field axis) can be expanded or contracted an integral number of times, e.g. replying *3. to the question "STEPS PER POINT (AS *N. OR /N.)?" will result in a three fold scale expansion. Similarly /5. will produce a five fold scale contraction. The position of the first point plotted on the plotter can be controlled using the Horizontal offset. e.g. for a 10 Gauss scan entering 2. for the horizontal offset will result in an 8 cm gap before the first point is plotted. Care must be exercised using horizontal offset and scale expansion together.

The scale of the Y-axis (the amplitude) can be controlled by one of three scaling options. Option 1, calculates the scaling factor to be applied by dividing the required height of the spectrum by the difference between the maximum and minimum amplitudes in the file. e.g. when plotting a simulation to a spectrum, the height of the centre line of which was 10 cm, this

option would be used and a height of 10cm input. Option 2 is similar, but the difference used is that between the maximum and minimum amplitudes in the part of the file being plotted. Option 3, is normally used to output collected spectra. The maximum and minimum values to be used are input at the console. For collected spectra the values input are, 4095. for the maximum value and 0. for the minimum value. The height of the spectrum is assumed to be 24.0 cm.

Two offsets are provided, one is simply a direct distance offset, e.g. move the spectrum 2.0 cm upwards. The second calculates the offset required to place the first point of the spectrum at some given height, and then uses this throughout.

The precise position of the pen can be fine tuned, using the fine tuning option, which allows the pen to be moved in any direction one point at a time.

The contents of the input disk file can be output in ASCII to an output file rather than plotted.

When using the A-60 plotter, the plotting of a file can be aborted simply by switching the plotter off.

Section 6 LNLOAD

LNLOAD is used to manipulate both Stick and Lineshape files. It can merge two Stick files with an offset, to simulate a difference in g-value, and with different intensities, to simulate different concentrations of the two species. If two sorted Stick files are merged the output is also sorted, but if either input file is unsorted the output file is also unsorted.

LNLOAD can add or subtract two Lineshape files to produce a weighted result. It can also produce a merged form. This is done by specifing the parts of the two files that are to be written to the output file, and ensuring that there is no overlap. e.g. if the region between 3240G and 3250G in one file, and 3250G and 3260G in the other file is to be used, a file of the region between 3240G and 3260G will be produced. An offset can be used with this option.

To merge two Collect files together, experimental scaling is used. To merge two Lineshape files together absolute scaling is used. see Appendix 2.4 for examples.

Section 7 GRAPHS

GRAPHS is a high resolution plotting program, the commands are identical to those of GRAPH, except that where GRAPH asks for a scale as *N. or /N., GRAPHS requires X/Y where X and Y are in the range 1 to 99. The algorithm used, is again linear interpolation. GRAPHS uses a more efficient version of ESRCON.M80, in that when doing a carriage return to the left hand margin of the E-12 plotter, the improved version tests for limit error rather than waiting a fixed 30 seconds for the plotter to do a carriage return. A plot being done on either plotter can be aborted by pressing CNTL 3. (i.e. hold down the control and 3 keys simultaneously.) The scaling factors to produce the usual scales are 2/1 for the E-12 plotter and 7/1 for the A-60.

APPENDIX 2.6

Modifications to ESRCON

(1) the size of the arrays were increased so that 15,000 rather than 1,000 points and 5,000 rather than 500 lines could be fitted.

(2) The centre of the spectrum was fitted on both axes.

(3) The program, as received, could only fit spectra consisting of one species. Modifications were made to allow spectra for which two species were present to be fitted, subject only to the constraint that the linewidth for both species was the same.

(4) The program was modified to allow for second order coupling constants.

(5) Alterations to the program were made to allow any, all or none of the coupling constants to be refined.

(6) Provision was made to allow a portion of the spectrum to be printed on a line-printer, so that it is possible to inspect the agreement between the calculated and experimental spectrum immediately.

(7) If the sum of the squares of the residuals rises from one iteration to another, the program can be instructed to check with the operator whether or not to continue. This means that on those occasions when the sum of the squares of the residuals does not decrease monotonically, the program will not automatically stop, but may, if so instructed, continue with the next iteration.

(8) Some of the spectra dealt with did not have a flat baseline, but rather had a broad curve. An option was added to

ESRCON to allow a lorentzian curve to be fitted to the baseline. This was found to significantly improve the fit, and also effect the values of the fitted coupling constants.

(9) The 'goodness of fit' parameter used in the original program was R, where

$$R = \sqrt{\frac{\sum (O_n - C_n)^2}{(N-k)}}$$

and O_n are the observed amplitudes, C_n are the calculated amplitudes, N is the number of observations and k the number of variables. Use of this parameter does not allow a comparison to be made between different spectra, as the actual value is dependent on the gain settings and the amplitude offset of the spectrum. Modifications were made such that the weighted parameter R_0 was also output, where

$$R_0 = \sqrt{\frac{\sum (O_n - C_n)^2}{\sum (O_n - Offset)^2}}$$

and Offset is the value of the signal amplitude for no microwave absorption.

The program calculates error limits for the fitted coupling constants and other parameters based on the assumption of a normal (gaussian) distribution of errors. These error limits would imply that the coupling constants were fitted to better than 0.1mGauss. Use of the program, on sets of spectra from one system under the same conditions, suggested that an overall error of $\pm$0.006 Gauss might be more reasonable. This is the error limit

of all coupling constants determined in this study, unless otherwise indicated. Some individual spectra might well be fitted to an accuracy considerably better than this, but it would be difficult to determine in individual cases what the error limits should be.

Appendix 3.1 Least Squares Refinement of Additivity Parameters for α Protons in Peri-alkylnaphthalene Anion Radicals

Parameter	Value (G)	Error[#] (G)
A	-1.826	0.042
^{5}F *	-0.544	0.049
^{5}N	0.747	0.049
^{7}F	-0.060	0.044
^{7}N	0.303	0.044
^{6}F	-0.576	0.049
^{6}N	0.751	0.049

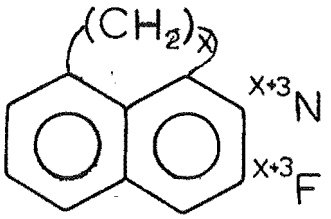

Compound	Position	Equation	Expt. (G)	Calc. (G)	Diff. (G)
naphthalene^{-}	2	A	-1.842	-1.826	-0.016
acenaphthene^{-}	4	A+^{5}F	-2.420	-2.370	-0.050
	3	A+^{5}N	-1.040	-1.079	0.038
pyracene^{-}	α	A+^{5}N+^{5}F	-1.580	-1.623	0.043
dipleiadane^{-}	α	A+^{7}N+^{7}F	-1.570	-1.582	0.012
pleiadane^{-}	1	A+^{7}N	-1.580	-1.523	-0.057
	2	A+^{7}F	-1.800	-1.885	0.085
5,7PN^{-}	$^{5}\alpha$	A+^{5}N+^{7}F	-1.220	-1.138	-0.082
	$^{7}\alpha$	A+^{5}F+^{7}N	-2.060	-2.067	0.007
phenalene^{-}	1	A+^{6}F	-2.420	-2.401	-0.019
	2	A+^{6}N	-1.040	-1.075	0.035

Appendix cont.

hexahydropyrene⁻		$A+{}^{6}N+{}^{6}F$	-1.670	-1.651	-0.019
6,7PN⁻	$^{6}\alpha$	$A+{}^{7}N+{}^{6}F$	-2.060	-2.098	0.038
	$^{7}\alpha$	$A+{}^{7}F+{}^{6}N$	-1.150	-1.135	-0.015

Standard Deviation 0.062

Gauss

* the parameter ^{x}N is defined as the change in proton due to an 'x'-membered ring adjacent to it. The parameter ^{x}F is defined as the change in an α proton due to an 'x'-membered across the more distant peri positions of the naphthalene ring.

#Estimated parameter standard deviation

Appendix 4.1 Coupling Constants for Methylnaphthalene Anions

Table A : Experimental Coupling Constants for Monomethylnaphthalene Anions

System	temperature ($\pm 2^0$C)	Coupling Constant ($\pm$0.005G)	Position[1]
1-MN/K^+/DEE	-86^0C	0.063	K^+
		1.491	
		1.546	
		2.007	
		2.296	
		3.508	Me (1)
		4.073	
		5.360	
		5.657	
1-MN/K^+/DME	-90^0C	1.409	
		1.529	
		1.964	
		2.290	
		3.854	Me (1)
		4.408	
		5.031	
		5.372	
1-MN/K^+/DME	-64^0C	1.437	
		1.519	
		1.973	
		2.271	
		3.812	Me (1)
		4.364	
		5.076	
		5.400	
1-MN/K^+/DME	-31^0C	1.465	
		1.526	
		1.984	
		2.247	
		3.753	Me (1)
		4.281	
		5.143	
		5.424	
1-MN/K^+/DME	0^0C	1.480	
		1.521	
		1.979	
		2.226	
		3.718	Me (1)
		4.251	
		5.172	
		5.438	

1-MN/K^+/MTHF	-78^0C	1.460	
		1.515	
		2.012	
		2.285	
		3.595	Me (1)
		4.119	
		5.281	
		5.571	
1-MN/K^+/MTHF	-44^0C	1.476	
		1.528	
		2.004	
		2.277	
		3.605	Me (1)
		4.140	
		5.275	
		5.568	
2-MN/K^+/DME	-88^0C	1.331	
		1.729	Me (2)
		2.269	
		2.322	
		4.602	
		4.764	
		5.063	
		5.063	
2-MN/K^+/DME	-62^0C	1.318	
		1.691	Me (2)
		2.259	
		2.319	
		4.588	
		4.705	
		4.994	
		5.050	
2-MN/K^+/DME	-27^0C	1.324	
		1.656	Me (2)
		2.299	
		2.368	
		4.654	
		4.658	
		4.940	
		5.128	
2-MN/K^+/DME	$+1^0$C	1.322	
		1.637	Me (2)
		2.301	
		2.369	
		4.629	
		4.674	
		4.903	
		5.152	

2-MN/K^+/DME	$+21^0$C	1.320	
		1.629	Me (2)
		2.307	
		2.371	
		4.623	
		4.683	
		4.894	
		5.160	
2-MN/K^+/MTHF	-73^0C	1.362	
		1.691	Me (2)
		2.303	
		2.371	
		4.577	
		4.792	
		4.825	
		5.243	
2-MN/K^+/MTHF	-44^0C	1.355	
		1.673	Me (2)
		2.318	
		2.367	
		4.565	
		4.768	
		4.834	
		5.232	
2-MN/K^+/MTHF	-14^0C	1.340	
		1.653	Me (2)
		2.309	
		2.359	
		4.551	
		4.730	
		4.814	
		5.192	
2-MN/K^+/MTHF	$+10^0$C	1.318	
		1.636	Me (2)
		2.282	
		2.346	
		4.529	
		4.685	
		4.791	
		5.160	
2-MN/K^+/DEE	-89^0C	0.061	K^+
		1.347	
		1.680	Me (2)
		2.315	
		2.361	
		4.538	
		4.747	
		4.799	
		5.193	

2-MN/K^+/DEE	-35^0C	0.067	K^+
		1.349	
		1.658	Me (2)
		2.315	
		2.381	
		4.539	
		4.762	
		4.792	
		5.230	
2-MN/Na^+/THF	-73^0C	1.337	
		1.733	Me (2)
		2.226	
		2.282	
		4.592	
		4.741	
		5.004	
		5.065	

[1]assignments given in Table C

TABLE B : Higher Methylnaphthalene Anions

System	temperature ($\pm 2^0$C)	Coupling Constant ($\pm$0.005G)	Position	Other
1,2,3,4-TMN/K^+/DME	-82^0C	5.167	5,8	5.32[1]
		3.650	Me(1,4)	3.74
		1.917	Me(2,3)	1.98
		1.730	6,7	1.75
1,3,5,7-TMN/K^+/DME	-81^0C	4.440	4,8	
		4.110	Me(1,5)	
		1.958	2,6	
		1.786	Me(3,7)	
1,2,3,4,5,8-HMN/K^+/DME	-87^0C	4.675	Me(1,4)	
		4.483	Me(5,8)	
		2.115	Me(2,3)	
		1.198	6,7	
OMN/K^+/DME	-83^0C	4.660	1,4,5,8	
		2.095	2,3,6,7	

[1] 72Ger

TABLE C Assignments for Methylnaphthalenes Anions[1]

Compound	Position	Value (Gauss)				
		This work	Kirk[2]	Gerson[3,4]	Moss[5]	Other
$N^{\cdot-}$	1		4.965	4.95		4.940[4,6]
	2		1.842	1.83		1.825
1-$MN^{\cdot-}$	4	4.408			4.425	4.414[9]
	5	5.372			5.402	5.354
	8	5.031			5.059	5.019
	2	1.409			1.421	1.402
	3	1.964			1.970	1.958
	6	1.529			1.536	1.531
	7	2.296			2.295	2.271
	1	3.854			3.867	3.885
2-$MN^{\cdot-}$	1	4.764			4.759	4.742[9]
	4	5.063			5.054	5.068
	5	5.063			5.054	5.037
	8	4.602			4.584	4.599
	3	2.322			2.313	2.286
	6	1.331			1.322	1.330
	7	2.269			2.256	2.225
	2	1.729			1.714	1.732
1,2-$DMN^{\cdot-}$	4		4.502			
	5		5.423			
	8		4.693			
	3		2.305			
	6		1.010			
	7		2.648			
	1		4.375			
	2		1.943			
1,3-$DMN^{\cdot-}$	4		4.242			
	5		5.074			
	8		5.239			
	2		1.880			
	6		2.032			
	7		1.759			
	1		3.950			
	3		1.867			
1,4-$DMN^{\cdot-}$	5		5.416	5.17		5.393[4,6]
	2		1.663	1.63		1.671
	6		1.829	1.79		1.832
	1		3.300	3.26		3.343
1,5-$DMN^{\cdot-}$	4		4.490	4.50		
	2		1.132	1.13		
	3		2.443	2.46		
	1		4.387	4.41		

Appendix 4.1 Table C cont.

1,6-DMN⁻	4		4.102			
	5		5.124			
	8		5.378			
	2		1.105			
	3		2.362			
	7		2.762			
	1		3.975			
	6		1.308			
1,7-DMN⁻	4	4.488				
	5	5.532				
	8	4.837				
	2		1.892			
	3		1.441			
	6		1.949			
	1		3.492			
	7		2.184			
1,8-DMN⁻	4		4.662	4.73		4.538[6]
	2		1.714	1.70		1.832
	3		1.657	1.70		1.671
	1		4.560	4.61		4.538
2,3-DMN⁻	1		5.033	4.93		
	5		4.733	4.67		
	6		1.797	1.76		
	2		1.714	1.69		
2,6-DMN⁻	1		4.835	4.79		
	4		4.681	4.65		
	3		2.724	2.68		
	2		1.222	1.22		
2,7-DMN⁻	1		4.413	4.32		
	4		5.231	5.12		
	3		1.797	1.76		
	2		2.200	2.16		
1,2,3,4-TMN⁻	5	5.167				5.32[8]
	6	1.730				1.75
	1	3.650				3.74
	2	1.917				1.75
1,3,5,7-TMN⁻	4	4.408				
	2	1.958				
	1	4.110				
	3	1.620				
2,3,6,7-TMN⁻	1					4.64[7]
	2					1.62
1,4,5,8-TMN⁻	2				1.411	
	1				4.354	

Appendix 4.1 Table C cont.

1,2,3,4,5,8-HMN⁻		
	6	1.198
	1	4.675
	2	2.115
	5	4.660
OMN⁻	1	4.660
	2	2.095

[1]coupling constants in K/DME at ca.-80^{0}C unless indicated otherwise, assignments based on the best fitting addivity relationship

[2]75Kir

[3]64Ger

[4]Na/DME

[5]69Mos

[6]from work by W.J.Campion quoted in 69Mos

[7]63Bol, conditions uncertain

[8]72Ger

[9]80Bru, Na/THF

Appendix 4.2 Least Squares Refinement of Proton Additivity Parameters for Methylnaphthalene Anion Radicals[3]

Table A : Best fit for α Coupling Constants

Parameter	Value (G)	Error[2] (G)
α	-4.965	0.027
A_B[1]	0.191	0.025
A_C	-0.166	0.027
A_D	0.577	0.027
A_E	-0.367	0.027
A_F	-0.099	0.023
A_G	0.358	0.025
A_H	-0.118	0.025

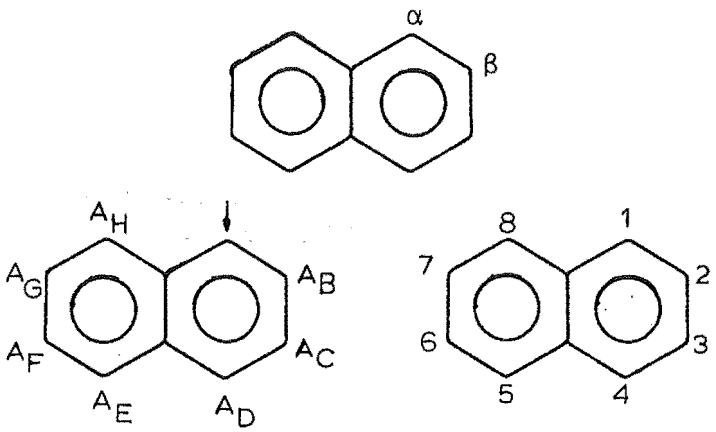

Compound	Position	Equation	Expt. (G)	Calc. (G)	Diff. (G)
1,5-DMN⁻	4	$\alpha+A_D+A_H$	-4.490	-4.506	0.016
1,8-DMN⁻	4	$\alpha+A_D+A_E$	-4.662	-4.755	0.093
1,4-DMN⁻	5	$\alpha+A_E+A_H$	-5.416	-5.450	0.034
2,7-DMN⁻	1	$\alpha+A_B+A_G$	-4.413	-4.416	0.003
	4	$\alpha+A_C+A_F$	-5.231	-5.230	-0.001
2,3-DMN⁻	1	$\alpha+A_B+A_C$	-5.033	-4.940	-0.093
	4	$\alpha+A_F+A_G$	-4.733	-4.706	-0.027
2,6-DMN⁻	1	$\alpha+A_B+A_F$	-4.835	-4.873	0.038
	4	$\alpha+A_C+A_G$	-4.681	-4.774	0.093
naphthalene⁻	1	α	-4.965	-4.965	0.000

Appendix 4.2 Table A cont.

2,3,6,7-TMN⁻	1	$\alpha+A_B+A_C+A_F+A_G$	-4.640	-4.681	0.041
1,2,3,4-TMN⁻	5	$\alpha+A_E+A_F+A_G+A_H$	-5.167	-5.191	0.024
1,3,5,7-TMN⁻	4	$\alpha+A_B+A_D+A_F+A_H$	-4.440	-4.414	-0.026
1-MN⁻	4	$\alpha+A_D$	-4.408	-4.389	-0.020
	5	$\alpha+A_E$	-5.372	-5.332	-0.040
	8	$\alpha+A_H$	-5.031	-5.083	0.052
2-MN⁻	1	$\alpha+A_B$	-4.764	-4.774	0.010
	4	$\alpha+A_C$	-5.063	-5.132	0.069
	5	$\alpha+A_F$	-5.063	-5.064	0.001
	8	$\alpha+A_G$	-4.602	-4.607	0.005
1,2-DMN⁻	4	$\alpha+A_C+A_D$	-4.502	-4.555	0.053
	5	$\alpha+A_E+A_F$	-5.423	-5.431	0.008
	8	$\alpha+A_G+A_H$	-4.693	-4.725	0.032
1,3-DMN⁻	4	$\alpha+A_B+A_D$	-4.242	-4.197	-0.045
	5	$\alpha+A_E+A_G$	-5.074	-4.974	-0.100
	8	$\alpha+A_F+A_H$	-5.239	-5.182	-0.057
1,6-DMN⁻	4	$\alpha+A_D+A_G$	-4.102	-4.031	-0.071
	5	$\alpha+A_B+A_E$	-5.124	-5.141	0.017
	8	$\alpha+A_C+A_H$	-5.378	-5.249	-0.129
1,7-DMN⁻	4	$\alpha+A_D+A_F$	-4.488	-4.487	-0.001
	5	$\alpha+A_C+A_E$	-5.532	-5.498	-0.034
	8	$\alpha+A_B+A_H$	-4.837	-4.892	0.055

Standard deviation = 0.0602G

[1] The contribution to the coupling constant of a proton at position A due to a methyl group at position J is defined as A_J

[2] estimated parameter standard deviation

[3] from 75Kir and this work

Table B : Assignments of Moss et al[1] for α Coupling Constants

Parameter	Value (G)	Error (G)
α	-4.972	0.041
A_B	0.285	0.037
A_C	-0.141	0.040
A_D	0.569	0.040
A_E	-0.349	0.040
A_F	-0.118	0.035
A_G	0.272	0.037
A_H	-0.111	0.037

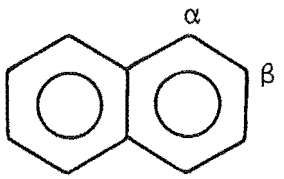

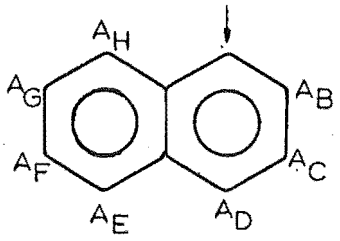

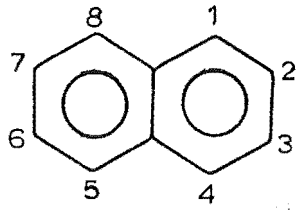

Compound	Position	Equation	Expt. (G)	Calc. (G)	Diff. (G)
1,5-DMN⁻	4	$\alpha+A_D+A_H$	-4.490	-4.515	0.025
1,8-DMN⁻	4	$\alpha+A_D+A_E$	-4.662	-4.752	0.090
1,4-DMN⁻	5	$\alpha+A_E+A_H$	-5.416	-5.432	0.016
2,7-DMN⁻	1	$\alpha+A_B+A_G$	-4.413	-4.416	0.003
	4	$\alpha+A_C+A_F$	-5.231	-5.230	-0.001
2,3-DMN⁻	1	$\alpha+A_B+A_C$	-4.773	-4.828	-0.095
	5	$\alpha+A_F+A_G$	-5.033	-4.818	-0.215
2,6-DMN⁻	1	$\alpha+A_B+A_F$	-4.681	-4.805	0.124
	4	$\alpha+A_C+A_G$	-4.835	-4.841	0.006
naphthalene⁻	1	α	-4.965	-4.972	0.007
2,3,6,7-TMN⁻	1	$\alpha+A_B+A_C+A_F+A_G$	-4.640	-4.667	0.034

Appendix 4.2 Table B cont.

1,2,3,4-TMN[1]	5	$\alpha+A_E+A_F+A_G+A_H$	-5.167	-5.279	0.112
1,3,5,7-TMN[1]	4	$\alpha+A_B+A_D+A_F+A_H$	-4.440	-4.348	-0.092
1-MN[1]	4	$\alpha+A_D$	-4.408	-4.403	-0.005
	5	$\alpha+A_E$	-5.372	-5.321	-0.051
	8	$\alpha+A_H$	-5.031	-5.083	0.052
2MN[1]	1	$\alpha+A_B$	-4.764	-4.687	0.085
	4	$\alpha+A_C$	-5.063	-5.112	0.049
	5	$\alpha+A_F$	-5.063	-5.090	0.027
	8	$\alpha+A_G$	-4.602	-4.700	0.064
1,2-DMN[1]	4	$\alpha+A_C+A_D$	-4.502	-4.544	0.042
	5	$\alpha+A_E+A_F$	-5.423	-5.439	0.016
	8	$\alpha+A_G+A_H$	-4.693	-4.812	0.119
1,3-DMN[1]	4	$\alpha+A_B+A_D$	-4.242	-4.119	-0.123
	5	$\alpha+A_E+A_G$	-5.074	-5.049	-0.025
	8	$\alpha+A_F+A_H$	-5.239	-5.201	-0.038
1,6-DMN[1]	4	$\alpha+A_D+A_G$	-4.102	-4.132	0.030
	5	$\alpha+A_B+A_E$	-5.124	-5.036	-0.088
	8	$\alpha+A_C+A_H$	-5.378	-5.223	-0.155
1,7-DMN[1]	4	$\alpha+A_D+A_F$	-4.488	-4.521	0.033
	5	$\alpha+A_C+A_E$	-5.532	-5.461	-0.071
	8	$\alpha+A_C+A_H$	-4.837	-4.799	-0.038

Standard deviation = 0.0901G

[1](69Mos), see footnotes p207

Table C : Best Least Squares Fit to β Coupling Constants

Parameter	Value (G)	Error (G)
β	-1.950	0.028
B_A	0.438	0.028
B_C	-0.397	0.032
B_D	-0.053	0.030
B_E	0.388	0.028
B_F	0.548	0.030
B_G	-0.376	0.028
B_H	-0.318	0.029

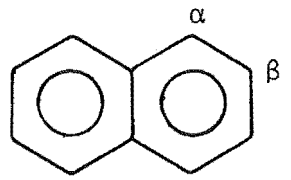

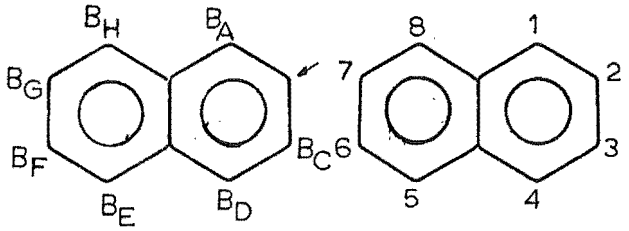

Compound	Position	Equation	Expt. (G)	Calc. (G)	Diff. (G)
1,5-DMN⁻	2	$\beta+B_A+B_E$	-1.132	-1.125	-0.007
	3	$\beta+B_D+B_H$	-2.443	-2.321	-0.122
1,8-DMN⁻	2	$\beta+B_A+B_H$	-1.714	-1.831	0.117
	3	$\beta+B_D+B_E$	-1.657	-1.615	-0.042
1,4-DMN⁻	2	$\beta+B_A+B_D$	-1.663	-1.565	-0.098
	6	$\beta+B_E+B_H$	-1.829	-1.881	0.052
2,7-DMN⁻	3	$\beta+B_C+B_F$	-1.797	-1.799	0.002
2,3-DMN⁻	6	$\beta+B_F+B_G$	-1.797	-1.779	-0.018
2,6-DMN⁻	3	$\beta+B_C+B_G$	-2.724	-2.723	-0.001
naphthalene⁻	2	β	-1.842	-1.950	0.108
1,4,5,8-TMN⁻	2	$\beta+B_A+B_D+B_E+B_H$	-1.480	-1.496	0.016
1,2,3,4-TMN⁻	6	$\beta+B_E+B_F+B_G+B_H$	-1.730	-1.709	-0.021
1,3,5,7-TMN⁻	2	$\beta+B_A+B_C+B_E+B_G$	-1.958	-1.898	-0.060

Appendix 4.2 Table C cont.

1,2,3,4,5,8-HMN$\bar{6}$		$\beta+B_A+B_D+B_E+B_F+B_G+B_H$	-1.198	-1.324	0.126
1-MN$^-$	2	$\beta+B_A$	-1.491	-1.512	0.021
	3	$\beta+B_D$	-2.007	-2.003	0.004
	6	$\beta+B_E$	-1.546	-1.562	0.016
	7	$\beta+B_H$	-2.296	-2.268	-0.028
2-MN$^-$	3	$\beta+B_C$	-2.322	-2.346	0.024
	6	$\beta+B_F$	-1.331	-1.402	0.071
	7	$\beta+B_G$	-2.269	-2.326	0.057
1,2-DMN$^-$	3	$\beta+B_C+B_D$	-2.305	-2.399	0.094
	6	$\beta+B_E+B_F$	-1.010	-1.015	0.005
	7	$\beta+B_G+B_H$	-2.648	-2.645	-0.003
1,3-DMN$^-$	2	$\beta+B_A+B_C$	-1.880	-1.909	0.029
	6	$\beta+B_E+B_G$	-2.032	-1.939	-0.093
	7	$\beta+B_F+B_H$	-1.759	-1.721	-0.038
1,6-DMN$^-$	2	$\beta+B_A+B_F$	-1.105	-0.965	-0.140
	3	$\beta+B_D+B_G$	-2.362	-2.379	0.017
	7	$\beta+B_C+B_H$	-2.762	-2.665	-0.097
1,7-DMN$^-$	2	$\beta+B_A+B_G$	-1.892	-1.889	-0.003
	3	$\beta+B_D+B_F$	-1.441	-1.455	0.014
	6	$\beta+B_C+B_E$	-1.949	-1.959	0.010

Standard deviation = 0.0735G

see footnotes p207

Table D : β Coupling Constants using Moss et al's Assignments[1]

Parameter	Value (G)	Error (G)
β	-1.950	0.030
B_A	0.447	0.031
B_C	-0.397	0.035
B_D	-0.062	0.032
B_E	0.378	0.030
B_F	0.548	0.032
B_G	-0.376	0.031
B_H	-0.309	0.031

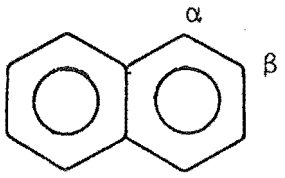

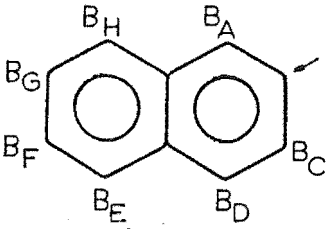

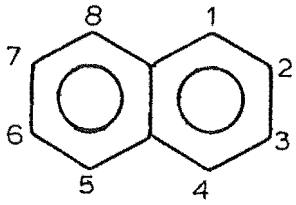

Compound	Position	Equation	Expt. (G)	Calc. (G)	Diff. (G)
1,5-DMN⁻	2	$\beta+B_A+B_E$	-1.132	-1.125	-0.007
	3	$\beta+B_D+B_H$	-2.443	-2.321	-0.122
1,8-DMN⁻	2	$\beta+B_A+B_H$	-1.657	-1.812	0.155
	3	$\beta+B_D+B_E$	-1.714	-1.634	-0.080
1,4-DMN⁻	2	$\beta+B_A+B_D$	-1.663	-1.565	-0.098
	6	$\beta+B_E+B_H$	-1.829	-1.881	0.052
2,7-DMN⁻	3	$\beta+B_C+B_F$	-1.797	-1.799	0.002
2,3-DMN⁻	6	$\beta+B_F+B_G$	-1.797	-1.779	-0.018
2,6-DMN⁻	3	$\beta+B_C+B_G$	-2.724	-2.723	-0.001
naphthalene⁻	2	β	-1.842	-1.950	0.108
1,4,5,8-TMN⁻	2	$\beta+B_A+B_D+B_E+B_H$	-1.480	-1.496	0.016
1,2,3,4-TMN⁻	6	$\beta+B_E+B_F+B_G+B_H$	-1.730	-1.709	-0.021
1,3,5,7-TMN⁻	2	$\beta+B_A+B_C+B_E+B_G$	-1.958	-1.898	-0.060

Appendix 4.2 Table D cont.

1,2,3,4,5,8-HMN	6	$\beta+B_A+B_D+B_E+B_F+B_G+B_H$	-1.198	-1.324	0.126
1-MN	2	$\beta+B_A$	-1.491	-1.503	0.012
	3	$\beta+B_D$	-2.007	-2.012	0.005
	6	$\beta+B_E$	-1.546	-1.572	0.026
	7	$\beta+B_H$	-2.290	-2.259	-0.037
2-MN	3	$\beta+B_C$	-2.322	-2.346	0.024
	6	$\beta+B_F$	-1.331	-1.402	0.071
	7	$\beta+B_G$	-2.269	-2.326	0.057
1,2-DMN	3	$\beta+B_C+B_D$	-2.305	-2.409	0.104
	6	$\beta+B_E+B_F$	-1.010	-1.024	0.014
	7	$\beta+B_G+B_H$	-2.648	-2.635	-0.013
1,3-DMN	2	$\beta+B_A+B_C$	-1.880	-1.899	0.019
	6	$\beta+B_E+B_G$	-2.032	-1.948	-0.084
	7	$\beta+B_F+B_H$	-1.759	-1.711	-0.048
1,6-DMN	2	$\beta+B_A+B_F$	-1.105	-0.955	-0.150
	3	$\beta+B_D+B_G$	-2.362	-2.388	0.026
	7	$\beta+B_C+B_H$	-2.762	-2.655	-0.107
1,7-DMN	2	$\beta+B_A+B_G$	-1.892	-1.879	-0.013
	3	$\beta+B_D+B_F$	-1.441	-1.464	0.023
	6	$\beta+B_C+B_E$	-1.949	-1.968	0.019

Standard deviation = 0.0794G

[1] 69Mos, see footnotes p207

Table E : β Coupling Constants using Brumby's Assignments[1]

Parameter	Value (G)	Error (G)
β	-1.942	0.041
B_A	0.431	0.041
B_C	-0.391	0.047
B_D	-0.102	0.043
B_E	0.390	0.040
B_F	0.540	0.043
B_G	-0.392	0.041
B_H	-0.271	0.042

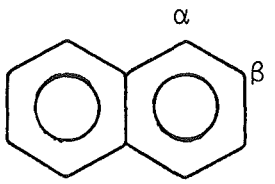

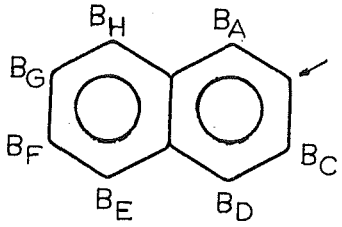

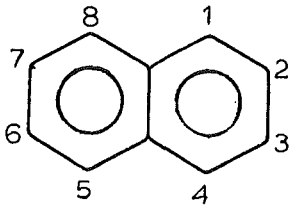

Compound	Position	Equation	Expt. (G)	Calc. (G)	Diff. (G)
1,5-DMN$^-$	2	$\beta+B_A+B_E$	-1.132	-1.122	-0.010
	3	$\beta+B_D+B_H$	-2.443	-2.315	-0.128
1,8-DMN$^-$	2	$\beta+B_A+B_H$	-1.714	-1.783	0.069
	3	$\beta+B_D+B_E$	-1.657	-1.654	-0.033
1,4-DMN$^-$	2	$\beta+B_A+B_D$	-1.663	-1.614	-0.050
	6	$\beta+B_E+B_H$	-1.829	-1.823	-0.006
2,7-DMN$^-$	3	$\beta+B_C+B_F$	-1.797	-1.794	-0.003
2,3-DMN$^-$	6	$\beta+B_F+B_G$	-1.797	-1.794	-0.003
2,6-DMN$^-$	3	$\beta+B_C+B_G$	-2.724	-2.725	0.001
naphthalene$^-$	2	β	-1.842	-1.942	0.100
1,4,5,8-TMN$^-$	2	$\beta+B_A+B_D+B_E+B_H$	-1.480	-1.494	0.014
1,2,3,4-TMN$^-$	6	$\beta+B_E+B_F+B_G+B_H$	-1.730	-1.674	-0.056
1,3,5,7-TMN$^-$	2	$\beta+B_A+B_C+B_E+B_G$	-1.958	-1.905	-0.054

Appendix 4.2 Table E cont.

1,2,3,4,5,8-HMN	6	$\beta+B_A+B_D+B_E+B_F+B_G+B_H$	-1.198	-1.345	0.147
1-MN	2	$\beta+B_A$	-1.529	-1.512	-0.017
	3	$\beta+B_D$	-2.290	-2.044	-0.246
	6	$\beta+B_E$	-1.491	-1.552	0.061
	7	$\beta+B_H$	-1.964	-2.213	0.249
2-MN	3	$\beta+B_C$	-2.269	-2.334	0.065
	6	$\beta+B_F$	-1.331	-1.402	0.071
	7	$\beta+B_G$	-2.322	-2.334	0.012
1,2-DMN	3	$\beta+B_C+B_D$	-2.305	-2.435	0.130
	6	$\beta+B_E+B_F$	-1.010	-1.012	0.002
	7	$\beta+B_G+B_H$	-2.648	-2.604	-0.044
1,3-DMN	2	$\beta+B_A+B_C$	-1.880	-1.903	0.023
	6	$\beta+B_E+B_G$	-2.032	-1.944	-0.088
	7	$\beta+B_F+B_H$	-1.759	-1.673	-0.086
1,6-DMN	2	$\beta+B_A+B_F$	-1.105	-0.972	-0.133
	3	$\beta+B_D+B_G$	-2.362	-2.436	0.074
	7	$\beta+B_C+B_H$	-2.762	-2.604	-0.158
1,7-DMN	2	$\beta+B_A+B_G$	-1.892	-1.903	0.011
	3	$\beta+B_D+B_F$	-1.441	-1.504	0.063
	6	$\beta+B_C+B_E$	-1.949	-1.943	-0.006

Standard deviation = 0.1067G

[1] 80Bru, see footnotes p207

Appendix 4.3 Least Squares Refinement of Additivity Parameters

Methyl Group Coupling Constants in Methylnaphthalene Anion Radicals[2]

Table A : Best fit for α Coupling Constants

Parameter	Value (G)	Error[3] (G)
P^1	3.878	0.051
A_B	0.381	0.093
A_C	-0.020	0.086
A_D	-0.604	0.088
A_E	0.490	0.090
A_F	0.198	0.095
A_G	-0.261	0.090
A_H	0.640	0.095

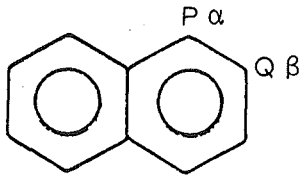

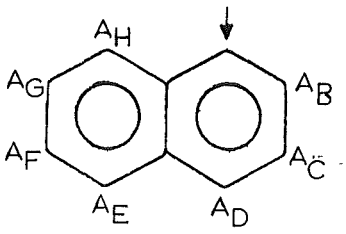

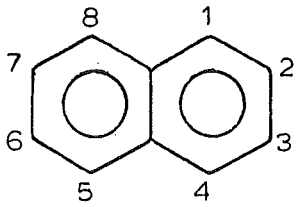

Compound	Position	Equation	Expt. (G)	Calc. (G)	Diff. (G)
1-MN⁻	1	P	3.812	3.878	-0.066
1,5-DMN⁻	1	$P+A_E$	4.387	4.368	0.019
1,8-DMN⁻	1	$P+A_H$	4.560	4.518	0.042
1,4-DMN⁻	1	$P+A_D$	3.300	3.273	0.027
1,2-DMN⁻	1	$P+A_B$	4.375	4.259	0.116
1,3-DMN⁻	1	$P+A_C$	3.950	3.858	0.092
1,6-DMN⁻	1	$P+A_F$	3.975	4.076	-0.101

Appendix 4.3 Table A cont.

1,7-DMN$^-$	1	$P+A_G$	3.492	3.617	-0.125
1,4,5,8-TMN$^-$	1	$P+A_D+A_E+A_H$	4.350	4.404	-0.054
1,2,3,4-TMN$^-$	1	$P+A_B+A_C+A_D$	3.650	3.635	0.016
1,3,5,7-TMN$^-$	1	$P+A_C+A_E+A_G$	4.110	4.087	0.023
1,2,3,4,5,8-HMN$^-$	1	$P+A_B+A_C+A_D+A_E+A_H$	4.675	4.765	-0.090
1,2,3,4,5,8-HMN$^-$	5	$P+A_D+A_E+A_F+A_G+A_H$	4.483	4.340	0.143
OMN$^-$	1	$P+A_B+A_C+A_D+A_E+A_F+A_G+A_H$	4.660	4.701	-0.041

Standard deviation = 0.1215G

[1] P is defined as the coupling constant for the hydrogens of a methyl group at position 1. The contribution to the coupling constant of a methyl proton of a methyl group at position A due to a methyl group at position J is defined as A_J [2] from 75Kir and this work, [3] estimated parameter standard deviation

Table B : Least Squares Fit to β Methyl Coupling Constants[2]

Parameter	Value (G)	Error[3] (G)
Q^1	1.719	0.021
B_A	0.202	0.040
B_C	-0.049	0.036
B_D	0.108	0.038
B_E	-0.370	0.039
B_F	-0.512	0.036
B_G	0.484	0.040
B_H	0.488	0.038

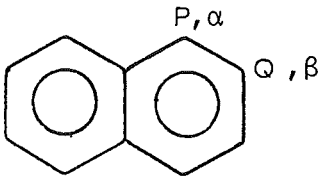

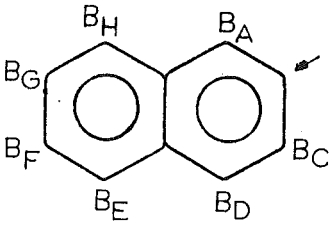

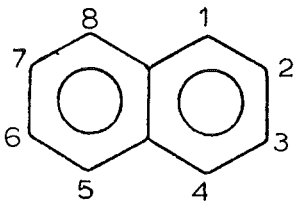

Appendix 4.3 Table B cont.

Compound	Position	Equation	Expt. (G)	Calc. (G)	Diff. (G)
2-MN$^-$	2	Q	1.729	1.719	0.010
2,7-DMN$^-$	2	$Q+B_G$	2.200	2.203	-0.003
2,3-DMN$^-$	2	$Q+B_C$	1.714	1.670	0.044
2,6-DMN$^-$	2	$Q+B_F$	1.222	1.207	0.015
1,2-DMN$^-$	2	$Q+B_A$	1.943	1.921	0.022
1,3-DMN$^-$	3	$Q+B_D$	1.867	1.827	0.040
1,6-DMN$^-$	6	$Q+B_E$	1.308	1.349	-0.041
1,7-DMN$^-$	7	$Q+B_H$	2.184	2.208	-0.024
2,3,6,7-TMN$^-$	2	$Q+B_C+B_F+B_G$	1.620	1.642	-0.022
1,2,3,4-TMN$^-$	2	$Q+B_A+B_C+B_D$	1.917	1.980	-0.063
1,3,5,7-TMN$^-$	3	$Q+B_D+B_F+B_H$	1.786	1.804	-0.018
1,2,3,4,5,8-HMN$^-$	2	$Q+B_A+B_C+B_D+B_E+B_H$	2.115	2.099	0.017
OMN$^-$	2	$Q+B_A+B_C+B_D+B_E+B_F+B_G+B_H$	2.095	2.070	0.025

Standard deviation = 0.0494G

[1] Q is defined as the value of the coupling constant for the methyl hydrogens of a methyl group at position 2. A_J is defined as the change produced in the coupling constant for the methyl hydrogens of a methyl group at position 2 due to a methyl group at position J.

[2] from 75Kir and this work

[3] estimated parameter standard deviation

Coupling Constants for Methylnaphthalene Derivative Cation Radicals

TABLE A : Coupling Constants for Methylnaphthalene Cation Radicals

Compound	Temperature	g	Constant (Gauss)	No.	Pos.	Other	
1,4-DMN^{+} [1]	-80^{0}C	2.0027	3.960[2]	2	5,8	3.84[3]	-3.74[7]
			9.726	6	1,4	9.63	+10.42
			2.189	2	2,3	3.75	-1.42
			1.346	2	6,7	2.36	-0.79
1,5-DMN^{+}	-72^{0}C	2.0029	7.095	6	1,5	7.07[3]	+7.93[7]
			5.348	2	4,8	5.34	-5.21
			1.772	2	2,6	1.69	-1.37
			1.584	2	3,7	1.69	-0.88
1,8-DMN^{+}	-84^{0}C	2.0028	8.305	6	1,8	8.25[3]	+10.14[7]
			5.725	2	4,5	5.73	-4.03
			2.480	2	2,7	2.45	-2.74
			1.136	2	3,6	1.16	+0.11
1,2,4-TriMN^{+}	-64^{0}C	2.0027	.729	1	7	-0.14[7]	
			.959	1	3	-0.34	
			2.042	1	6	-1.45	
			3.306	1	5	-3.01	
			3.855	3	2	+3.98	
			4.227	1	8	-4.12	
			8.993	3	4	+9.59	
			9.891	3	1	+10.92	

Appendix 5.1 Table A cont.

1,2,3,4-TMN†	-84°C	2.0030	9.451	6	1,4	9.36[4]
			3.691	2	5,8	3.71
			2.386	6	2,3	2.41
			1.403	2	6,7	1.33
1,3,5,7-TMN†	-85°C	2.0027	6.450	6	1,5	
			5.042	6	3,7	
			5.078	2	4,8	
			.068	2	2,6	
1,4,5,8-TMN†				12	1	7.84[6]
				4	2	1.76
1,2,3,4,5,8-HMN†	-90°C	2.0030	7.879	6	1,4	7.87[5]
			6.335	6	5,8	6.32
			1.938	6	2,3	1.99
			1.630	2	6,7	1.55
1,2,3,4,6,7-HMN†				6	1,4	8.48[5]
				6	2,3	2.40
				6	6,7	2.06
				2	5,8	4.25
OMN†			6.54	12	1,4	6.45[5]
			1.85	12	2,3	1.85

[1] abbreviations used; DMN is dimethylnaphthalene, TMN is tetramethylnaphthalene, PMN is pentamethylnaphthalene, HMN is hexamethylnaphthalene and OMN is octamethylnaphthaene

[2] $\pm$0.006 Gauss, [3] 72Yos, [4] 71Ger, [5] 69Roo, [6] 69How, [7] INDO Molecular Orbital calculations

TABLE B : Methylnaphthalenedisulphide Cation Radical ESR Parameters

Compound	Temp.	g	Coupling Constant (in Gauss)	Position
NDS^{+}[1]	-60^{0}C	2.0083	0.883[2]	2,5
			4.416	1,6
			5.260	3,4
1-MNDS^{+}	-60^{0}C	2.0084	0.628	5
			0.990	2
			3.971	6
			4.525	Me(1)
			4.992	3
			5.140	4
3-MNDS^{+}	-60^{0}C		0.588	2
			0.754	5
			4.002	6
			4.286	1
			4.978	4
			6.001	Me(3)
3-MNDS^{+}	-55^{0}C		0.591	
			0.764	
			3.993	
			4.281	
			4.972	
			5.988	Me
3-MNDS^{+}	-41^{0}C		0.593	
			0.757	
			4.015	
			4.289	
			4.988	
			6.010	Me
3-MNDS^{+}	-30^{0}C	2.0082	0.583	
			0.754	
			4.018	
			4.284	
			4.995	
			6.034	Me
1,2-DMNDS^{+}	-38^{0}C	2.0082	0.661	5
			0.848	Me(2)
			4.102	6
			4.304	Me(1)
			5.292	4
			5.074	3

Appendix 5.1 Table B cont.

1,3-DMNDS†	-52^{0}C 2.0079	0.495	5
		0.716	2
		3.655	6
		4.308	Me(1)
		5.107	4
		5.833	Me(3)
1,4-DMNDS†	-67^{0}C	0.349	5
		0.881	2
		3.936	6
		4.044	Me(1)
		4.887	3
		5.726	Me(4)
1,5-DMNDS†	-35^{0}C 2.0080	0.485	Me(5)
		1.029	2
		3.574	6
		4.761	Me(1)
		5.295	3
		5.343	4
1,6-DMNDS†	-2^{0}C 2.0081	0.793	2,5
		4.060	Me(1,6)
		4.904	3,4
2,4-DMNDS†	-62^{0}C	0.631	5
		0.631	Me(2)
		3.610	1
		4.481	6
		5.314	3
		6.167	Me(4)
3,4-DMNDS†	-39^{0}C 2.008	0.45	2,5
		3.85	1,6
		6.4	Me(3,4)

[1] abbreviations used; NDS is naphthalenedisulphide, MNDS is methylnaphthalenedisulphide and DMNDS is dimethylnaphthalenedisulphide.

[2] error in coupling constants is estimated to be $\pm$0.006 G

TABLE C : Coupling Constants from Miscellaneous Cation Radicals

Compound	Temp.	g	Coupling Constant[1]	Number	Other
perylene$^+$	-60^{0}C		4.033[2]	4	4.11[3]
			3.030	4	3.09
			0.414	4	0.46
signal from 1-methyl naphthalene	-60^0	2.006	4.770	6	
			2.306	2	
			0.440	4	
			0.270	2	
			0.020	2	
perylene$^+$ from 1,7-dimethyl-naphthalene			6.735	6	
			1.712	2	
			0.930	2	
			0.843	2	
			0.326	6	
			0.099	2	
3,9-dimethylperylene$^+$			4.389	6	
			3.877	2	
			2.905	2	
			2.818	2	
			0.395	2	
			0.235	2	
2,8-dimethylperylene$^+$			2.635	2	
			0.464	2	
			0.299	6[4]	
dimer$^+$ from 2,6-dimethyl-naphthalene			4.888	4	
			2.572	8	
			0.117	12	
			or		
			4.888	8	
			2.572	4	
			0.117	12	

[1] error in coupling constants $\pm$0.006 G

[2] from Scholl Condensation of naphthalene

[3] (67Rey)

[4] other coupling constants uncertain.

Appendix 5.2

Least Squares Refinement of Additivity Parameters for Methylaphthalenedisulphide Cation Radicals

Table A : Least Squares Fit to α Proton Coupling Constants

Parameter	Value (G)	Error[3] (G)
A	-4.380	0.028
A_B[1]	0.413	0.030
A_C	0.061	0.030
A_D	0.355	0.030
A_E	-0.139	0.030
A_F	0.395	0.024

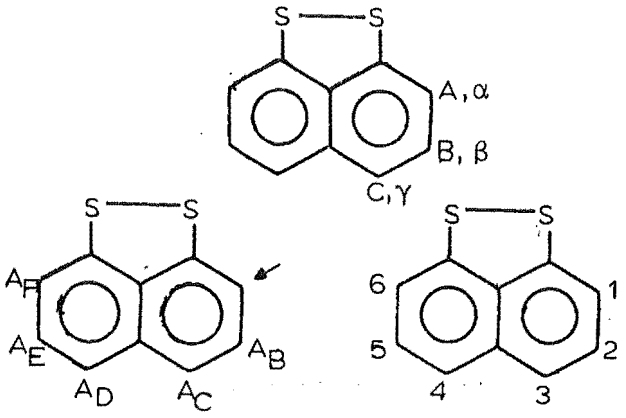

Compound	Position	Equation	Expt. (G)	Calc. (G)	Diff. (G)
NDS^{+}[2]	1	A	-4.416	-4.380	-0.036
1-MDS^{+}	6	$A+A_F$	-3.971	-3.986	0.015
3-MDS^{+}	1	$A+A_C$	-4.286	-4.320	0.034
	6	$A+A_D$	-4.002	-4.025	0.023
1,2-DMDS^{+}	6	$A+A_E+A_F$	-4.102	-4.125	0.023
1,3-DMDS^{+}	6	$A+A_D+A_F$	-3.655	-3.630	-0.025
1,4-DMDS^{+}	6	$A+A_C+A_F$	-3.936	-3.925	-0.011
1,5-DMDS^{+}	6	$A+A_B+A_F$	-3.574	-3.572	-0.002
2,4-DMDS^{+}	1	$A+A_B+A_D$	-3.610	-3.612	0.002
	6	$A+A_C+A_E$	-4.481	-4.458	-0.023

Standard Deviation = 0.035G

[1]The contribution to the coupling constant in position K due to a methyl group at position J is defined as K_J

[2]abbreviations used: naphthalenedisulphide (NDS), methyl-naphthalenedisulphide (MDS), dimethylnaphthalenedisulphide (DMDS)

[3]estimated parameter standard deviation

Table B : Least Sqaures Fit to β Proton Coupling Constants

Parameter	Value (G)	Error[3] (G)
B^{1}	(-)0.874	0.011
B_A	(-)0.132	0.009
B_C	(+)0.284	0.010
B_D	(+)0.129	0.011
B_E	(-)0.030	0.010
B_F	(+)0.239	0.009

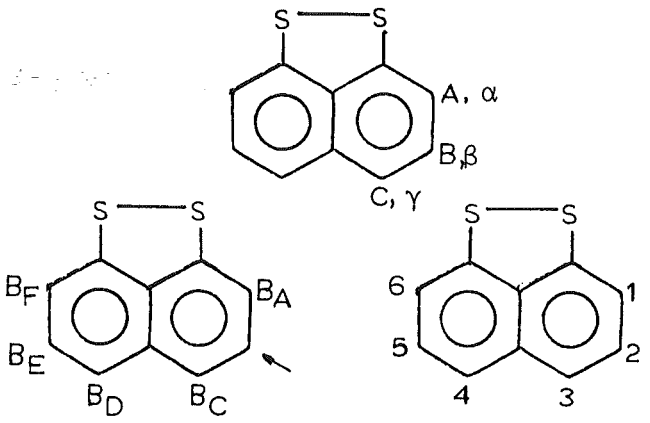

Compound	Position	Equation	Expt. (G)	Calc. (G)	Diff. (G)
NDS[2]	2	B	(-)0.883	-0.874	-0.009
1-MDS	2	$B+B_A$	(-)0.990	-1.006	0.016
	5	$B+B_F$	(-)0.628	-0.635	0.007
3-MDS	2	$B+B_C$	(-)0.588	-0.590	0.002
	5	$B+B_D$	(-)0.754	-0.746	-0.008
1,2-DMDS	5	$B+B_E+B_F$	(-)0.661	-0.665	0.004
1,3-DMDS	2	$B+B_A+B_C$	(-)0.716	-0.722	0.006
	5	$B+B_D+B_F$	(-)0.495	-0.507	0.012
1,4-DMDS	2	$B+B_A+B_D$	(-)0.881	-0.878	-0.003
	5	$B+B_C+B_F$	(-)0.349	-0.351	0.002
1,5-DMDS	2	$B+B_A+B_E$	(-)1.029	-1.036	0.007
1,6-DMDS	2	$B+B_A+B_F$	(-)0.793	-0.767	-0.026
2,4-DMDS	5	$B+B_C+B_E$	(-)0.631	-0.620	-0.011

Standard Deviation = 0.015G

[1]The contribution to the coupling constant in position K due to a methyl group at position J is defined as K_J

[2]abbreviations used: naphthalenedisulphide (NDS), methyl-naphthalenedisulphide (MDS), dimethylnaphthalenedisulphide (DMDS)

[3]estimated parameter standard deviation

Table C : Least Squares Fit to γ Proton Coupling Constants

Parameter	Value (G)	Error[3] (G)
C^1	-5.203	0.069
C_A	0.219	0.060
C_B	-0.169	0.062
C_D	0.103	0.062
C_E	-0.231	0.074
C_F	-0.061	0.060

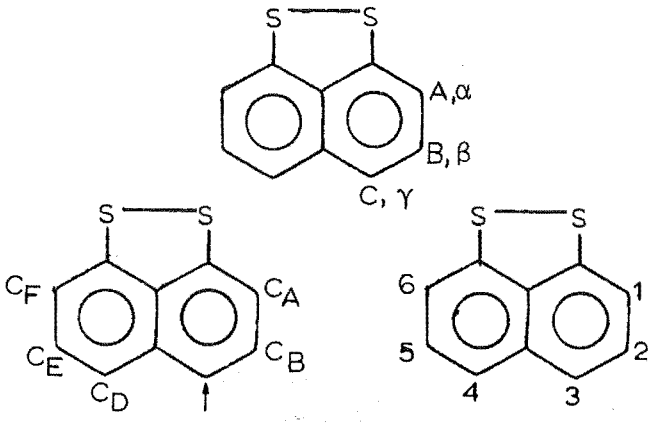

Compound	Position	Equation	Expt. (G)	Calc. (G)	Diff. (G)
NDS†[2]	3	C	-5.260	-5.203	-0.057
1-MDS†	3	$C+C_A$	-4.992	-4.983	-0.009
	4	$C+C_F$	-5.140	-5.142	0.002
3-MDS†	4	$C+C_D$	-4.978	-5.099	0.121
1,2-DMDS†	3	$C+C_A+C_B$	-5.074	-5.152	0.078
	4	$C+C_E+C_F$	-5.292	-5.373	0.081
1,3-DMDS†	4	$C+C_D+C_F$	-5.107	-5.038	-0.069
1,4-DMDS†	3	$C+C_A+C_D$	-4.887	-4.880	-0.007
1,5-DMDS†	3	$C+C_A+C_E$	-5.295	-5.214	-0.081
	4	$C+C_B+C_F$	-5.343	-5.311	-0.032
1,6-DMDS†	3	$C+C_A+C_F$	-4.904	-4.922	0.018
2,4-DMDS†	3	$C+C_B+C_D$	-5.314	-5.268	-0.046

Standard Deviation = 0.087G

[1]The contribution to the coupling constant in position K due to a methyl group at position J is defined as K_J

[2]abbreviations used: naphthalenedisulphide (NDS), methyl-naphthalenedisulphide (MDS), dimethylnaphthalenedisulphide (DMDS)

[3]estimated parameter standard deviation

Table D : Additivity Parameters for Methyl Coupling Constants

Parameter	Value (G)	Parameter	Value (G)
A	4.525	C	6.001
-	-	C_A [1]	-0.89
A_B	-0.16	C_B	-
A_C	-0.27	-	-
A_D	-0.48	C_D	-0.40
A_E	+0.23	C_E	+0.17
A_F	-0.46	C_F	-0.28

[1]The contribution to the coupling constant in position K due to a methyl group at position J is defined as K_J

REFERENCES

26Bje N. Bjerrum, Kgt. dauske Vidensk. Selsk., 7, 9 (1926), cited in 72Szw

33DeB E. De Barry Barnett and F. G. Sanders, J. Chem. Soc. (London), 136, 434 (1933)

44Zav E. Zavoisky, J. Phys. (U.S.S.R.), 8, 377 (1944), C.A. 39:3186[1]

46Blo F. Bloch, Phys. Rev., 70, 460 (1946)

54Sad H. Sadek and R.M. Fuoss, J. Am. Chem. Soc., 76, 5905 (1954)

53Gut H.S. Gutowsky, D.W. M^{c}Call, and C.P. Slichter, J. Chem. Phys., 21, 279 (1953)

54Win S. Winstein, E. Clippinger, A.H. Fainberg, and G.C.Robinson, J. Am. Chem. Soc., 76, 2597 (1954)

57Ehr H.W.W. Ehrlich, Acta. Cryst., 10, 699 (1957)

58Ada F.C. Adam and S.I. Weissman, J. Am. Chem. Soc., 80, 1518 (1958)

58deB E. de Boer and S. Weissman, J. Am. Chem. Soc., 80, 4549 (1958)

58M^{c}C M^{c}Connell, J. Chem. Phys., 28, 1188 (1958)

59M^{c}L A.D. M^{c}Lachlan, Mol. Phys., 2, 271 (1959)

59Ven B. Venkataraman, B.G. Segal, and G.K. Fraenkel, J. Chem. Phys., 30, 1006 (1959)

59Vil C.E. Villars, thesis as quoted in Thesis Abstracts 20 No. 4534 (1960)

60And J.M. Anderson, A.D. Campbell, G.W. Emerson, and J. Murray, J. Chem. Soc., 163, 410 (1960)

60Hel C. Heller and H.M. M^{c}Connell, J. Chem. Phys., 32, 1535 (1960)

61Ath N.M. Atherton and S.I. Weissman, J. Am. Chem. Soc., 83, 1330 (1961)

61Bol J.R. Bolton and A. Carrington, Mol. Phys., 4, 497 (1961)

62Hor A. Horsfield, J.R. Morton, and D.H. Whiffen, Mol. Phys., 5, 115 (1962)

62Mit W.J. Mitchell, R.D. Topsom, and J. Vaughan, J. Chem. Soc. (London), 2526 (1962)

62Miy I. Miyagawa and K. Itoh, J. Chem. Phys., 36, 2157 (1962)

63Bol J.R. Bolton, Thesis, Cambridge University, Cambridge (1963)

63deW C. de Waard and J.C.M. Henning, Phys. Lett., 4, 31 (1963)

63Fre J.H. Freed and G.K. Fraenkel, J. Chem. Phys., 39, 326 (1963)

63Rei P.H. Reiger, I. Bernal, W.H. Reinmuth, and G.K. Fraenkel, J. Am. Chem. Soc., 85, 683 (1963)

64Bar B.L. Barton and G.K. Fraenkel, J. Chem. Phys., 41, 1455 (1964)

64Bol J.R. Bolton and G.K. Fraenkel, J. Chem. Phys., 40, 3307 (1964)

64Col J.P. Colpa and E. de Boer, Mol Phys., 7, 333 (1964)

64deB E. de Boer and A.P. Praat, Mol. Phys., 8, 291 (1964)

64Fre J.H. Freed and G.K. Fraenkel, J. Am. Chem. Soc., 86, 3477 (1964)

64Ger F. Gerson, B. Weidmann, and E. Heilbronner, Helv. Chim. Acta., 47, 1951 (1964)

65Bal A.T. Balaban and C.D. Nenitzescu, "Friedel-Crafts and Related Reactions", Vol II, ch 23, John Wiley and Sons, New York (1963-1965)

65deB E. de Boer, Rec. Trav. Chim., 84, 609 (1965)

65Hyd J.S. Hyde, J. Chem. Phys., 43, 1806 (1965)

65Ish K. Ishizu, H. Hasegawa, H. Chikaki, N. Nishiguchi, and Y. Deuchi, Kogyo Kagaku Zusshi, 68, 1522 (1965), CA 63:16180d

65Lew I.C. Lewis and L.S. Singer, J. Chem. Phys., 43, 2712 (1965)

65Mob K. Mobuis, Z. Naturforsch., 20a, 1102 (1965)

65Zwe A. Zweig and A.K. Hoffmann, J. Org. Chem., 30, 3997 (1965)

66Ved V.I. Vedeneev, L.V. Gurvich, V.N. Kondrat'yev, V.A. Madvedev, and Y.L. Frankevich, "Bond Energies, Ionization Potentials and Electron Affinities." Edward Arnold, London (1966)

67Bol J.R. Bolton, J. Chem. Phys., 46, 408 (1967)

67Can P. Canonne and A. Regnault, Can. J. Chem., 45, 1267 (1967)

67Car A. Carrington and A.D. McLachlan, "Introduction to Magnetic Resonance", Harper and Row. (1967)

67Her A.M. Hermann, A. Rembaum, and W.R. Carper, J. Phys. Chem., 71, 2661 (1967)

67Iwa M. Iwaizumi, M. Suzuki, T. Isobe, and H. Azumi, Bull. Chem. Soc. J., 40, 2754 (1967)

67Law R.G. Lawler, J.R. Bolton, M. Karplus, and G.K. Fraenkel, J. Chem. Phys., 47, 2149 (1967)

67Nel S.F. Nelson, J. Am. Chem. Soc., 89, 5925 (1967)

67Oku A. Oku, T. Kakihana, and H. Hart, J. Am. Chem. Soc., 89, 4554 (1967)

67Rey A. Reymond and G.K. Fraenkel, J. Phys. Chem., 71, 4570 (1967)

68Law R.G. Lawler and G.K. Fraenkel, J. Chem. Phys., 49, 1126 (1968)

68Rie R.D. Rieke, C.F. Meares, and L.I. Rieke, Tet. Lett., 5275 (1968)

69Bev P.R. Bevington, "Data Reduction and Error Analysis for the Physical Sciences", McGraw-Hill, New York. (1969)

69How O.W. Howarth and G.K. Fraenkel, J. Chem. Phys., 52, 6258 (1969)

69Mos R.E. Moss, N.A. Ashford, R.G. Lawler, and G.K. Fraenkel, J. Chem. Phys., 51, 1765 (1969)

69Roo K.D.J. Root and M.T. Rogers, J. Magn. Res., 1, 568 (1969)

70Cla R.F.C. Claridge and B.M. Peake, Mol. Phys., 18, 137 (1970)

70Fis A. Fischer, D.R.A. Leonard, and D.A.R. Happer, Can. J. Chem, 48, 1446 (1970)

70Gol I.B. Goldberg and J.R. Bolton, J. Phys. Chem., 74, 1965 (1970)

70Red A.H. Reddoch, C.L. Dodson, and D.H. Paskovich, J. Chem. Phys., 52, 2318 (1970)

70Sul P.D. Sullivan and J.R. Bolton, Advances in Magnetic Resonance, 4, 39 (1970)

71Bau N.L. Bauld, C.E. Hudson, and J.S. Hyde, J. Chem. Phys., 54, 1834 (1971)

71Cav P. Cavaleiri D'Oro, R. Danieli, C. Maccagnani, G.F. Pedulli, and P. Palmieri, Mol. Phys., 20, 365 (1971)

71Cla R.F.C. Claridge, D.R.A. Leonard, and B.M. Peake, Mol. Phys., 19, 737 (1971)

71Fis A. Fischer, D.R.A. Leonard, and D.A.R. Happer, Can. J. Chem., 49, 1343 (1971)

71Owe G.S. Owen and G. Vincow, J. Chem. Phys., 54, 368 (1971)

71Pea B.M. Peake, Thesis, University of Canterbury (1971)

71Pij F.W. Pijpers, M.R. Arick, B.M.P. Hendricks, and E. de Boer, Mol. Phys., 22, 781 (1971)

71Red A.H. Reddoch, Chem. Phys. Lett., 10, 108 (1971)

71Sha A.L. Shain, Mol. Phys., 22, 733 (1971)

71Ste B.I. Stepanov, W.Ya. Rodionov, A.Ya. Zheltov, and V.V. Orlov, Tet. Lett. 1079 (1971)

72All R.D. Allendoerfer, P.E. Gallagher, and P.T. Lansbury, J. Am. Chem. Soc., 94, 7702 (1972)

72Bal S.E. Bales and R.D. Rieke, J. Org. Chem., 37, 3866 (1972)

72Boc H. Bock and B. Solouki, Angew. Chem. Int., 11, 436 (1972)

72Cla1 R.F.C. Claridge, B.M. Peake, and R.M. Golding, J. Magn. Res., 6, 29 (1972)

72Cla2 R.F.C. Claridge and B.M. Peake, Aust. J. Chem., 25, 2353 (1972)

72Des R.M. Dessau and S. Shih, J. Chem. Phys., 57, 1200 (1972)

72Dew M.J.S. Dewar and D.W. Goodman, J. C. S. Faraday II, 68, 1784 (1972)

72Fas D.J.M. Fassaert and E. de Boer, Rec. Trav. Chim, 91, 273 (1972)

72Ger F. Gerson, B.M. Peake, and G.M. Whitesides, Org. Magn. Res., 4, 361 (1972)

72Hud C.E. Hudson and N.L. Bauld, J. Am. Chem. Soc., 94, 1158 (1972)

72Pas D.H. Paskovich and A.H. Reddoch, Can. J. Chem., 50, 1523 (1972)

72Sai A. Saika ,A. Kawamori, and R. Takagi, J. Magn. Res., 7, 324 (1972)

72Sch J.V. Schutz and H. C. Wolf, Z. Naturforsch. A, 27, 42 (1972), C.A. 76:119614n

72Szw M. Szwarc, Ed. "Ions and Ion Pairs in Organic Reactions", Wiley-Interscience, New York.

72Tom K.B. Tomer, J. Turk, and R.H. Shapiro, Org. Mass. Spectrom., 6, 235 (1972)

72Wer J.E. Wertz and J.R. Bolton, "Electron Spin Resonance", M^{c}Graw-Hill, New York (1972)

72Yos H. Yoshimi and K. Kuwata, Mol. Phys., 23, 297 (1972)

73Bri D. Bright, I.E. Maxwell, and J. de Boer, J. C. S. Perkin II, 2101 (1973)

73Chr T.C. Christidis and F.W. Heineken, Chem. Phys., 2, 239 (1973)

73Jon M.T. Jones, T.C. Kuechler, and S. Metz, J. Magn. Res., 10, 149 (1973)

73Nel S.F. Nelsen and J.P. Gillespie, J. Am. Chem. Soc., 95, 2940 (1973)

74Bau N.L. Bauld and F.R. Farr, J. Am. Chem. Soc., 96, 5633, (1974)

74Boc H. Bock and B. Solouki, Chem. Ber., 107, 2299 (1974)

74Ped J.A. Pederson, Mol. Phys., 28, 1031 (1974)

74Red A.H. Reddoch, J. Magn. Res., 15, 75 (1974)

74Rie R.D. Rieke, S.E. Bales, C.F. Meares, L.I. Rieke, and C.M. Milliren, J. Org. Chem., 39, 2276 (1974)

75Eva T.I. Evlasheva, V.V. Puchkova, V.K. Potapov and E.N. Gur'yanova, Russ. J. Phys. Chem., 49, 453 (1975)

75Huf A.S. Huffadine, B.M. Peake, and L.W. Deady, J. C. S. Perkin II, 1263 (1975)

75Ishl K. Ishizu, F. Nemoto, K. Yamamoto, and M. Nakazaki, Bull. Chem. Soc. J., 48, 2168 (1975)

75Ish2 K. Ishizu, F. Nemoto, K. Mukai, M. Kohno, and H. Hasegawa, Bull. Chem. Soc. J., 48, 1635 (1975)

75Kir C.M. Kirk, Thesis, Canterbury University (1975)

75Nel G.V. Nelson and A. von Zelewsky, J. Am. Chem. Soc., 97, 6219 (1975)

75Nem F. Nemoto and K. Ishizu, J. Phys. Chem., 79, 1730 (1975)

75Rou R.A. Rouse and M.T. Jones, J. Magn. Res., 19, 294 (1975)

75Sol B. Solouki, H. Bock, and R. Appel, Chem. Ber., 108, 897 (1975)

76Lad K.H. Ladner, D.K. Dalling, and D.M. Grant, J. Phys. Chem., 80, 1783 (1976)

76Ste A. Streitwieser and C.H. Heathcock, "Introduction to Organic Chemistry", Collier Macmillan Publishers, London (1976)

76von C. von Borczyskowski and K. Mobius, Chem. Phys., 12, 281 (1976)

77Dom L.N. Domelsmith, L.L. Munchausen, and K.N. Houk, J. Am. Chem. Soc., 99, 6506 (1977)

77Cla R.F.C. Claridge, unpublished results (1977)

77Gol I.B. Goldberg and B.M. Peake, J. Phys. Chem., 81, 571 (1977)

77Ish K. Ishizu, M. Ohnishi, and H. Shikata, Bull. Chem. Soc. J., 50, 76 (1977)

77Jon M.T. Jones, S. Metz and, T.C. Kuechler, Mol. Phys., 33, 717 (1977)

77Lan Landolt Bornstein "Magnetic Properties of Free Radicals" New Series Group II Vol 9 Parts d1 and d2 (1977)

78Bra F.B. Bramwell, R.C. Haddon, F. Wudl, M.L. Kaplan, and J.H. Marshall, J. Am. Chem. Soc., 100, 4612 (1978)

78Sch T. Schmidt, W. Kraemer, and E. Kranz, U.S. Patent 4,127,728 (1978)

79Lam K. Lammertsma and H. Cerfontain, J. C. S. Perkin II, 673 (1979)

79Sau M. Saunders, D. Cox, and J.R. Lloyd, J. Am. Chem. Soc., 101, 6656 (1979)

79Sha1 K.K. Sharma and R.J. Boyd, Theor. Chim., 53, 309 (1979)

79Sha2 K.K. Sharma and R.J. Boyd, J. C. S. Faraday II, 75, 494 (1979)

79Yos K. Yoshida and S. Nagase, J. Am. Chem. Soc., 101, 4268 (1979)

80Bar M. Barzaghi, C. Oliva, and M. Simonetta, J. Phys. Chem., 84, 1959 (1980)

80Bru S. Brumby, J. Magn. Res., 40, 157 (1980)

80Buc A.C. Buchanan III, R. Livingston, A.S. Dworkin, and G.P. Smith, J. Phys. Chem., 84, 423 (1980)

80Dub J.E. Dubois, M. Delmar, and P.C. Lacaze, ElecChim. Acta., 25, 429 (1980)

80Iwa M. Iwaizumi, S. Kita, M. Kohno, and T. Isobe, Bull. Chem. Soc. J., 53, 1745 (1980)

81Boc H. Bock, G. Brahler, D. Dauplaise, and J. Meinwald, Chem. Ber., 114, 2622 (1981)

81Bru S. Brumby, J. Magn. Res., 44, 429 (1981)

81Thu R.P. Thummel and T. Fuchigami, J. Org. Chem., 46, 5217 (1980)

81Van H.L. Vancamp and A.H. Heiss, Magn. Res. Rev., 7, 1 (1981)

83Jac R.A. Jackson, J. C. S. Perkin II, 523 (1983)

83Poo C.P. Poole, "Electron Spin Resonance", John Wiley and Sons, New York (1983)

83Tan L.K. Tan and S. Brownstein, J. Org. Chem., 48, 302 (1983)

84Mak R. Makela, M. Oksanen, and M. Vuolle, Acta. Chem. A., 38, 73 (1984)

List of Figures

List of Tables